Addis Ababa University

Addis Ababa Institute of Technology

School of Mechanical and Industrial Engineering

Mechanical Design Engineering Stream

NUMERICAL MODELING OF THERMO-MECHANICAL STRESS FIELD ASSOCIATED WITH MODE-I AND MIXED-MODE FRACTURE IN HOMOGENOUS ISOTROPIC MATERIALS

A Thesis Submitted to Graduate Studies for School of Mechanical and Industrial Engineering in Addis Ababa University in Partial Fulfillment for the Requirement of the Degree of Master of Science in Mechanical Engineering

(Mechanical Design Stream)

Prepared By:

Wondimu Dessalegn Gatu

ID No: - GSR/8629/11

Main Advisor: Dr. Addis Kidane

Co-Advisor: Dr. Araya Abera

November, 2021 G.C.

Addis Ababa, Ethiopia

Declaration

I highly declare that the thesis work presented here entitled "***Numerical Modeling of Thermo-Mechanical Stress Field Associated with Mode-I and Mixed-Mode Fracture in Homogenous Isotropic Materials***" is my own work and all source of materials are duly acknowledged. The thesis was not written or defended previously for any award of degree in academic institutions. Besides, the work meets the rule and regulations of the university and agreed with the standard of originality and quality.

Wondimu Dessalegn Gatu		15/02/2022
Name of Candidate	Signature	Date

This is to certify that the above declaration made by the above candidate is correct to the best of my knowledge.

Addis Kidane (Dr.)		15/02/2022
Advisor	Signature	Date

ADDIS ABABA UNIVERSITY
ADDIS ABABA INSTITUTE OF TECHNOLOGY
SCHOOL OF MECHANICAL AND INDUSTRIAL ENGINEERING

NUMERICAL MODELING OF THERMO-MECHANICAL STRESS FIELD ASSOCIATED WITH MODE-I AND MIXED-MODE FRACTURE IN HOMOGENOUS ISOTROPIC MATERIALS

By
Wondimu Dessalegn Gatu

Approved by the Board of Examiners

Addis Kidane (Dr.) Advisor	Signature	15/02/2022 Date
Araya Abera (Dr.) Co-Advisor	Signature	Date
Mulugeta Habtemariam (Dr.) Internal Examiner	Signature	02/18/2022 Date
Haileloul Sahle (Dr.) External Examiner	Signature	Feb. 15, 2022 Date
Araya Abera (Dr.) Mechanical Design Chairman	Signature	Date
Yilma Tadesse (Dr.) SMiE Dean	Signature	15/02/2022 Date
Ermias Tesfaye (Dr.) Director of Post-Graduate	Signature	Date

Abstract

Engineering components exposed to different loading include mechanical, thermal or combined thermo-mechanical loading. Some of the components subjected to thermomechanical loading are gas turbines, engines, reactor components, fuel chambers, and so forth. Defects and flaws are primal causes for materials failure and exist in almost all materials. In this work, the effect of thermomechanical loading on the stress fields was investigated under pure Mode-I and Mixed Mode fracture by assuming a two-dimensional model under plane strain condition. To study the combined effect of thermo-mechanical loading on the stress field around the crack tip, sequentially coupled thermal-stress analysis employed by ABAQUS software was used under different conditions. The parameters used in this work i.e., material dimension selected based on BS standard, the applied remote stress also calculated analytically using limit load formula as 20MPa, 50MPa and 100MPa. The temperature gradient employed at the surface of the model is taken from literature ranges from $20℃$ *to* $89℃$. *The crack was considered as thermally insulated means adiabatic crack and the temperature field used as an input for the thermomechanical stress. This temperature field was solved by the assumption of steady-state heat transfer and the heat transfer procedure is utilized to solve it. The temperature field is incorporated as an input for the stress analysis as a predefined field in the static general procedure for developing a thermomechanical stress field. The extended finite element method (XFEM) was employed to model the crack for reducing the time of meshing and processing and to define the temperature and displacement discontinuity along the crack. The thermomechanical stress field was solved by applying different parameters i.e., remote stress, crack angle, crack length and temperature gradient. The mechanical and thermo-mechanical stress fields were evaluated and extracted from the crack tip for the radian value of* $r = 0.002\text{m}$ *and angular position value between* $-180° \leq \theta \leq 180°$ *for both Mode–I and Mixed Mode fracture cases.*

Based on the result, the stress fields i.e., σ_{xx}, σ_{yy} *and* τ_{xy} *around the crack tip were affected by the temperature gradients. The extreme thermo-mechanical stress field values* σ_{xx} *and* σ_{yy} *were rise by 13.4 to 36.39% and 4 to 17.6% respectively while the in-plane stress* τ_{xy} *drop by 8 to 43.49% relative to extreme mechanical stress value for temperature change* ΔT_1 *to* ΔT_3 *in case of considering the maximum value in pure mode-I loading case. Even though, the phenomenon of the extreme values for the case of mixed and pure mode-I loading cases are differ, the mixed mode thermo-mechanical stress field values* σ_{xx} *and* τ_{xy} *are drop by 6.78 to 25.64% and 12.85 to 30.3% respectively while the in-plane stress* σ_{yy} *rise by 4.75 to 25.09% in rising of temperature change* ΔT_1 *to* ΔT_3 *in case of considering the maximum value. This extreme values variation was because of the temperature gradient from the boundary of the plate as compared to mechanical stress field. Besides the angular position of the extreme stress field values shifted for a certain angle as compared to the isothermal stress field. The contour of these stress fields around the crack tip developed numerically has a good agreement with the analytical developed results.*

Key Words*: Adiabatic crack, XFEM, Thermo-mechanical stress fields, Mechanical stress field, In-plane stresses, Temperature gradient*

Acknowledgments

First and above all, I would like to thank the Almighty God to owe me here in the existence of the globe and for providing me the opportunity for making me capable of doing the master's program.

Next, my deepest heartfelt gratitude goes to my advisors Dr. Addis K. and Dr. Araya A. for giving me a supportive idea and commitment to the response to questions while doing the research paper. Their door was always open whenever I had a question about my research or writing their consistently allowed this paper to be my work, and also steered me in the right direction whenever they thought I need them. All in all, I thank them for the continuous response to the research idea shaping for making it into specific.

Last but not the least, I would like to thank the community of Mechanical Engineering staff of Addis Ababa Institute of Technology for giving me a chance to do my research.

Table of Contents

List of Tables

List of Figures

Nomenclatures

a	Crack length	$[mm]$
σ	Normal tensile stress	$[MPa]$
σ_{max}	Maximum stress	$[MPa]$
$\dot{\sigma}$	Stress rate	$[MPa/s]$
T	Temperature	$[K]$
$NT11$	Nodal Temperature	$[K]$
t	Time	$[s]$
K_{eff}	Effective stress intensity factor	$\left[MPa\sqrt{m}\right]$
K_{Ic}	Static fracture toughness	$\left[MPa\sqrt{m}\right]$
c_R	Rayleigh wave speed	$[m/s]$
c_d	Dilatational wave speed	$[m/s]$
v	Poisson's ratio	$[mm/mm]$
$\dot{a}$	Crack tip speed	$[m/s]$
u	Displacement in x-direction	$[mm]$
v	Displacement in y-direction	$[mm]$
k	Thermal conductivity coefficient	$W/m.K$
α	Coefficient of thermal expansion	$[1/k]$
M	High order term	[-]
G	Shear modulus	$[GPa]$
K	Degree kelvin	$[K]$
Y	Shape factor	[-]
$\sigma_{xx}, \sigma_{yy}, \tau_{xy}$	In-planes stress field components	$[MPa]$
θ	Angular position	[°]
α	Crack angle	[°]
ΔT	Temperature gradient	$[K]$
σ_o	Remote stress	$[MPa]$
a/w	Crack ratio	$[m/m]$

Abbreviations

FEM	Finite Element Method
FEA	Finite Element Analysis
XFEM	Extended Finite Element Method
FGM	Functionally Graded Materials
BEM	Boundary Element Method
DOF	Degree Of Freedom
DENT	Double Edge Notched Tension
LEFM	Linear Elastic Fracture Mechanics
EPFM	Elastic Plastic Fracture Mechanics
ES-FEM	Edge-Based Smoothed Finite Element Method
SFEM	Smoothed Finite Element Method
IC	Internal Combustion
CPE4R	Linear Quadrilateral Plane Strain Continuum Element
CPE3	Linear Triangular Plane Strain Continuum Element
HIMs	Homogeneous Isotropic Materials
CTOD	Crack Tip Opening Displacement
BS	British Standard
DSIF	Dynamic Stress Intensity Factor
PUM	Partition Unity Method
QUADS	Quadratic Nominal Stress Criterion
QUADE	Quadratic Nominal Stress Criterion
MAXS	Maximum Nominal Stress Criterion
MAXE	Maximum Nominal Strain Criterion
EFGM	Element Free Galerkin Method
MSED	Minimum Strain Energy Density Criterion
MCS	Maximum Circumferential Stress Criterion
MAXPS	Maximum Principal Stress Criteria
MAXPE	Maximum Principal Strain Criteria
MSF	Mechanical Stress Field
TMSF	Thermo-Mechanical Stress Field
MLS	Moving Least Squares

Chapter One
1 Introduction

1.1 Overview

The anticipated life expectancy of engineering components is a primal question concerning the safety of components of engineering machines utilized for manufacturing, production and aviation industries. However, the material selection for withstanding the imposed load is a vital role in the reliability of the part. The materials needed for different applications have to withstand various loading in the real-world arena. Especially in engineering utilization, materials are exposed through a lifetime to mechanical, thermal or combined thermo-mechanical loading. A few of the foremost common examples of components bare to thermo-mechanical loadings are gas turbines, engines, reactor components, fuel chambers, and so forth(Yadav *et al.*, 2020). It is obvious that engineering parts failure happens. This phenomenon is not only by mechanical load but also due to the cause of thermal loads/stresses or thermal fatigue(Pant et al., 2011) and also by crack propagation results in catastrophic failure engineering components. The thermomechanical load may influence initiating the new crack or propagating the pre-existing crack in the components. To alleviate and overcome such phenomenon special or advanced materials developed for instance Metal-Ceramic matrix and FGMs. FGMs were developed for the sake of filling the constraints of different materials to make a good response for the exerted thermal and mechanical loading simultaneously in various application.

Structural failure happens as engineering materials are subjected to mechanical loading in addition intensified by changing environmental conditions like fluctuation of temperature under forced or normal conditions. Generally, failure may be caused by various mechanisms including corrosion, buckling, fatigue, fretting, wear, stress corrosion cracking, fracture and so on. Among them, the fracture has no priority precaution but it is a common and omnipresent event with difficulty to anticipate and also it physically inescapable phenomenon and it is one of the failure mechanisms important for designing and analyzing engineering structures and materials(Nguyen et al., 2017). So, in this manner, how to precisely anticipate the failure of materials with the thought of temperature varieties is an interesting area, while the issue is more challenging(Ye et al., 2020).

Therefore, the need for fracture mechanics and its application has picked up tangible importance in the current time in many different industries: civil engineering, automobile industry, aerospace engineering, etc. Since fracture mechanics is a mechanism of failure investigation in engineering structures because of cracks or flaws exists in some degree of all structures(Owen & Fawkes,

1983). This consideration is due to the high expenditure of maintenance because of the existence of flaws/cracks, dislocation and defects that leads to failure or rupture due to the rapid crack growth and propagation at the crack tip, which requires substantial attention, time, maintenance strategies, etc. For reality, it is important to consider the real environmental condition i.e., the temperature gradient to which the materials are subjected. This temperature change, according to (Habib *et al.*, 2018) expression, can endanger the mechanical load and the stress accumulation in the vicinity of the crack tip under the constraint of deformation. Therefore, it is important to consider the thermoelastic fracture mechanics to account for the thermal and thermo-mechanical loadings.

Nevertheless, the homogenous isotropic materials utilized in designs withstanding a unique performance in overall structural developments. For instance, the primary goal of structural steel in the construction of a building is to withstand and hold the weights and loads exerted on the structure. Therefore, the material property needed in such application is its mechanical strength rather than any other properties. Hence, the combined thermo-mechanical loading implied in any of the materials might not be by deliberate applying heat transfer, it can dedicate by natural environmental effect due to fluctuation of the weather condition. For instance, steels in structural engineering are more appropriate for standing mechanical loadings rather they may lose their productivity undergo with thermal loadings while other materials such as ceramics are safer against thermal loadings than mechanical effects(Hosseini *et al*., 2013). As in through, the combined effect of the two types of loading should be tested in materials under different circumstances. One of the assets is the fracture behavior of materials under thermal and mechanical effects in the crack.

Through the materials manufacturing or development due to the voids, dislocations, or vacuum generally, preexisting flaws initiate and develop a crack. Therefore, the existence of various loading the crack will grow over time. This growth of crack tends to lower the intended goal of the structure to uphold the required strength by the accumulation of the stress around the tip of the crack. The propagation of the flaw decreases the material's strength to withstand the allowable load in the proper design of the structure. This tends to the material to fail by sudden load or fracture under the required load besides with the time(Broek, 1986) as depicted in the figure below.

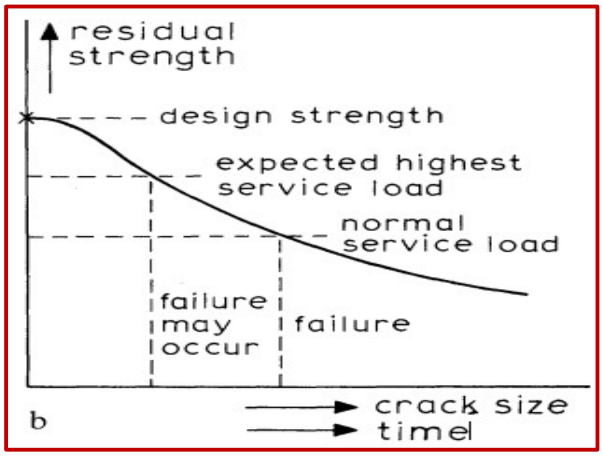

Figure 1-1. Strength of material with respect to crack size and time. Source: (Broek, 1986)

Therefore, due to the existence of the flaws in materials, the theory of ordinary analysis criteria that is based on the tensile strength, yield strength, and buckling have lacks on considering it. So, the adequate science for considering the discontinuity in materials is fracture mechanics, it emerges for considering cracks in materials. Engineering structures and problems are subjected to different loadings since the mechanical property couldn't remain consistent throughout the life whereas it changes under service life. One of the loads that combine with their extreme property is thermo-mechanical load. Upon this load, the crack in materials initiates and propagate which leads to a sudden failure(Shukla *et al.*, 2010). The initiation of the cracks by the existence of microcracks and defects that developed together to macro cracks that extensively influences materials. Due to the thermomechanical loadings also, the cracks unstable and intensified(Hosseini *et al*., 2013).

At the vicinity of the crack tip also the temperature field is established due to the plastic deformation occurrence, this also leads to introducing the thermal stress that alters the stress field in the crack tip and influences the fracture parameters like the stress intensity factor. This phenomenon is called the thermo-mechanical effect associated with crack propagation(Kotousov, 2002). It is recognized that the generation of heat around the vicinity of the crack tip tends to create the temperature field around the crack tip(Zehnder & Rosakis, 1991). Hence, much of the fracture energy converted to heat dissipation in metals around 90% and polymers around 60-80% while the rest of the energy converted to the form of a modified atomic/molecular/grain structure in the vicinity of the crack tip (Kotousov, 2002). Bearing in mind this, the temperature field around the crack tip leads to affecting the stress field as well as the behavior of the fracture. This heat production at the crack tip tends to develop the temperature field but it is assumed neglected and

also not considered in this work rather only the external exposure of temperature on the boundary of material considered.

The stress field in the crack end according to the theory is singular but in reality it is not because materials cannot sustain infinite stress(Anderson, 2005). This is due to the inelastic and irreversible deformation that occurred in the vicinity called plastic deformation. The plastic zone at the crack tip tendency in brittle or ductile fracture, despite their magnitude, the tendency of crack propagates with temperature raises, which is proofed experimentally(Kotousov, 2002) and analytically (Abotula et al., 2012; Shukla et al., 2010; Kidane et al., 2010). The property of materials varies under temperature variation. The temperature change in material runs off for the generation of thermal stress, if it exceeds the material strength break or failure happens but also it alters the mechanical properties(Fu *et al*., 2017). The elastic property of an isotropic material decreases when it undergoes in a temperature environment for instance the elastic modulus and yield strength of materials. The hypothesis was validated as truth by working on the steel material under different temperatures at a constant strain rate(Carla *et al.,* 2017).

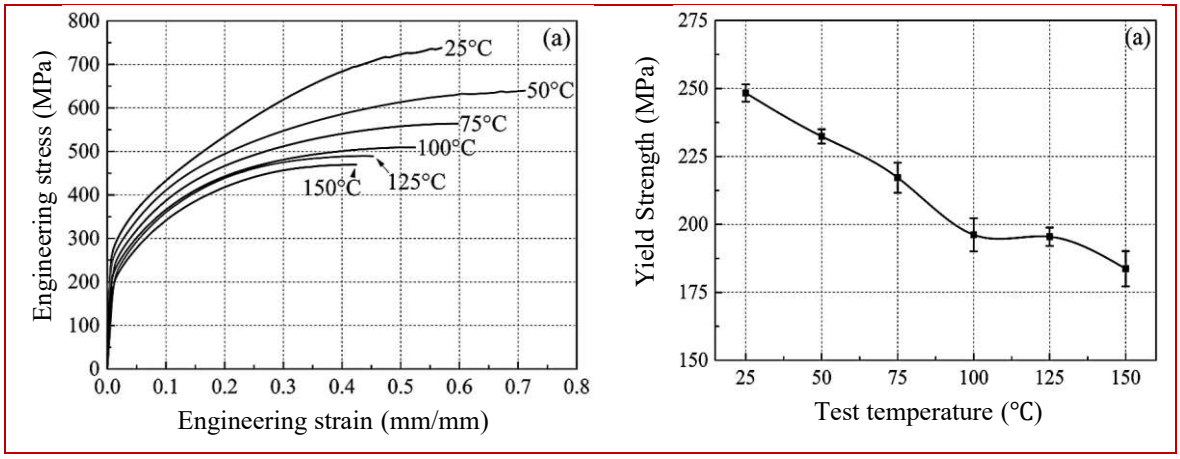

Figure 1-2. The effect of temperature change in mechanical property of steel material under tensile testing. Source: (Carla et al., 2017)

Similarly, the temperature gradient might have a change in the stress field along the propagated crack. For instance, the temperature effect in polyimide resin (PMR-15) material results in lowering its stiffness and flexural strength in cross laminar and trans laminar directions results in softening in the matrix of a composite material(Aglan *et al*., 1992). However, the dynamic fracture toughness also varied with the temperature gradient in which the fracture toughness was tested under the loading rate function by the Charpy test(Broek, 1986). Besides, the temperature gradient in material results in thermal stress, this becomes a failure of the structure if it exceeds the limit of the strength of the material. This is proved by (Fu *et al*., 2017) in which the crack initiated and

propagated in brittle material of the thick wall cylinder model among the temperature given in the boundaries of the model.

Since cracks cannot be eliminated under any circumstances; this prompts engineers to guide their efforts towards winning strategies in prevention, design, and especially analysis that can be provided by the tool of numerical modeling. Therefore, the difficulty, complexity, and time-consuming in solving problems analytically modeling and experimentally, computational methods are chosen for simplifying the problem and reducing time. So, in this paper numerical method is employed to define the phenomenon of the stress field around the crack tip by the coupled thermo-mechanical loading.

1.2 Motivation for the Research

The operation of numerous mechanical systems or their components regularly works suspected to both mechanical and thermal loading conditions, which is commonly experienced in many applications such as engines, fuel cells, and pressure vessels, etc. Also, the nature of the engineering components couldn't force a single load subjection during performing a certain application. For instance, the vehicle components like the IC engine components are subjected to mechanical as well as thermal fatigue in operation also some automotive components as well. This implication stands to consider the fracture of the components needs to be considered not only the mechanical load but also the thermal load. This and other scenarios lead to consider the thermal effect on failure investigation materials by many scholars. Reminding this, the thermal effect in combination with the fracture mechanics subject motivated to consider the area of the research should consider the thermo-mechanical effect on the surrounding of crack by the exposure of temperature change on the boundary of the model is the starting point of conducting this study in addition to the work of colleagues.

1.3 Statement of the Problem

Many researchers and scholars investigate the failure of engineering materials and structures with dislocations, voids and flaws under the subjection of external loads. These voids, dislocations and flaws growth to crack and the failure mechanism of materials executed by fracture mechanics considering the mechanical stress. However, several engineering components are subjected to heat transfer that works under high operating temperature for instance engines, fuel cells, furnaces, heat pump, turbine blades, pressure vessels and so on. And their failure mechanism investigation by considering both the effect of mechanical load and thermal load is essential. Reminding the above problem, different approaches are utilized to investigate the failure of materials under the existing

crack that accommodates the thermo-mechanical loading condition these methods are analytical/mathematical, experimental and numerical approaches.

Therefore, to expand the analytical methods, a numerical approach utilized in this work because it enables for a dynamic manipulation of parameters such as applied load, crack orientation, crack angle, and temperature gradient and fracture modes. Besides, by incorporating the parameters mentioned above, this work is an extension of the analytical modeling of thermomechanical stress field which is done by (Kidane et al., 2010) modified by considering fracture modes and stationary crack using a numerical approach utilizing the ABAQUS software tool.

1.4 The Objective of the Research

1.4.1 General Objective

The intended goal of conducting this study is to model the thermo-mechanical stress field associated with Mode-I and Mixed Mode fracture around the vicinity of crack tip using numerical tool.

1.4.2 Specific Objectives

To accomplish the main aim of the research the following specific objectives needed to be done. So, the precise goals of the research are: -

- Modeling the temperature field and mechanical stress field around crack tip numerically by ABAQUS/CAE
- To investigate the effect of thermo-mechanical loading on stress field at the crack tip for mode-I and mixed mode fracture cases
- To determine the variation of stress components due to temperature change

1.5 Scope of the Research

The primary goal of the study focuses on the modeling of the stress field around the crack tip for homogeneous isotropic material under thermo-mechanical loading by using numerical methods i.e., extended finite element method to model the crack. Even though the analytical modeling of the thermo-mechanical stress field around the crack tip has developed but the numerical analysis is needed to justify and testing of the fracture problem in different dimensions considering the type of loading varied, mixed-mode fracture, temperature variations can be considered easily in numerical approach.

As of all, the research intended for analyzing the phenomena of stress field on the vicinity of the crack tip numerically by ABAQUS software under the combined thermal and mechanical

loading. However, the direction of the crack propagation is not included. But the study is limited to consider the property of materials change under temperature gradient effect, inhomogeneous materials like composite and functional graded materials and how the three-dimensional stress field looks like are not prescribed in the paper.

1.6 Significance of the Research

Engineering components are under the subjection of thermal and mechanical loading(Pant et al., 2011). The theoretical researches consider the effect of temperature on the materials/components' integrity. This is also the same for fracture of materials in the preexisted crack. Since materials consist of flaws that enlarged to crack under the exposure of external stresses. Considering the fracture of materials under the effect of thermal loads the crack initiate and propagate. However, the crack-tip velocity in the formulation of the theoretical modeling is considered while the numerical analysis on the thermo-mechanical loading on the crack has a limitation. So, the research contributes to fracture mechanics in consideration of thermal effects on stationery crack by applying the remote stress for Mode-I and Mixed Mode fracture. After all, this work suggests in designing and implementation of engineering materials by thermo-mechanical effects during the design needed to consider because of the tendency of the crack in materials affected by the thermal and mechanical loading. Besides, it contributes to the scholars who are involved in the study in this area for becoming the input for further study.

1.7 Research Methods and Methodology

1.7.1 Research Methods

The study is performed numerically to achieve the objective of the research. Based on these, methods and tools used in the analysis is taken by reviewing related papers.

1.7.1.1 Literature Review

A variety of literature like proceedings, periodicals, different articles, websites, and different materials was under surveyed for the sake of assessing the methods used for developing the thermo-mechanical stress field in the crack tip. A literature review is also needed to understand and select the correct procedures to be followed in utilizing the numerical methods to analyze the stress field in the crack tip.

1.7.1.2 Techniques and Tools

Among different approaches of simulating and analysis of the fracture problem the extension of the finite element method which is called the extended finite element method (XFEM) is utilized for modeling the crack. Since the accuracy of simulating the crack tip and crack surface is by using additional enrichment function (Section 2.5.3), also, no need for re-meshing during the propagation of the crack. This method is also incorporated in ABAQUS software so it can be easily implemented for fracture problems.

1.7.2 Research Methodology

The procedure for attaining the objective of the research is by attending the sequences of the methods and tools by cross-checking with the literature to validate each of the methods. Therefore, gathering the important concept in the analysis of the thermo-mechanical stress field can be gathered from the literature. The input for the numerical software is determined following the existing scholars. This includes the material property, boundary conditions such as the traction load, the temperature field, the heat flux given for the two-dimensional modeled geometry based on the theory of analytical modeling of the stress field for fracture problem. The numerical method used in this study is a finite element method to simulate the stress and heat transfer fields by using ABAQUS software utilizing the XFEM method for modeling the crack in the case static general procedure. After all, the numerical stress field based on the superimposing effect of the mechanical and thermal loading on the vicinity of crack tip simulated for different temperature boundary conditions, crack orientation, remote stresses and crack length. All in all, the stress field is the in-

plane stresses in the vicinity of the crack tip extracted from the crack tip with varied temperatures. Then the result will be compared and validated with the mechanical/analytical stress fields. The framework of the research is generalized in the following Figure 1-3.

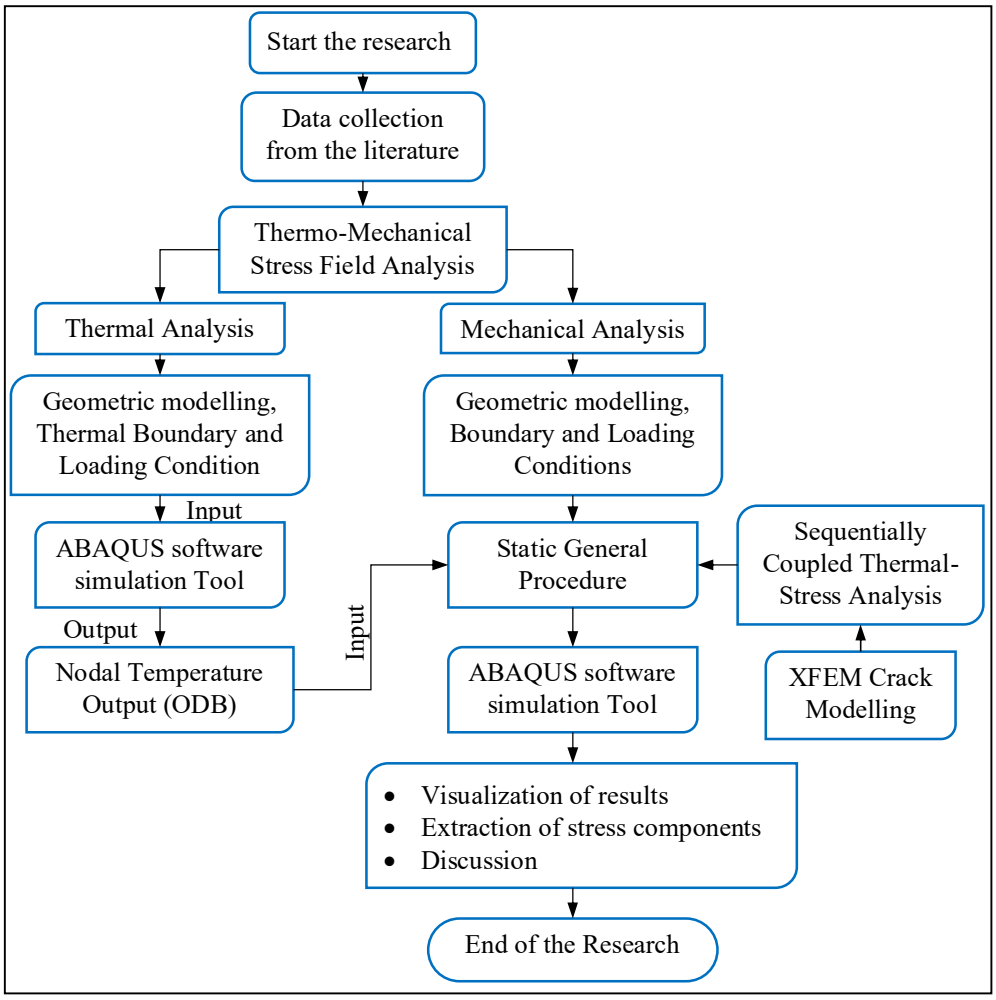

Figure 1-3. Research Methodology. Source: Author's MS Visio

1.8 Organization of the Document

The paper studies the numerical analysis of the thermo-mechanical stress field associated with mode-I and mixed-mode fracture using the finite element method by the ABAQUS software tool. To accomplish this objective the document is organized into five chapters.

The first chapter introduces the overall concept of fracture happen not only by mechanical load but also by thermal loads in addition to the basic notes on the effect of temperature on material properties. Besides, it will mention other important points of the research that should include for instance the basement for initiation of the research that is the problem that enforces for upholding the study, the scope of paper which it covers, the methodology used to accomplish the research with the objectives. And also, the opportunity that creates while after accomplishing the research and the obstacles in progressing the study is included in this part.

The second chapter portion of the research paper will explain the theory of fracture mechanics for dynamically loaded body and propagating crack, reviewing the important scientific papers from the scholars and the finite element tool used for simulating the crack also presented. The third chapter discusses the numerical modeling approach tools and the procedures followed in the numerical software mentioned. The fourth chapter is about the clarification of the outcome from the analysis and discusses the result with that of mechanical stress field for different fracture configurations. In the last chapter, the conclusion is drawn based on the result and recommendations shown.

Chapter Two
2 Literature Review

2.1 Introduction

The effect of thermo-mechanical load on material integrity has been the research area in fracture mechanics. Upon this different researcher studies the fracture analysis numerically, analytically, and experimentally to develop the phenomenon of engineering materials under the thermo-mechanical loading on the cracked body. This has been investigated in a variety of material types such as homogeneous, non-homogeneous and composite materials. In this study, the isotropic homogeneous material is under investigation. Doing so in this part of the research different concepts related to thermoelastic fracture, dynamic fracture and XFEM method are discussed in addition to the works of scholars related to the thermo-mechanical stress field in a pre-existing crack in the two-dimensional flat plate body.

2.2 Fracture Mechanics

It has been obvious that materials tend to withstand the allowable stress below the strength of materials. However, the existence of cracks in almost all structures tends to the development of fracture mechanics which is a new area founded in the early 20th century. The existence of pre-existing flaws or discrepancies in materials born the existence of the field of fracture mechanics(Sheng, 2018). Fracture mechanics is a solid mechanics that studies materials failure, strength in which the materials contain one or more cracks(Anderson, 2002). According to (Kanninen & Popelar, 1985), it is applied for relating the maximum permissible stress exerted on the engineering components to the geometry and position of real or hypothetical cracks that exist on the materials. Generally, fracture mechanics is a field of solid mechanics concerns about the crack and crack propagation in addition to the fracture of materials and components with measuring and characterizing of materials to resistance of the crack growth. Furthermore, fracture stands for separation of parts or components into two whereas crack stands for discontinuity in materials that exist within the components i.e., without segregation of a body in any of parts(Ai, 2018). The main aim of the fracture mechanics is to assess the achievement of defective materials for engineering utilization.

The first attempt applied for fracture mechanics by the concept of an elliptical hole at the center of the flat plate assuming infinite geometry in which the geometry of the material doesn't influence the hole is by Inglis in 1913(Anderson, 1995). The figure depicted below describes the Inglis notation of stress concentration at the end of the major axis of the elliptical hole.

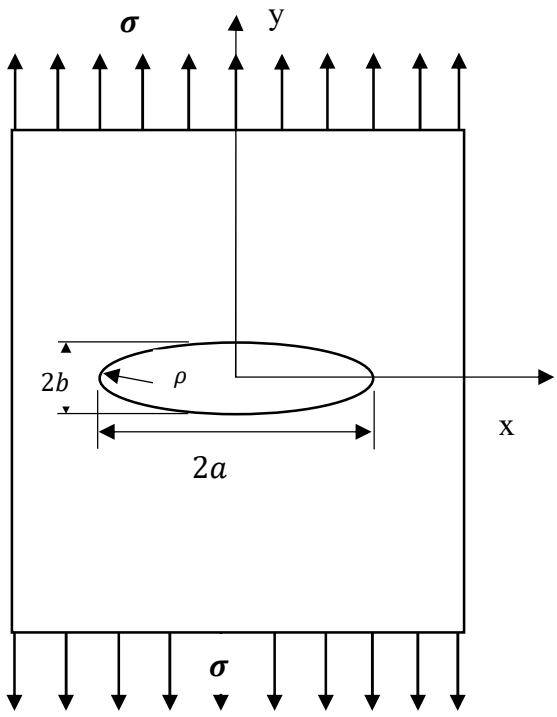

The plate subjected to uniform tensile stress in both upper and lower part of the infinite plate as shown in figure. The maximum stress exists in the tip of the major axis of the ellipse given by Inglis as:

$$\sigma_{max} = \sigma\left(1 + 2\frac{a}{b}\right) \tag{2.1}$$

Bearing in mind of increasing the major axis $2a$ relative to minor axis $2b$, the ellipse tends to being the advent of sharp crack. For this case Inglis also found a convenient expression by letting of radius of curvature, ρ as:

$$\rho = \frac{b^2}{a} \tag{2.2}$$

Figure 2-1. Elliptical hole in a flat plate model. Source: (Anderson, 2005)

Therefore, the maximum stress is written in terms of the radius of curvature, ρ and by letting $a \gg b$ as:

$$\sigma_{max} = \sigma\left(1 + 2\sqrt{\frac{a}{\rho}}\right) \tag{2.3}$$

The elliptical hole tends to the appearance of the crack as the $\rho \to 0$ the applied stress neglected compared to the left end of an expression. So, the equation can be expressed as:

$$\sigma_{max} = 2\sigma\sqrt{\frac{a}{\rho}} \tag{2.4}$$

The Inglis relationship between the applied loads with the hole introduced in the object leads to failure of the material is happens with a small load. And also, any material couldn't sustain infinite stress to withstand. This deficiency of the principle leads to innovation in any other model by the energy balance concept by Griffith. The theory if the rate of release of the strain energy is more than the critical value (material resistance) the crack will propagate.

2.2.1 Modes of Fracture

The pre-existed crack in the body deformed in a different manner of the application of the load on the body. Due to this, different types of motion of the crack are observed in a body. So, the same types of mode of fracture observed in the dynamic fracture mechanics also. The difference is the applied load is whether it is dynamically applied that varies with time or the crack propagates by crack tip speed on the cause of the time-independent loading. So, the fracture modes, in this case, are also the same as the static one in orientation, line of action of the load, etc. these modes are: -

1. Opening mode of fracture (Mode-I)

The applied loads tend to open the initiated crack which is perpendicular to the plane of the crack. The action of the loading is symmetric to the crack plane and the loading intensifies the crack surfaces by pulling outward from the plane of crack. It is also called symmetric in-plane mode(Anderson, 2002).

2. Shearing mode of fracture (Mode-II)

The applied load is parallel to the crack plane in both the upper and lower part of the crack and perpendicular to the face of the crack. The load makes the crack slide each other and the forced shear on the plane of the crack is called in-plane shear.

3. Tearing mode of fracture (Mode-III)

The crack moves out of the crack plane by the shear load applied in parallel with the crack face in the upper and lower part from the crack surface in opposite directions. This causes the crack surface to deform out of the plane of crack called out-plane shear (tearing).

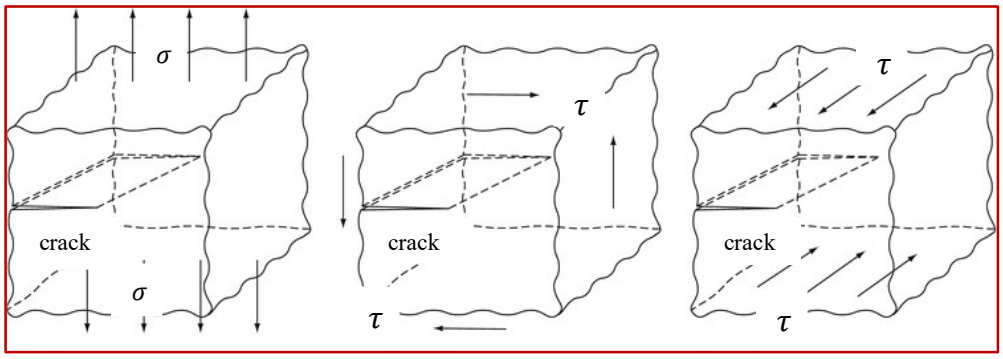

Figure 2-2. Schematic of the modes of fracture: Mode I opening (left), Mode II shearing (middle), and Mode III tearing (right). Source: (Zehnder, 2012)

However, the loading type on a certain body is not only by a single mode of fracture but maybe a combination of the above modes. The most common combination of loading is a mode I and

mode II called a mixed-mode fracture. Besides, other types of loading are also applied in material for instance the thermal load by implication of the temperature gradient in the body combined with mechanical load called a thermomechanical load. The fracture phenomena are parameterized by the stress intensity factor and the energy release rate for Linear Elastic Fracture Mechanics and described in the following section.

2.2.2 Stress Intensity Factor(K)

The SIFs are intended for predicting the intensity of stress on the crack tip in which the load is applied remotely from the crack face. More generally, SIF is used to characterize the displacement, strain and stress fields in the region of the crack tip in LEFM. Also, its implication confirms to use of the failure criteria for brittle materials. The material resistance for crack propagation under the exerted stress remotely is called fracture toughness. If the stress intensity factor is equitable with the fracture toughness, it is intrinsic material property independent of the geometry of materials but it is measured under plane strain condition, the crack tends to be unstable leads to propagation called the critical intensity factor.

The stress intensity factor magnitude varies corresponding to the type of loading(tensile/compressive, shear), the geometry of the specimen, crack size, and magnitude of the force exerted on the material (Anderson, 1995).

$$\begin{aligned} &\text{For mode-I} && K_I = Y\sigma_O\sqrt{\pi a} \\ &\text{For mode-II} && K_{II} = Y\tau\sqrt{\pi a} \\ &\text{For mode-III} && K_{III} = Y\tau_{tear}\sqrt{\pi a} \end{aligned} \tag{2.5}$$

Y: Stands for shape factor depends on the loading type and the geometry of the sample

$\sigma_O, \tau\ and\ _{tear}$: Stands for normal, shear and tearing stress with respect to crack respectively.

a: Stands for crack length

2.2.3 Energy Release Rate(G)

The energy release rate is another fracture parameter that used to determine the tendency of the crack in a material i.e., whether the crack extended or stationary based on the energy available for the crack growth. It is defined as measure of the energy available for an increment of crack extension and also called as the ***crack driving force or crack extension force***(Anderson, 2005). As the fracture behavior of materials characterized by the fracture toughness using displacement/crack tip stress theory, the energy approach introduced to describe the fracture of materials behavior by using energy release rate parameter. For linear elastic materials, the energy

and the stress field approaches can be considered equivalent and related to each other as follow(Sun & Jin, 2012). The relation between the energy release rate and the stress intensity factor for two dimensional problems in case of plane strain, plane stress and anti-plane shear conditions are stated below(Anderson, 2005).

For Mode-I $$G_I = \frac{{K_I}^2}{E'}$$

For Mode-II $$G_{II} = \frac{{K_{II}}^2}{E'} \quad (2.6)$$

For Mode-III $$G_{III} = \frac{{K_{III}}^2}{2\mu}$$

If all modes of fracture present in a certain loading, the energy release rate related with fracture toughness is stated as follow.

$$G = \frac{{K_I}^2}{E'} + \frac{{K_{II}}^2}{E'} + \frac{{K_{III}}^2}{2\mu} \quad (2.7)$$

$E' = E$ For plane stress

$E' = \frac{E}{1-\upsilon^2}$ For plane strain

$\mu =$ Shear modulus

2.3 Thermoelastic Dynamic Fracture

Thermoelasticity stands for studying the property of elastic bodies under the effect of the non-uniform temperature field(Parkus, 1976). The temperature field influences the elastic property of materials the stress field in the body should also consider the thermal stress developed by the gradient of temperature. The equations for characterizing the material property need to add the temperature-dependent variables. For instance, the constitutive equation i.e., strain and stress add the thermal strain and stress components due to the temperature gradient. Thermoelastic dynamic fracture brings about to study the effect of temperature field develops thermal stress on the propagating preexisted crack moving with the specified crack tip speed(Kanninen & Popelar, 1985).

The material which is subjected to both the thermal and mechanical load under the propagating crack is governed by the mechanical and thermal governing equations. For propagating crack, the equation of motion is utilized instead of the equilibrium equation due to the motion of the crack tip. For thermal load condition assuming the steady-state heat conduction with no heat source i.e., neglecting the heat generated during crack propagation by plastic deformation.

For two-dimensional rectangular thermo-mechanical problem on the preexisted crack under plane strain condition with negligible body force governed by: -

1. Equilibrium Equation

For the static equilibrium condition, the governing equation for the thermo-elastic problem is depicted below(Parkus, 1976).

$$\frac{\partial \sigma_{xx}}{\partial x} + \frac{\partial \tau_{xy}}{\partial y} = 0$$
$$\frac{\partial \sigma_{yy}}{\partial y} + \frac{\partial \tau_{xy}}{\partial x} = 0 \tag{2.8}$$

2. Heat Equation

The temperature change incorporated in the problem tends to change in the temperature field in the medium of the problem as well as in the crack tip. Under the steady-state with no heat generation in the flat plate, the governing equation for the two-dimensional problem can be: -

$$\frac{\partial}{\partial x}\left(k\frac{\partial T}{\partial x}\right) + \frac{\partial}{\partial y}\left(k\frac{\partial T}{\partial y}\right) = 0 \tag{2.9}$$

Since the temperature gradient in material results in material property changes. But, in this case, the property k assumed constant in a small region around the crack tip. so, the equation (2.12) can be written as: -

$$\frac{\partial^2 T}{\partial x^2} + \frac{\partial^2 T}{\partial y^2} = 0 \tag{2.10}$$

The temperature change creates thermal strain and stress in addition to mechanical stress. So, the total strain and stress are the sum of both the thermal and mechanical strain and stress respectively.

$$\varepsilon_{ij}^{tot} = \varepsilon_{ij}^{thermal} + \varepsilon_{ij}^{stress}$$
$$\sigma_{ij}^{tot} = \sigma_{ij}^{thermal} + \sigma_{ij}^{stress} \tag{2.11}$$
$$i, j = x, y, z$$

The thermal strain is written as: -

$$\varepsilon_{ij}^{thermal} = \alpha \Delta T \tag{2.12}$$

From the generalized Hook's law, the constitutive equation in terms of stress depicted for 2D plane strain condition demonstrated as: -

$$\sigma_{xx} = 2G\left(\varepsilon_{xx} + \frac{v}{1-2v}(\varepsilon_{xx} + \varepsilon_{yy}) - \frac{1+v}{1-2v}\alpha\Delta T\right)$$
$$\sigma_{yy} = 2G\left(\varepsilon_{yy} + \frac{v}{1-2v}(\varepsilon_{yy} + \varepsilon_{xx}) - \frac{1+v}{1-2v}\alpha\Delta T\right) \tag{2.13}$$

$$\tau_{xy} = 2G\varepsilon_{xy}$$

$$\sigma_{zz} = v(\sigma_{xx} + \sigma_{yy})$$

2.4 Scholar Works Related to Different Methods

2.4.1 Numerical Modeling

The effect of thermal and the combined thermo-mechanical influence on the crack propagation on elastic materials was investigated by different models. This thermo-mechanical analysis is a vital area in the real-world application for instance in an engine, nuclear plants, fuel cells, etc. The constraints on simulation of the thermo-mechanical failure modeling generate the synergy of the Mesh Free Method and (XFEM) to utilize the combined advantage of modeling with accuracy and efficiency in node distribution and for the asymptotic approximation of fields respectively which is called the eXtended Element Free Galerkin (XEFG) method introduced by (Bouhala et al., 2012) to model the crack propagation. They enhance the accuracy and better simulation by the partition of unity principle. Develops the shape function in mesh free method by Moving Least Squares (MLS). The direction of the propagation of the crack growth is known by proceeding to calculate the stress intensity factor (SIF) by interaction energy integral after that assumption held by the crack tends to propagate in the maximum shear stress. After all, by utilizing the boundary condition of the static crack by adiabatic and isothermal, the influence of different loading conditions was validated with the published literature with a different modeling tool. The temperature change in the 2D model of the plate affects the stress intensity factor i.e., lowers the fracture toughness of the material.

The need for predicting the fracture mechanics of a problem and propagation of crack without introducing the conforming mesh numerical methods chosen. One of the methods is Boundary Element Method. But recently much attention was given to XFEM since the end of millennia. Thus, (Duflot, 2008) introduced the XFEM for thermoelastic fracture problems by the formulation of the problem in which the crack is subjected to different thermal loadings. The XFEM is selected for this paper due to its representation of the discontinuous temperature, heat flux, traction across the crack surface, displacement and also singular heat flux and stress at the crack front. As a result, in a different configuration of the crack and geometry of the 2D model, the modified SIFs concluded as it is independent of the domain of the path in the crack front. Besides, the results from the different orientations of crack (edge, center, inclined and arc-shaped), the calculated modified SIF is closely agreed with other methods (i.e., Dual Boundary Element Method) and

papers in considering the crack either adiabatic or isothermal. So, the proposed method to simulate and calculate the SIF is recommended for similar works.

With the need for better simulation and accurate results, different methods developed. Due to the drawbacks of the finite element method and boundary element methods of modeling the crack problems of conformal mesh, remeshing and crack tip singular element, (Yadav et al., 2020) uses extended isogeometric analysis (XIGA) for analysis of the thermo-mechanical loading on elastic materials incorporated with cracks. The method needs the combined configuration of CAD isogeometric analysis for correcting the errors to arise in different basis functions for defining the geometry and solution. The normal and modified (normalized) SIFs extracted by modified domain-based interaction integral approach for different loading in an adiabatic and isothermal crack. The result using the XIGA method agrees with other methods from the literature. The result showed due to the thermal loading in conjugate with the mechanical loading, the stress intensity factor increased this become the material to become a vulnerable influence due to thermomechanical loading compared with each of the loadings.

(Grégoire *et al*., 2007) proposes the methodology to assess dynamic crack propagation under mixed-mode crack propagation. Due to the challenges to control the loading condition, the exact position of the crack location and variation of propagation parameters in dynamic mixed mode loading condition by experiment unlike quasi-static condition, numerical simulation was performed to assess by comparing with the experimental results. XFEM simulation is utilized for numerical validation of the experimental works because the crack is not described explicitly by mesh besides as Réthoré et al. (2005) proofed and verify among any other numerical tools it does not pose or waste energy numerically during crack growth. The parameters evaluated from the experimental work i.e., the input velocity for striker bar, were utilized for input in the numerical investigation for the sake of determining the dynamic crack initiation and propagation stress intensity factor.

(Nguyen et al., 2017) studies about thermoelastic fracture problems in which the body is under thermomechanical loading. They compare the recently developed numerical tool of the extended consecutive 4-node quadrilateral element (XCQ4) with other tools XFEM XQ4 element, XEFG and meshfree tools for dynamic and quasi-static thermoelastic fracture mechanics. The method works with the principle of based on consecutive interpolation approach which enables the derivatives and trial solutions to continuous across the boundary of the element since nodal gradients enhanced in finite element interpolation as well as the neighborhood nodes are

considered in the interpolation whereas the standard FEM and its extension are nonphysical discontinuous across the nodes which affect the accuracy and requires treatment. Due to the existence of discontinuity such as crack and flaws the enrichment functions incorporated in CIP to form XCQ4 element. To simulate the crack tip enrichment function jump Heaviside function is not enough it only simulates the crack surface. So, crack tip simulated in conjugate with Ramp function which has the advantage of less DOF and only one Ramp function enriches the crack tip not like in XFEM needs four enrichment function. In this study, in quasi-static thermomechanical loading, the SIF is the fracture parameter to characterize the crack growth and fracture property. Besides, in dynamic thermomechanical loading, the inertia effect is considered and the fracture parameter is DSIF which is determined by interaction integral. The maximum hoop stress criterion is also utilized to determine the crack growth in thermoelastic fracture problems. So, this approach is needed to show the crack growth in dynamic and quasistatic cases of rectangular, square, cruciform bodies under edge, center and curved crack subjected to thermal, mechanical and thermomechanical loading. Generally, the fracture parameters are in close accuracy with other approaches such as the XFEM, meshfree and XEFG methods with different orientations and geometry of crack. Also, the crack growth in the cruciform plate under thermal, mechanical and thermo-mechanical loading is different this is because of the loading type.

Another approach utilized by (Kumar *et al*., 2016) is to model the dynamic crack under the step and blast loading considering stationary and moving crack under constant velocity on the linear homogeneous and bi-materials. The numerical approach proposed in the study is three different enrichment functions/schemes with XFEM. These are the Heaviside function, Heaviside function with linear ramp function and Heaviside function along with cubic ramp function to model the crack tip parameters. While the XFEM tip enrichment scheme is very popular in fracture mechanics but the Heaviside function along with cubic ramp function is advantageous because it reduces the DOF at crack tip node i.e., eight DOF is required in the XFEM tip enrichment scheme whereas the latter one utilizes two DOF to model the crack tip nodes which leads to computationally more effective than the former one. Among them, the last scheme is the more accurate and better result is overcome compared with the analytical results as expressed in the case of stationary crack under step loading. Also, for time integration to construct the DSIFs and dynamic response the Newmark Time Integration Scheme is adopted since it is broadly used in fracture mechanics. Generally, the number of nodes affects the DSIFs but when it is large, it converges to the analytical and asymptotic results. And also, when the loading increases the

dynamic response that is the stress intensity factor also increases but in the case of blast loading the rate of increment is slower than that of step loading.

The need for better accuracy in numerical results initiates a proposal of an investigation of a new methodology to capture the true phenomenon of the fracture parameters in different loading. Bearing in mind this, (Chen *et al*., 2016) presents the behavior of crack growth and stress intensity factors of linear homogeneous isotropic material under thermo-mechanical load on two-dimensional thermoelastic fracture problems by using the modified finite element method. Since thermal or mechanical stresses are singular at the crack tip and to model them singular elements are employed. But the standard FEM has drawbacks of overly stiff phenomena and distorted mesh that affects the stress accuracy and SIFs. So, they have used the edge-based smoothed finite element method (ES-FEM) among other classifications of SFEM because it has good convergence, stability, high accuracy and applied for mechanics problems that utilize strain smoothing technique. This tool also advanced to singular ES-FEM for ordering of singularity by the addition of enrichment terms for the application of thermo-elastic fracture problems. The concept of this approach is the same with FEM, but soothing is held by connecting the centroid of the linear triangular element with that of the endpoints of the element. The temperature and displacement are smoothed by the same approach called the gradient smoothing technique. The singularity of the stress field in the vicinity of the crack tip is modeled by employing an additional node on the crack tip element edges between the two endpoints results in a layer of five-node crack tip element which enables to have accurate stress fields around the crack tip. Generally, the singular ES-FEM method employed for simulating the thermal, mechanical also thermo-mechanical loading for cracked fracture problems agrees with any other methods like standard XFEM and XFGM in case of crack growth direction, SIF in different incline crack angle orientation as well as crack length. In comparison with the FEM and ES-FEM, the method is more accurate and better convergence rate to determine the thermal SIFs.

(Pant *et al*., 2010) also used the element-free Galerkin method (EFGM) to simulate the thermo-elastic fracture problems on isotropic homogeneous and bi-materials. The investigation is needed because of the catastrophic failure that occurs in combustion chambers, engines and turbines due to thermal loading leads the propagation of the crack. Under all different numerical methods are involved to solve such methods like FEM, meshless method and XFEM. However, the EFGM method can model the crack by intrinsic enrichment, extrinsic enrichment and smoothing technique. But, the XFEM method models the crack by extrinsic enrichment. So, the intrinsic

enrichment in the paper is due to its simplicity in coding but the extrinsic enrichment approach is efficient than the currently utilized approach. The M-integral is modified to extract the mixed-mode stress intensity factor for the thermoelastic fracture problems. After all, the numerical simulation is held on the center, inclined and edge cracked 2D models by considering adiabatic and isothermal crack. After all the extracted normalized stress intensities by EFGM has a good agreement with the literature that uses FEM, analytical/numerical methods. This leads to the capability of EFGM applicable for real-life fracture problems.

(Menouillard *et al.*, 2010) proposed a new enrichment method based on the time function for stationary and moving crack propagation. Due to the limitation of the classical FEM, they propose a time-dependent XFEM method to model the crack tip by utilizing different enrichment functions i.e., Heaviside function for discontinuous crack surface and time-dependent crack tip enrichment displacement function. They employed also Kalthoff's experiment to validate the numerical result and analytical method. The stress intensity factors for crack propagation are determined based on the interaction integral and utilizing near crack tip auxiliary fields. Singular, quadratic and Heaviside enrichment on the crack tip is applied to verify the accuracy of the functions on the crack tip element and surrounding elements around the crack tip. As a result, the same type of curve to time vs normalized SIF is observed in both moving and stationary cracks. But, the singular enrichment at the crack tip gives a more agreed result with the analytical solution compared to the quadratic enrichment. The error is large for the case of utilizing the Heaviside enrichment function for both moving and stationary crack. Like the above paper, the SIF in moving crack observed as oscillates this is because the crack tip jumps in the elements perhaps differ from the graph of an analytical solution but the difference is significant up to 20%. The oscillation can be decreased by the utilization of enlarging enrichment elements in the zone of the crack tip.

(Liu et al., 2004) presented the utilization of the extended finite element method (XFEM) for determining the mixed-mode stress intensity factor for the homogeneous, isotropic materials and bi-materials by advancing the method to mixed mode fracture by enriching the crack face and crack tip using the enrichment function. The numerical integration for displacement fields in the utilized for elements cut by the crack is by seven order Gauss quadrature while for the element of crack tip DECUHR adaptive quadrature package is used. For better accuracy more layers of enrichment elements at the crack tip reduced the error by less than 10%. It is concluded that the better the approximation of the crack surface and tip the more the accuracy of the result can achieve. So, the XFEM presented in this paper enhances for determination of not only the mode I

SIF but also the mixed-mode extraction of the SIFs and its result better accuracy with the analytical calculation of the SIFs ($K_I = \sigma\sqrt{\pi a}\, co\ ^2(\beta), K_{II} = \sigma\sqrt{\pi a}\, cos(\beta)sin(\beta)$) and another numerical method called boundary element method.

(Gracie *et al*., 2010) focuses on the application of the XFEM method for thermoelastic fracture mechanics for the determination of the stress intensity factor accurately. The enrichment in the vicinity of the crack face and tip adds the temperature field in addition to the displacement enrichment function. They develop the method of extracting the SIFs from the first-order asymptotic term for all nodes of a crack tip by high order asymptotic terms in the crack tip for the thermoelastic problems. This enhances better accuracy and benefits for such thermoelastic fracture problems compared with elastic and heat transfer problems individually. The extraction of the SIFs directly from the enriched nodes by XFEM and by interaction method is compared for a straight and curved crack for elastic and thermoelastic problems. For reducing the error on the convergency result the crack surface and crack tip elements are integrated with the standard Gauss quadrature, 4th order direct Gauss quadrature formula and 15th order bidirectional Gauss quadrature utilized for the elements non-enriched, enriched by branch function (elements cut by crack) and the crack tip elements respectively for removing the ill-conditioning. However, the high order enrichment terms with the interaction integral overcome the better result of SIFs compared to literature for the thermoelastic fracture problem and also from the direct extraction from the XFEM also, instead of the accuracy. The high order terms for $1 \leq M \leq 7$ errors decrease with interaction integral monotonically for both temperature and displacement enrichment fields.

2.4.2 Analytical Modeling

Considering influences on the crack propagation in fracture mechanics, different parameters considered studying the effect on the fracture property of materials. (Kidane *et al.,* 2010) develop the mathematical modeling of the stress field in FGM materials around crack tips considering thermal and mechanical loading. The uniqueness of the modeling from (Parameswaran & Shukla, 1999) is it incorporates the thermal stress effects due to temperature. But the methodology followed to develop the stress fields in different modes of fracture is the same. They introduce the thermo-mechanical stress field from the theory of steady-state heat transfer principle by first developing the temperature field around the crack tip using the asymptotic approach since the temperature at crack-tip couldn't singular. The displacement potentials utilized for finding the displacement and strain around the crack-tip. By substituting the displacement potentials and temperature field equation on the elastic stress field equation, finally, the thermo-mechanical stress

field equation was established. However, parameters in the field equation tend to vary the normal phenomenon of the fracture parameters. For instance, the temperature variation has an effect on the crack direction, strain energy, stress components and stress field in the crack tip. Besides, the crack speed tends to vary the crack direction angle. The stiffness index(non-homogeneity), as in the index affects the mechanical stress field showed in (Parameswaran & Shukla, 1999) in FGM, also has an effect on the fracture parameters in thermomechanical loading based on the analytical work of the scholars.

(Abotula *et al.,* 2012) develops the thermomechanical stress field equation in the vicinity of the curved crack for varying of the material properties such as shear modulus, density, coefficient of thermal expansion and thermal conductivity exponentially in the direction of gradation by considering Young's Modulus and Poisson's ratio constant and the material assumed as continuum i.e., at a point the property is isotropic. The investigation held because of a lack of the development of the thermo-mechanical stress field equation on the dynamically propagated curved crack. This was succeeded by using the asymptotic equation for developing the temperature field equation, displacement equation by using displacement potentials later on the thermomechanical stress equation has been developed from the displacement and temperature field equation. Generally, the stress fields are highly affected by the inhomogeneity parameters, temperature, and velocity of a crack tip as well as curvature of the crack seam.

Similar work also held for developing the thermomechanical stress field and displacement field on the propagating crack in FGM materials using asymptotic analysis and displacement potentials by considering the exponential variation of mass density, shear modulus, coefficient of thermal expansion by (Lee *et al*., 2008). And also, the heat flux and temperature distribution fields are derived by considering exponential thermal conductivity gradient. It is unique by displaying the stress field by developing the isochromatic contours to show the phenomenon of the crack tip fields in mode I and mixed-mode of thermomechanical loading conditions under heating and no heating. The contour change observed from the isochromatic fringes for instance the fringes large and tilt to crack face in the case of heating mode I load condition in decreasing material property head of crack tip the reverse is true for increasing material gradient. In mixed mode also in decreasing material gradient the stress intensity increases in the third quadrant whereas it decreases in the first quadrant. It also reverses the case of increasing material gradient at the end of the crack tip.

A similar approach was attended also for homogeneous isotropic materials like the above. Due to the shortcoming of using a closed-form solution for extracting the stress intensity factor or

fracture parameters from the experimental stress or deformation field, another methodology is needed for filling the gap. Therefore, (Kidane *et al.*, 2010) introduced an asymptotic approach to finding out the displacement potentials and temperature field equation at the crack tip for the input of the general thermo-mechanical stress field equation under a constant velocity propagating crack. To model the analysis the Hook's law, equation of motion and steady-state heat transfer equations were utilized for simulating the stress field around the crack tip analytically. After all, the temperature field around the crack tip generated by crack propagation is assumed to be neglected, the temperature change affects the in-plane stress components (σ_{xx}, σ_{yy} and τ_{xy}), crack direction, maximum hoop stress, maximum shear stress and principal stress around the tip of the crack. And they compare the direction of crack growth by the Minimum Strain Energy Density (MSED) criterion and Maximum Circumferential Stress (MCS) criterion under different varied parameters.

The requirement of functionally or structurally combined with metallic materials for application electronics, electro energy of ceramics materials subjected to thermomechanical loads under the interfacial crack is analyzed by (Boutabout *et al*., 2009) to understand the superimposed effect of thermal and mechanical loading on the crack propagation and initiation. The research is held because of the limitation on understanding on the study of the brittle/ductile interfacial toughness. So, due to the difference or mismatch between the thermal property of the ductile and brittle material (i.e., copper and alumina in case of this work), residual stress occurred at the interface. The residual stress and the applied stress effect on the interfacial crack were studied. The internal stress developed due to the mismatch of material property results in different residual stresses under a homogeneous temperature gradient. Whatever the temperature gradient the stress at the vicinity of the crack tip maximizes, maximum compressive residual stress in transversal (σ_{yy}) and tangent (τ_{xy}) to crack tip whereas tensile residual stress in the normal direction to crack tip (σ_{xx}) but their magnitude is different. Generally, different loading has their own influence on the crack growth behavior of the j-integral. This effect is analyzed by the finite element method. The J-integral increase with temperature gradient increase in parallel with crack length linearly. Also, vary increasingly with the applied load in the form of an exponential curve with crack length increment however it rapidly changes its curve when the load reaches more than 100N. Under thermomechanical load, the J-integral has increased with temperature gradient with the form of parabolic form at small fixed crack length but it changes its phenomenon when the crack length increased and also has the form of increase exponentially after the load reaches 180N while till to

it parabolic. At fixed temperature gradient the j-integral has a form of increase exponentially with large crack length.

2.5 Numerical Methods

Different approaches are utilized for simulating and analyzing engineering problems. These methods are following the analytical derivations and integrations that are derived from the pillar theoretical equation i.e., Hooks law, equation of motion, constitutive matrixes, and so forth. The fracture problems are analyzed through different theories and numerically by different approaches. Some of the numerical methods used to solve are described hereafter and the selection of the method for this work is justified in basement literature.

2.5.1 Finite Element Method

The finite element numerical tool is utilized for solving complex engineering problems by discretizing the partial differential equations converging to an approximation solution. It is the most popular numerical tool to solve problems. FEM was developed for carrying out in civil engineering for structural analysis utilizing triangular elements. Later on, the development has grown to solve problems in plate and shell elements for plane stress analysis. This extension of usage emerges to utilizing it in three-dimensional problems by developing elements like tetrahedral elements, however, it also developed to carry out analysis in plasticity, biomechanics, and structural analysis, etc. Nevertheless, on the side of the development to cover any other problems also the difficulties happen in solving the problems of damage, penetration and fracture(Ai, 2018). To alleviate this problem different modeling methods evolved basing FEM for instance BEM which utilizes different interpolation and approximation methods.

The tool is cumbersome when applied to fracture mechanics. Since the discontinuities, the interfaces, the cracks and so on, the engineering problems need another tool since it models the problem by smooth polynomial approximation which is an inadequate approximation characteristic. And FEM is ill-conditioned in representing and modeling problems with discontinuity, interfaces, boundary layers and singularities(Khoei, 2015). So, modeling crack growth is difficult since remeshing is needed to conform to the phenomenon of the crack surface in FEM(Khoei, 2015). Even if the usage of high order polynomial function as interpolation function raises the error i.e., the convergence rate cannot improve and utilization elements in the crack tip by fining the mesh also the same(Liu *et al.*, 2004). For the crack growth and propagation phenomena, re-meshing is needed throughout the time step and it is tedious and time-consuming. Hence, in the case of analyzing the crack in FEM, the cracks aligned with the elements conforming,

and the singular meshing around the crack tip is necessarily. As a result, the crack growth dependent on the mesh. All in all, the finite element method and boundary element method has advantage and also drawbacks on the analysis of fracture problems which incorporates the crack that needs to have the singular element at the crack tip, conformal mesh and remeshing to simulate crack propagation(Yadav et al., 2020).

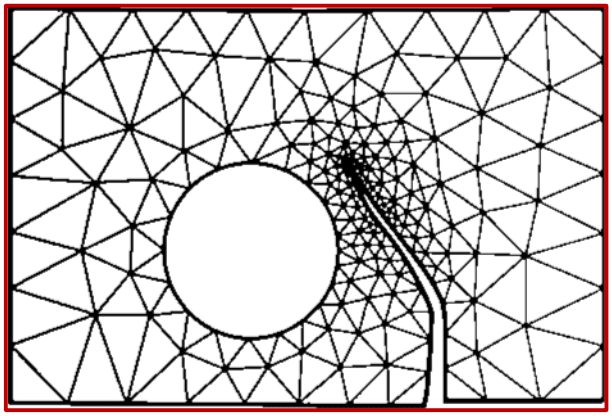

Figure 2-3. Standard FEM the mesh conforms to the geometry of the discontinuities. Source: (Khoei, 2015)

2.5.2 Extended Finite Element (XFEM)

The technique was presented in late 1999 by Belytschko and Black(Bordas & Duflot, 2007). It empowers the exact solution of BVPs with discontinuities and singularities openly found inside elements of the discretization(Fries, 2018). Also, it is an expansion of the standard finite element method for approximating the results of a problem by the classical way of discretizing a problem and finding the sum solution for all nodes and elements. The difference is by incorporating additional shape function for the discontinuities by using partition of unity concept. The method is applicable for solving problems in different circumstances for instance in fracture mechanics, composite materials, phase transition, fluid-structure interaction, fluid mechanics, etc. It is also applicable for fatigue crack propagation by ABAQUS software with a restricted protocol that needs another development investigation(Duan *et al*., 2020). The method is also more powerful and robust than other developed techniques such as the extended isogeometric method, meshless method and phantom node technique in accuracy and efficiency for capturing as well as simulating the fracture problems like crack propagation(Goli *et al*., 2014). Generally, its working principle is based on the standard FEM framework but accounts for the existence of the discontinuity on the body and the remeshing is continuous to permit the propagation of the crack by allowing special displacement function using the level set method to track the crack propagation(Duan *et al*., 2020).

In fracture mechanics, it is used to simulate accurately the fracture problems incorporated with the discontinuities and cracks rather than classical FEM especially for crack growth and propagation and primarily developed for it. The key feature in the eXtended Finite Element Method is the partition unity, which allows the introduction of a non-polynomial function to finite elements in a domain for approximation. The method enables to model the interfaces in static as well as dynamic discontinuities for different problems such as rock mechanics, fatigue, tool machining, hydraulic fracturing, delamination in composites, fragmentation and reinforced concrete(Moës *et al*., 2017).

Some of the benefits of XFEM as compared with FEM is (Goli *et al*., 2014):-

- Reproducing the singular field near a crack tip
- Avoiding expensive remeshing procedures
- Extraordinary flexibility for crack propagation problems
- Simple formulation and independent definition of crack

In the XFEM method, the crack growth and the crack propagation are independent of mesh i.e., the crack can also propagate along with the elements not conform to the element edges as in FEM see Figure 2:4. This discontinuity in elements makes the nodes and elements enriched with additional DOFs and enrichment function which uses the same formulation as FEM but additional terminologies included due to the separation.

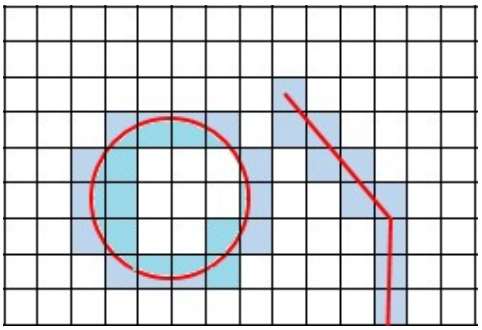

Figure 2-4. XFEM method the elements cut by discontinuity and enriched. Source: (Khoei, 2015)

The displacement field generally can be written as the sum of the standard approximation field variable and the added enrichment function expressed explicitly as follow(Fries, 2018).

$$u(x) = \sum_{i=1}^{N} N_i(x)u_i + added\ terms \tag{2.14}$$

The former approximation function stands for standard finite element approximation after equivalent. The $N_i(x)$ denotes the standard FE interpolation or shape functions stands for capturing

the smooth part of $u(x)$. $u(x)$ is the field variable it may be vector stands for displacement, velocity, etc. u_i stands for the standard degree of freedom. N stands for the total number of nodes in the discretized model.

2.5.3 Enrichment Function

For two-dimensional fracture problems, there are two enrichment functions used to model the fracture behavior of the material cut by the preexisting crack.

2.5.3.1 The Heaviside Enrichment Function

The added term in the above equation is due to discontinuity. The discontinuity can be strong and weak. The crack in a body is considered a strong discontinuity because of the jump from the interpolation function from one side of the node to the other. The added terms can be assigned by the crack tip enrichment and Heaviside enrichment from the crack interface function as described below in Figure 2-5. The Heaviside enrichment function is applied for the elements which are completely cut by the crack. Therefore, the element splitting results in jump or discontinuity in the displacement or temperature field and the enrichment function which is the Heaviside function provided to model such characteristics using a mathematical approach.

Let consider the two-dimensional deformable-body Ω includes the continuous curve Γ that specifies the crack domain within the boundary as shown below.

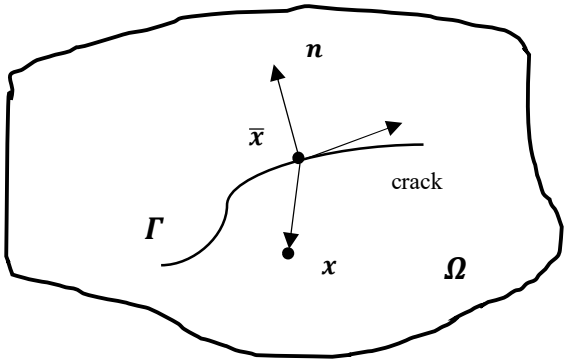

Figure 2-5. The Heaviside enrichment function representation

The point $\boldsymbol{x}(x, y)$ represent an arbitrary point in the deformable body and $\bar{\boldsymbol{x}}(x, y)$ is the nearest point on the crack curve which closes to $\boldsymbol{x}(x, y)$ and the direction $\boldsymbol{n}$ represents the normal vector along the path Γ at point $\bar{\boldsymbol{x}}(x, y)$. Therefore the Heaviside function is used to represent the location of an arbitrary point $\boldsymbol{x}(x, y)$ concerning the location of crack defined as: -

$$\mathrm{H(x,y)} = \begin{cases} 1 \text{ for } (\mathbf{x} - \bar{\mathbf{x}}).\mathbf{n} > 0 \\ -1 \text{ for } (\mathbf{x} - \bar{\mathbf{x}}).\mathbf{n} < 0 \end{cases} \tag{2.15}$$

The function includes acknowledging the discontinuity that arises along the crack face.

2.5.3.2 Asymptotic Crack Tip Enrichment Function

The Heaviside function is not enough to enrich the crack domain at all since the crack tip may not align on the element edge so another enrichment function is needed to represent the elements that hold the crack tip called the crack tip enrichment function. This function was first introduced by Fleming later used by others to formulate the XFEM and the function contains four-function to describe the displacement field in the crack tip(Bostanci, 2019). This four-function may differ based on the type of problems for instance for thermomechanical loading, to represent the temperature field the function of enrichment for crack tip differ from the displacement field function.

The function has been utilized for the fracture problem and also for the XFEM formulation. The functions are used to represent the crack tip displacement field in the polar coordinate base from the tip. This function also represents the asymptotic strain and stress fields at the vicinity of crack tip leads to specify the stress intensity factors and are utilized for the improvement of the accuracy of the SIFs but not all functions. For instance, the leading term in Equation (2.16 is used to define discontinuity over the vicinity of the crack tip since it is discontinuous over the crack face. Whereas the rest terms are utilized for the surrounding of the crack tip only to advance the approximation solution of the finite element and the SIFs(Sepehri, 2014). The branch function for tip enrichment domains the elements in which the crack tip laid or may cover the surrounding elements to enrich the connected nodes. This enrichment method is utilized for convergence of the analysis and accuracy.

These enrichment methods are called the geometrical or topological enrichments, shown in Figure 2-6. In geometrical enrichment, the nodes accommodated by a subdomain around the vicinity of the crack tip are enriched. The method leads to having a large more degree of freedom of nodes in a model that can cause ill-conditioning in stiffness matrix and may have an accurate result whereas in topological enrichment the nodes only on the crack tip element are enriched and the added DOF on the element is lesser than the former and leads convergence. This leads to a conclusion the topological enrichment is preferable(Esmati *et al*., 2018).

Generally,

The XFEM approximation function for the displacement field that combines the FEM and enrichment functions is(Khoei, 2015)

$$u(x) = \sum_{i=1}^{N} N_i(x)u_i + \sum_{j=1}^{N_1} N_j(x)H(x)b_j + \sum_{j=1}^{N_{tip}} N_j(x)\left(\sum_{k=1}^{4} R_k\, a_j^k\right) \quad (2.16)$$

Where $H(x)$ stands for the Heaviside function that assigns the value of +1 and -1 for the nodes in either side of the crack interface correspondingly. It stands for the enrichment of the nodes that are cut by the crack surface. N_1 is denotes the sets of nodes belongs to the elements intersect by crack totally and N_{tip} is also stands for the set of nodes that belongs to elements that contained the vicinity of the crack tip. b_j and a_j^k are the additional degree of freedoms nodal enriched unknowns due to the crack and R_k are components of the crack-tip asymptotic enrichments functions based on Westergaard's crack tip displacement solution(Sheng, 2018), $\boldsymbol{R}$ as:

$$\boldsymbol{R}(r,\theta) = \left[\sqrt{r}\,sin\frac{\theta}{2}, \sqrt{r}\,cos\frac{\theta}{2}, \sqrt{r}\,sin\theta\,sin\frac{\theta}{2}, \sqrt{r}\,sin\theta\,cos\frac{\theta}{2}\right] \quad (2.17)$$

Where r and θ are the relative polar coordinates at the crack tip. The function represents elements in which the crack tip resembles or for all nodes in radius at the crack tip.

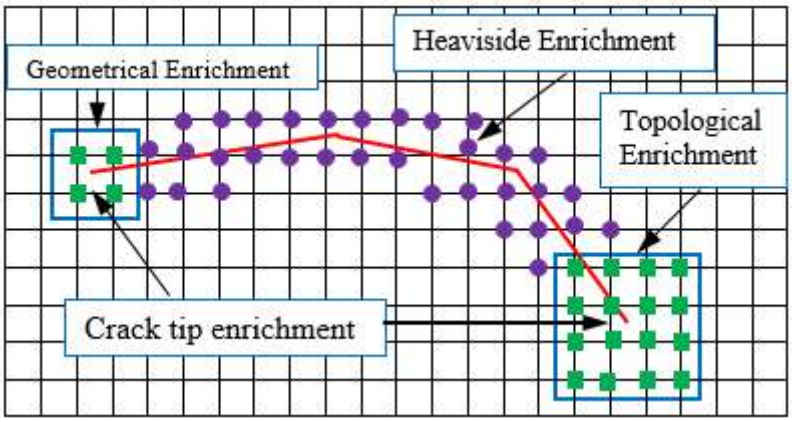

Figure 2-6. The enriched nodes of structured mesh with the crack interface discontinuity. Source: (Sepehri, 2014)

The same field equation is also applicable for the temperature field except for the crack tip asymptotic branch function. In the temperature field function, the former branch function is utilized. But, for the temperature solution, only one singular term is utilized for both the isothermal or adiabatic cracks so the asymptotic function is one to represent the singularity terms(Bouhala et al., 2012). Therefore the temperature field equation became except the tip enrichment function with only the second branch function for adiabatic crack because the temperature along the crack is discontinuous whereas the heat flux is continuous with zero flux(Duflot, 2008):-

$$T(x) = \sum_{i=1}^{N} N_i(x)T_i + \sum_{j=1}^{N_1} N_j(x)H(x)b_j + \sum_{j=1}^{N_{tip}} N_j(x)\left(\sum_{k=1}^{4} R_k\, a_j^k\right) \tag{2.18}$$

The branch function for adiabatic crack is: -

$$\boldsymbol{R}(r,\theta) = \left[\sqrt{r}\, sin\frac{\theta}{2}\right] \tag{2.19}$$

For the adiabatic crack case, like displacement field, the temperature field is discontinuous across the crack face while the heat flux is singular at the front side of the crack tip with the singularity of $1/\sqrt{r}$ same as mechanical loading where the r indicates the distance from the crack tip. For adiabatic crack i.e., thermally insulated crack the temperature and heat flux field distribution across the crack is given as (Duflot, 2008).

$$T = -\frac{K_T}{k}\sqrt{\frac{2r}{\pi}}sin\left(\frac{\theta}{2}\right) \tag{2.20}$$

$$q = \frac{K_T}{\sqrt{2\pi r}}\begin{pmatrix} -sin\left(\frac{\theta}{2}\right) \\ cos\left(\frac{\theta}{2}\right) \end{pmatrix} \tag{2.21}$$

To model the isothermal crack, the continuous function with the discontinuous derivative temperature field equation is utilized to model its continuity of the prescribed temperature on the crack face and also its discontinuous heat flux along the crack face. That means the crack is thermally conductive with the prescribed temperature value. Therefore, the temperature boundary condition is defined in the crack surface. The tip enrichment function for modeling the crack tip for the case of isothermal crack utilized as (Duflot, 2008) depicted as:-

$$\boldsymbol{R}(r,\theta) = \left[\sqrt{r}\, cos\frac{\theta}{2}\right] \tag{2.22}$$

The jump function called the Heaviside function, $H(x)$ used to represent the discontinuity of the displacement function for the case of the displacement field also utilized in case of representing the temperature field discontinuity in isothermal crack condition.

2.5.4 Numerical Integration

In the classical finite element method, the integration point is used to integrate numerically the equation on the fixed position of an element. Also, the integration function is smooth. But in the case of discontinuity direct utilization of these points is problematic(Bäker *et al.*, 2019). Therefore, a subdivision of the elements into a triangle is needed to conform to the crack face for numerical integration in case of discontinuity because of the discontinuity in the crack face and the singularity

at the crack tip. The integration classification is depending on the type of function in which integration is performed and the type of element on which the integration is performed. In light of this, in fracture problem of a body contained the cracks and incorporates the discontinuity function the standard Gauss quadrature integration scheme couldn't be utilized unless the elements discretized into some sub triangles with the edges on the crack faces and element edges(Zamani & Eslami, 2010) as described below. The non-enriched elements are integrated with the standard Gauss quadrature while the crossed elements and crack tips are enriched with Heaviside and crack tip enrichment function respectively. Therefore, the crack face elements are subdivided with triangles align with the crack line also the crack tip element is also subdivided into triangles making the vertex of the crack tip but the 4th order direct Gauss quadrature formula and 15th order bidirectional Gauss quadrature are utilized respectively and for the crack tip elements the triangles are performed mapped singularly this is because of increases the accuracy of the integration(Gracie *et al*., 2010).

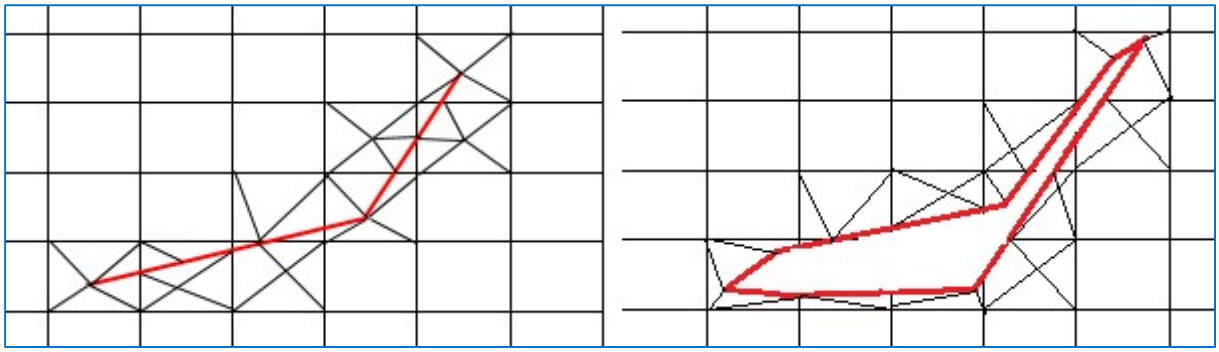

Figure 2-7. Numerical integration in sub triangles on undeformed and deformed elements. Source: (Zamani & Eslami, 2010)

2.5.5 Implementation of XFEM Method in ABAQUS

Abaqus is one of a powerful finite element tool used to offer complete solutions for sophisticated and routine engineering problems which covers a wide spectrum of applications for instance for impact, linear and non-linear problems, thermal loadings, static, dynamic, vibration, etc., It is launched by Dassault Systems which is the product of SIMULIA software tool categorized in structure product of Dassault Systems. Bearing in mind this, the Abaqus software was utilized for fracture analysis to solve the problems related to the initiation and propagation of crack in a body. This can be done using the conventional FEM (contour integral) and another incorporated method of the XFEM method.

However, the innovation of the XFEM method goes back to 1999 as described in the above section therefore the numerical software tools were not incorporate. Nevertheless, many trials and attempts were made over a year to apply the XFEM method in commercial software of FEA and user-created codes(Sepehri, 2014). After a while, the XFEM method included in multi-purpose commercial FEM software the most known software is the LS-DYNA and Abaqus. The XFEM method was incorporated in Abaqus in 2009 when the Dassault system released the 6.9 version of the Abaqus software upholds the basics functions of XFEM(Bostanci, 2019). The method implemented in the software in which the Abaqus working principle is based on the phantom node method. It stands for the interpolation of the field variable(displacement) along with the elements cut by the crack between the real nodes (above crack) and phantom node domain (below crack) and to reproduce or recognizing the discontinuity presence on the element.

In fracture analysis of the cracked body, the surface and tip of the crack location are identified by the numerical procedure of the Level Set Method. In the procedure of the analysis, includes from the part modeling to solution analysis, the discretized element connected by the nodes characterized by the DOF in a global coordinate system and any other additional parameters to characterize the crack is the PSILSM and PHILSM. The parameters are nonzero on the above and below of crack surface and are used to represent the coordinate of enriched node centered at the fracture tip which is normal and tangent to crack surface at the crack tip.

Type of XFEM analysis

The initiation and propagation of the crack in the XFEM method were analyzed by two approaches in Abaqus. These are: -

1. Traction-separation cohesive behavior
2. Linear elastic fracture mechanics (LEFM) based on VCCT

Traction separation cohesive behavior

The Abaqus software by default used the traction separation law to model the crack initiation and propagation of the material using different damage modeling criteria. The principle is based on the constitutive behavior between the relative displacement between two points and the traction. Abaqus allows two different methods in the finite element model. The surface-based and element-based cohesive behavior. The method follows the framework of the surface-based cohesive behavior. The surface-based cohesive behavior is characterized as a surface interaction property and can be utilized to demonstrate the delamination at interfacing specifically by employing a traction - separation constitutive model(Bostanci, 2019). The method utilized for the fracture of brittle and ductile materials.

The initiation of the crack stands for the beginning of the degradation of the cohesive response at the enriched element. The process of deprivation starts when the stresses or the strains fulfill the specified criteria of crack initiation. In Abaqus, the crack initiation is based on the stress and strain relationship. These damage modeling criteria are:

- Maximum principal stress (MAXPS) and strain (MAXPE) criteria

The maximum principal stress and strain criterion are expressed as follows respectively.

$$f = \left\{ \frac{\langle \sigma_{max} \rangle}{\sigma^o_{max}} \right\}$$
$$f = \left\{ \frac{\langle \varepsilon_{max} \rangle}{\varepsilon^o_{max}} \right\} \tag{2.23}$$

σ^o_{max} and ε^o_{max} stands for maximum allowable principal stress and strain respectively. The Macaulay bracket symbol $\langle \quad \rangle$ used to represent that the compressive stress or strain state does not initiate damage and signifies the value to be positive. The initiation of damage is assumed to start when the above stress or strain ratio reaches the value of one.

- Maximum nominal stress (MAXS) and strain (MAXE) criterion

The maximum nominal stress and strain criterion are represented as follows respectively.

$$f = max\left\{ \frac{\langle t_n \rangle}{t^o_n}, \frac{t_s}{t^o_s}, \frac{t_t}{t^o_t} \right\}$$
$$f = max\left\{ \frac{\langle \varepsilon_n \rangle}{\varepsilon^o_n}, \frac{\varepsilon_s}{\varepsilon^o_s}, \frac{\varepsilon_t}{\varepsilon^o_t} \right\} \tag{2.24}$$

In the above equation, t represents the nominal traction stress vector (consists of two in 2D problems otherwise three). t_n and ε_n are normal components of stress and strain of the cracked surface respectively while the t_s, ε_s and t_t, ε_t represents the shear component of stress and strain

respectively on the cracked surface. Damage initiation is assumed to occur when the maximum nominal stress and strain ratio components reach a value of one.

- Quadratic nominal stress (QUADS) and strain (QUADE) criterion

The criterion of the quadratic nominal stress and strain can be expressed as follow.

$$f = \left\{\frac{\langle t_n \rangle}{t_n^o}\right\}^2 + \left\{\frac{t_s}{t_s^o}\right\}^2 + \left\{\frac{t_t}{t_t^o}\right\}^2$$
$$f = \left\{\frac{\langle \varepsilon_n \rangle}{\varepsilon_n^o}\right\}^2 + \left\{\frac{\varepsilon_s}{\varepsilon_s^o}\right\}^2 + \left\{\frac{\varepsilon_t}{\varepsilon_t^o}\right\}^2 \quad (2.25)$$

Initiation of the damage is assumed to start when the quadratic nominal stress and strain ratio in the above expression tends to the value of one(Abaqus manual, 2016).

Linear Elastic Fracture Mechanics (LEFM) based on VCCT

The virtual crack closure technique is based on the presumption that for a very small crack opening, the strain energy released is equivalent to the amount of work required to close the crack. This method is more appropriate for fracture propagation problems in brittle materials. In this method, only the displacement jump function in the cracked element is considered and the fracture has to propagate the entire element at once to avoid the need to model the stress singularity. The strain energy release rate at the fracture tip was calculated based on the modified virtual crack closure technique (VCCT). Using this approach fracture propagation along an arbitrary path can be simulated without the need for to fracture path to be known a priori. The modeling technique is similar to the XFEM-based cohesive segment approach. In this method also phantom nodes are introduced to represent the discontinuity of the enriched elements. The fracture criterion is satisfied when the equivalent strain energy release rate exceeds the critical strain energy rate at the fracture tip in the enriched element(Sepehri, 2014).

2.6 Summary of Literature Review

Main topics related to the thesis objectives are covered and explained in which these thesis work concerns in addition to the related papers done in different methods i.e., analytical, numerical, etc. methods. Even though many works go through a thermomechanical fracture in different analytical and numerical approaches in different boundary thermal conditions, some others focus on considering thermal stress effect on crack growth in addition to mechanical stress simultaneously applied in a two-dimensional model. The majority of the works as seen in the literature show that no papers have to find the thermomechanical loading effect on the crack tip stress using XFEM numerical method to model the crack. Since different literatures such as on

particular applications on pressure vessel numerically and analytically for propagating crack by considering constant crack velocity has done related to thermo mechanical loading but in this case, it considers the simultaneous effect of thermo-mechanical loading numerically on the particular effect of crack tip on stationery crack for different scenarios. This thesis work has got the value of filling the gap of considering sharp cracks introduced into two-dimensional part modeling by varying the mechanical and thermal boundary conditions in different scenario of crack to study the mechanical stress and temperature effect on crack tip stress utilizing a productive mathematical formulation tool that accommodates both the temperature and displacement boundary condition that found in ABAQUS called extended finite element method (XFEM). The method utilized for modeling the crack for stationery crack because the numerical tool allows for static crack by disallowing the XFEM crack growth(Abaqus 6.12, 2016).

Chapter Three
3 Numerical Analysis and Modeling

3.1 Material

The material selected for the research is titanium which represents homogeneous isotropic materials based on the works of (Kidane et al., 2010). And also, this titanium material has same property in all direction at a point. Since the work is an extension of Kidane et al., 2010, titanium is considered (which is the primary interest for their further experimental research) but this paper considers the stationary crack and application of load also static and the temperature input is at boundaries of plate as mentioned in Section 4. Besides, titanium is a metallic material that attracts the researchers and industries focus on it due to its good mechanical property with specific strength, corrosion resistance, stiffness, fracture toughness, ability to withstand low and high temperature, etc. due to its property of excellent specific strength and capability to withstand extreme temperature and good heat transfer capability it is applicable for the aviation and space shuttle technologies(Bathini *et al.*, 2010). The reason for experimental investigation for further study is due to its property mentioned above.

The important material property that becomes an input for the numerical analysis are the elastic properties, thermal properties and fracture material property and physical property i.e., the density of the titanium included. In the next table, the thermal properties are needed because the numerical analysis included the temperature effect and also the analytical solution has been incorporated the terminologies during the equation development for thermomechanical loading in governing equation of the problem i.e., from Fourier law and the steady-state heat equation.

Table 3-1. Room temperature material property of pure Titanium (Ti). Source: (Callister, 2001)

Type of Property	***Parameters***	***Value***
Physical property	Density (ρ)	$4.51\ g/cm^3$
Thermal property	Coefficient of thermal expansion (α)	$8.6 \times 10^{-6}/K$
	Thermal conductivity (K)	$16\ W/m.K$
Mechanical property	Elastic modulus (E)	*103 GPa*
	Shear modulus (G)	*45 GPa*
	Tensile strength (σ_u)	*240 MPa*
	Yield strength (σ_y)	*170 MPa*
	Poisson's ratio (v)	*0.34*
Fracture property	Fracture toughness (K_c)	$[50-60]\ MPa\sqrt{m}$

3.2 Geometrical Modeling

The basement for numerical analysis of the fracture problem is the geometrical model. So, the two-dimensional plane strain condition is considered. Since the verification of the paper compared

with other literature which has been done via plane strain condition. The geometrical modeling for two-dimension is modeled with different orientations of the crack initiation. The crack initiation modeling includes the edge crack, the center crack and the inclined center crack parallel with different mechanical and thermal boundary conditions to accommodate the thermomechanical loading.

The modeling of the geometry is simple and can be specified easily with the numerical analysis software. The part module interface in ABAQUS/CAE software enables to model the two-dimensional features easily by considering the interaction of the crack on the geometry so no other modeling software is used for modeling this simple geometry. The geometry of the model is according to standards using British standard using Single Edge Notched Tension (SENT) specimen established in BS 8571 catalog while in ASTM standard this type of material specimen is not specified. The recommended dimension of the material is taken based on(Zhu, 2016) because the standard recommendation dimensions existed on the paper. The dimension of a material taken based on: -

$$\begin{gathered} {}^{1}/_{2} \leq {}^{B}/_{W} \leq 2 \\ H = 10W \\ {}^{a}/_{W} = 0.2 \; to \; 0.5 \end{gathered} \tag{3.1}$$

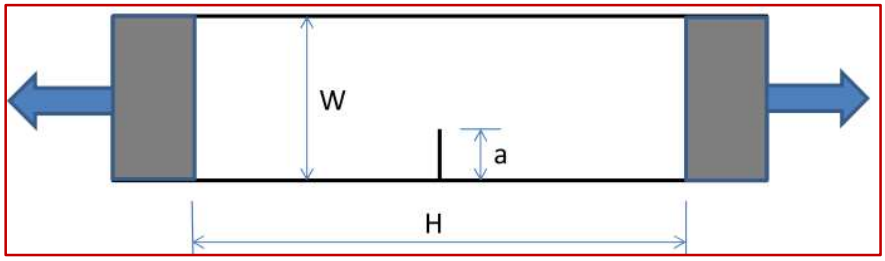

Figure 3-1. Schematic diagram of the single edge notched tension specimen

The dimension of this material specimen utilized for simulation doubled to its width w to $2w$ and its crack length a to $2a$ for using through center crack but their correction factor is different analytically. But more accurate solutions for a through crack in a finite plate have been obtained from finite-element analysis as compared to closed-form solution(Anderson, 1995), the finite element analysis method accommodates this correction factor and no input inserted in finite element software tools to accommodate it.

The limit load capacity of the material model according to the expression of (Anderson, 2005) is depicted below for the different types of specimen for plane strain condition and the applied stress is based on the calculation below.

For the middle tension (MT) panel

$$P_L = \frac{4}{\sqrt{3}} Bb\sigma_Y \tag{3.2}$$

For single edge notched tension (SENT) specimen

$$P_L = 1.455\eta Bb\sigma_Y \tag{3.3}$$

Where:

η is non-dimensional constant

$$\eta = \sqrt{1 + \left(\frac{a}{b}\right)^2} - \frac{a}{b} \tag{3.4}$$

b is ligament size

$$b = W - a \tag{3.5}$$

σ_Y is average of yield strength and ultimate strength

$$\sigma_y = \frac{\sigma_{ys} + \sigma_{us}}{2} \tag{3.6}$$

3.3 Justification on Plane Strain Condition

In this section the reason of using the plane strain condition and its justification explained graphically authenticate with the theoretical plastic zone shape by comparing the plane stress and plane strain plastic zone by modeling the plate and input the value of fracture parameters.

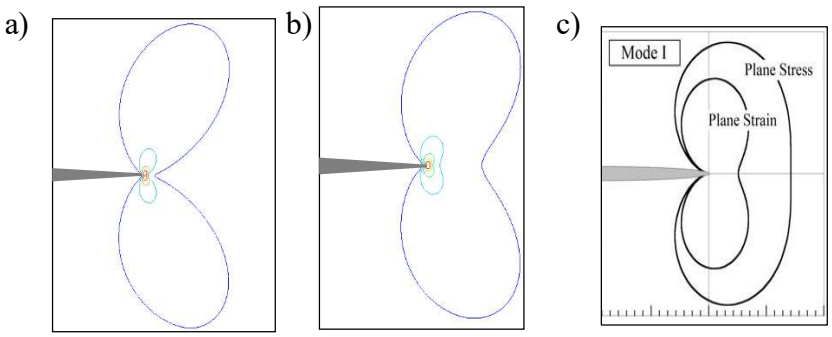

Figure 3-2. Crack-tip plastic zone shapes predicted by finite element method. (a). Plane Strain (b). Plane Stress and (c). Theoretical(Anderson, 2005)

The figure shown above the plastic zone for the plane stress Figure 3-2(b) and plane strain conditions Figure 3-2(a) and it reveals that the more bean shape is observed for plane strain condition and a less bean shape is observed for case of plane stress condition as compared with plane strain. These map shows closer to the theoretical crack tip plastic zone shown in Figure 3-2(c). Also, for plane strain condition the strain along z −direction become null but there is stress along z −direction for two dimensional problems. This condition is also confirmed by strain

component graphical representation as shown in Figure 3-3 below. The figure shows there is no strain for plane strain condition $\varepsilon_{zz} = 0$.

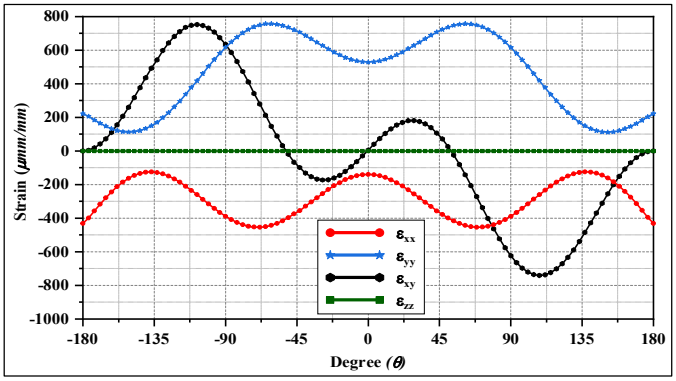

Figure 3-3. The strain components for plane strain condition

3.4 Fracture Modelling Approach

As mentioned in the literature review, the extension of crack is determined based on the two fracture criteria. These are the stress/displacement approach or energy approach. The former one is based on the new crack is formed when the stress in the vicinity of the crack tip reached the intrinsic material property of which is the critical stress intensity factor. In the later one, the new surface is created when the energy release rate exceeds the strain energy of the material property.

In the thesis, the energy approach is used to model the crack whether it propagates or not (at static). The crack in the body is subjected to different loading pure mode I or mixed-mode loading. The stress fields in the vicinity of the crack tip are modeled by the assumption of the linear elastic fracture mechanics. The loadings applied in the plate are pure mode I and mixed-mode. But the mixed-mode would consider only a two-dimension plate. The local stresses in the crack tip are analyzed.

According to the energy approach, the energy release rate i.e., fracture energy in Abaqus can be calculated as follow.

Fore pure mode I loading

$$G_I = \frac{{K_I}^2}{E'} \tag{3.7}$$

Fore pure mode II loading

$$G_{II} = \frac{{K_{II}}^2}{E'} \tag{3.8}$$

Mixed-mode loading (mode I + mode II)

$$G_{mixed} = \frac{1}{E'}\left({K_I}^2 + {K_{II}}^2\right) \tag{3.9}$$

$$E' = \frac{E}{1 - v^2} \quad For\ plane\ strain\ condition \tag{3.10}$$

Therefore, most materials are severed failure happens due to mode I loading condition. So, the material property of fracture energy is calculated based on this model and the value of the intrinsic material property of fracture energy is determined as: -

$$G_c = \frac{{K_{Ic}}^2}{E'}$$
$$G = \frac{(1 - v^2){K_C}^2}{E} \tag{3.11}$$

The material property of v, K_c and E are listed in Table 3-1.

$$G = \frac{(1 - 0.34^2)(55\ MPa\sqrt{\text{m}})^2}{103\ GPa}$$
$$G = 25{,}974\ \ N\ /\ m \tag{3.12}$$

The value inserted in the material property module for modeling the fracture of material if exceeds the energy the crack is unstable and leads to propagation unless it is stationery.

3.5 Numerical Analysis Tool

For numerical analysis of engineering problems, a different platform of finite element method computational software has been developed. For instance, the Ansys and Abaqus. Both are utilized for fracture problems but due to the extension of the usage of XFEM, ABAQUS/CAE software is in demand for the current research. The computation of the fracture parameters by numerical modeling software called ABAQUS is vast and multi-function software used to solve static, quasi-static and dynamic transient problems. But also, other problems like thermal, electrical and magnetic and also coupled problems analyzed and solved.

Abaqus is a powerful program suite for engineering problems, works based on the finite element method that can unravel issues ranging from generally basic linear problems to the foremost challenging nonlinear problems. Abaqus contains a broad library of components that can demonstrate for all intents to model any geometry. It has a similarly broad list of fabric models that can reenact the behavior of most typical engineering materials counting metals, elastic, polymers, composites, reinforced concrete, foams, and geotechnical materials such as rocks and soils. Outlined as a general-purpose simulation apparatus, Abaqus can be utilized to ponder more than fair auxiliary (stress/displacement) problems. It can evaluate and simulate engineering

problems in such different ranges as heat transfer, mass dissemination, coupled thermal-electrical problems, acoustics, soil mechanics, piezoelectric analysis, fluid dynamics and electromagnetic analysis.

3.6 Finite Element Modeling Procedures

The finite element analysis is performed by the numerical analysis software called ABAQUS/CAE. The procedure in the analysis is performed step by step from the part modeling to visualization of the result. The selection of the type of element, the mesh size, the time, etc. is based on the convergence of the outcome and the type of modeling of the part. Each of the conditions is discussed in the later section of the procedure. In Abaqus software, any of the procedures/modules can be done without keeping the consequences of the modules. Therefore, the steps can be done that can be suitable for the user so the following procedures are utilized in this work case.

3.6.1 Part Modeling

The two-dimensional plate geometry of the analysis can be modeled in the part module of the section of the Abaqus software since the Abaqus/CAE feature enable to model any type of simple geometries also it has the platform to import the complex geometries from other modeling software like CATIA, SOLIDWORKS, etc. So, the analysis is held in the different orientations of the crack and the sample of the geometry depicted below in the part module.

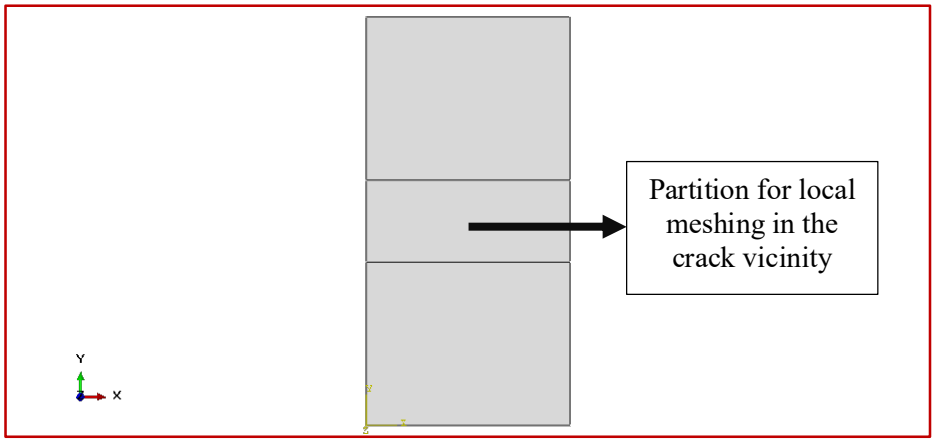

Figure 3-4. Two-dimensional plate part modeling

3.6.2 Assign Material Property

In the property module section of the numerical tool, the property of the material used (values and type of material i.e., isotropic, orthotropic, etc.) and the body section is specified (if the different sections or parts are existing in the model). Since the material used is an isotropic homogeneous material, only a single material property and section are specified and assigned in

the property module. The material property includes mechanical and thermal properties. The plastic property also should define in the module. Its property is taken from the experimental literature in which the properties are dependent on the temperature at a constant strain rate(Guo & Cheng, 1999). This property is extracted by converting the pdf data to numeric data using Get Data Graph Digitizer as depicted in the Appendix including the plastic property as well.

Table 3-2. Assignment of the material property of the 2D plate in property module

Model name	***Material property***	***Type of material***	***Values***		***Section type***
			E	***V***	
2D plate	Elastic	Isotropic	103 GPa	0.34	Solid, Homogenous

3.6.3 Assembly Module

In the assembly module, the parts modeled in the part module are combined for creating instances of parts and making the right position of the parts relative to each other based on the analysis type i.e., for the edge crack, inclined and center crack the assembly of the instances are different. The model comprises the 2D plate and crack instances and is assembled in the correct orientation of the crack on the plate. Since no other parts are assembled and modeled only the crack and 2D part instances are assembled for the case of the XFEM method because in this method the crack is created as a unique part as wire geometry in 2D or as planar geometry for 2D analysis.

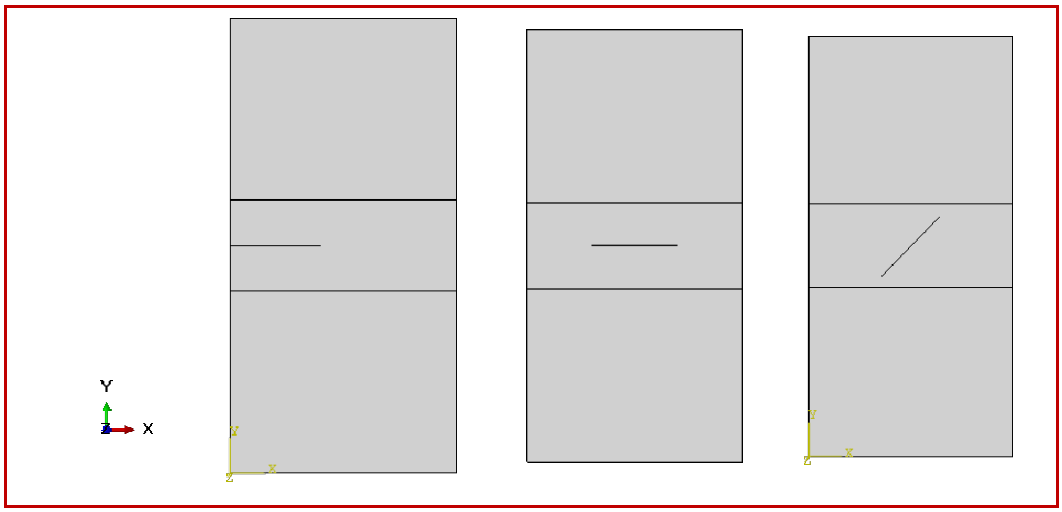

Figure 3-5. Assembly of the different orientation of XFEM crack and 2D part

3.6.4 Step Module

In this section, the type of analysis hold in the software is ordered and selected. Different type of procedures is available including the heat transfer, mechanical stress analysis, electrical analysis, and the combined analysis on each of conjunction of the listed procedures either jointly or separately. The type of analysis may static or dynamic.

For thermomechanical problems, the Abaqus software can solve heat transfer and Thermal-Stress analysis in a different approach. These approaches used to solve thermomechanical analysis are illustrated in the diagram below.

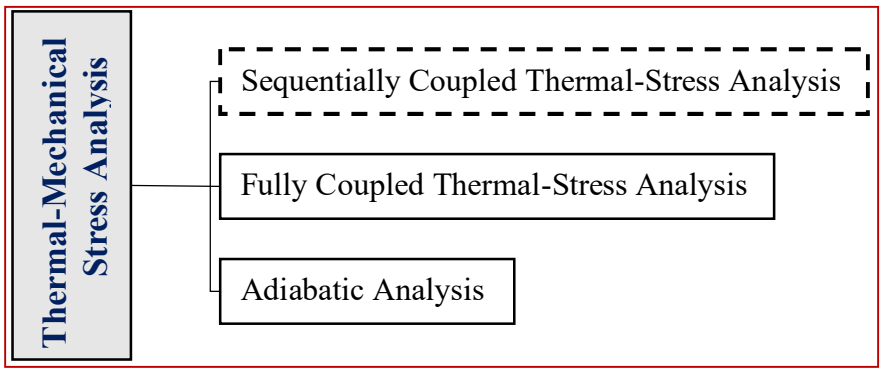

Figure 3-6. Approaches of solving thermomechanical problems in Abaqus

1. **Sequentially Coupled Thermal-stress Analysis**
   The analysis is based on the dependency of stress/displacement solution on the temperature distribution while the inverse is not. This analysis is performed sequentially first by conducting uncoupled(pure) heat transfer analysis and then the stress analysis performed by reading the temperature output from the previous analysis as a predefined field(Abaqus User's Manual, 2016).
2. **Fully Coupled Thermal-Stress Analysis**
   In this analysis, the stress/displacement and temperature fields are dependent on each other and solved simultaneously. In Abaqus, the coupled temperature-displacement procedure is utilized to solve such problems for example metalworking problems(Abaqus User's Manual, 2016).
3. **Adiabatic Analysis**
   In adiabatic analysis, it can be utilized when the mechanical deformation leads to heating hence the event should fast and the heat hasn't time to diffuse in the material(Abaqus User's Manual, 2016).

In the case of this work, sequentially thermal-stress analysis is used. This means, the heat transfer analysis has been analyzed separately and then the output from the analysis becomes the input for the stress analysis later on. Since the stress solution is dependent on the temperature field, the sequentially coupled thermal-stress analysis in Abaqus/Standard is performed by first solving the pure heat transfer problem, then reading the temperature solution into a stress analysis as a predefined field(Abaqus 6.12 User's Manual). The Abaqus software can allow the solution from different meshes. The figure below describes the procedure of the analysis used.

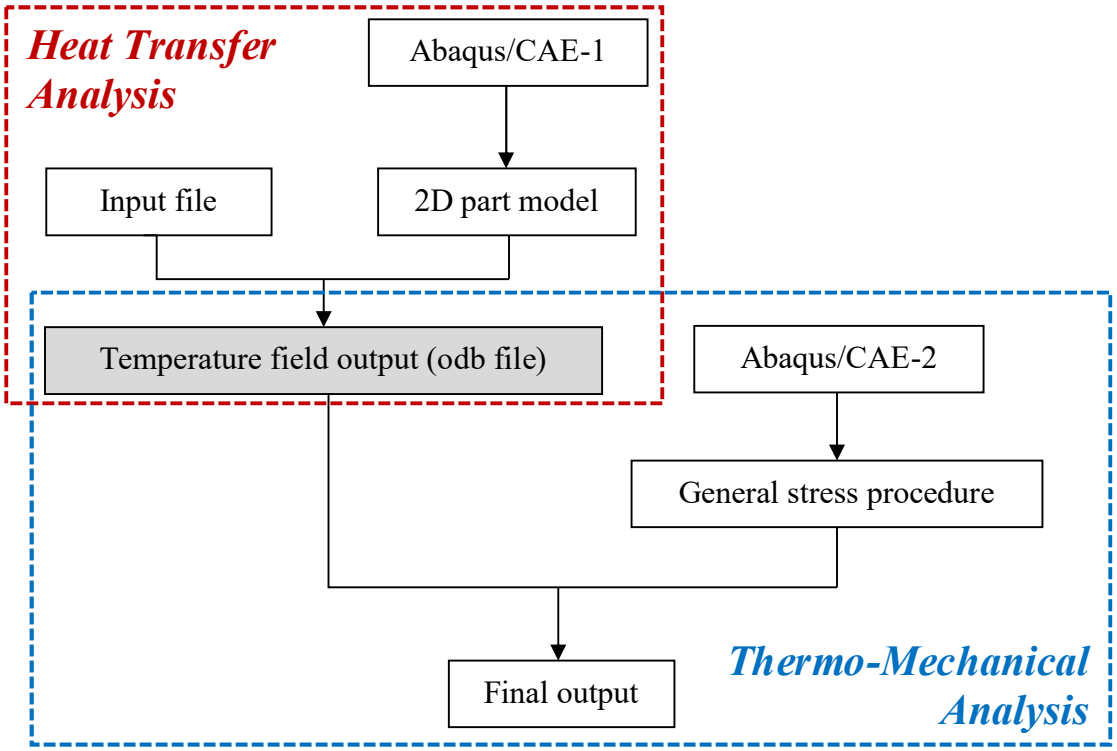

Figure 3-7. General steps of the overall procedure followed in the analysis

In each procedure i.e., heat transfer and static general analysis, the initial procedure is used to define the boundary conditions and to check whether the model is correctly defined or the requests in the step are possible or not. In each procedure the final output is different. The maximum and minimum limit of each increment including the total maximum increment number is set until the processor displays as the analysis is complete. In the heat transfer procedure, the output request can be the temperature field that can be input for the next analysis as a predefined field in the load module.

Table 3-3. Heat transfer procedure analysis inputs

Step	Step Name	Procedure	Time Period	Increment Size			Increments
				Initial	Minimum	Maximum	
0	Initial	Initial	N/A	N/A	N/A	N/A	N/A
1	Temperature	Heat transfer	0.1	0.001	0.000001	0.01	1000000

In static general analysis the strain, the STATUSXFEM, stress, displacement, PHILSM, PSILSM, etc. are requested. The heat transfer load i.e., the temperature in the boundary of the model, and in general static procedure the remote mechanical stress is applied in the needed conditions.

Table 3-4. The general static procedure analysis inputs in the step module

Step	Step name	Procedure	Time period	Increment size			Increments
				Initial	Minimum	Maximum	
0	Initial	Initial	N/A	N/A	N/A	N/A	N/A
1	Mech_stress	General, static	0.1	0.001	0.0000001	0.01	1000000

3.6.5 The Interaction Module

In the model, the interaction is between the crack and the 2D plate at the appropriate location. Since the XFEM crack is defined as a wire part in the part module, the interaction between the crack and the plate is defined in a special toolbar by selecting the crack and the type is XFEM or by selecting an engineering feature in the assembly module. No other interaction between surfaces is required in the analysis for instance geometric contact.

3.6.6 Type of Loading and Boundary Conditions

The analysis including both the heat transfer and general static analysis, the boundary and loading conditions in both procedures are different. In the former analysis, the temperature in the boundary of the model has been applied instead in the latter case the remote stress in mode I and mode II are applied in y-direction along with the initial conditions (initial temperature, fixed boundary conditions, etc.).

Table 3-5. Loading and boundary conditions

Procedure type	Boundary condition	Loading type
Heat transfer	Initial temperature	Step temperature
Static, general	Fixed displacement/rotation	Remote stress and ODB input

3.6.7 The Mesh Module

The XFEM method utilized in the Abaqus needs no more conforming the singularity behavior at the crack tip these become eliminate the limitation of the standard FEM method. It permits to study of the crack parameters without the remeshing on the vicinity of the crack. Besides the mesh structure is independent of the geometry of the crack, the singularity and the discontinuity of the stress, displacement and other parameters modeled by utilizing the enrichment functions. However, the mesh around the crack should be orthonormal and a high density of meshing is needed even if it doesn't depend on it for sake of overcoming more accurate results (Zen, 2013). Since the model is 2D and all the input parameters consider plane strain conditions, the type of element used in the analysis is a two-dimensional, 4-node, plain strain quadrilateral reduced integration element.

The mesh size at the section of the crack is fine and then the coarse mesh is utilized far from the crack region gradually. The discretization of the body into the finite element is done by using Abaqus by choosing element shape, element type and structure of the mesh for the consistency of the result in contrast with a mathematical formula.

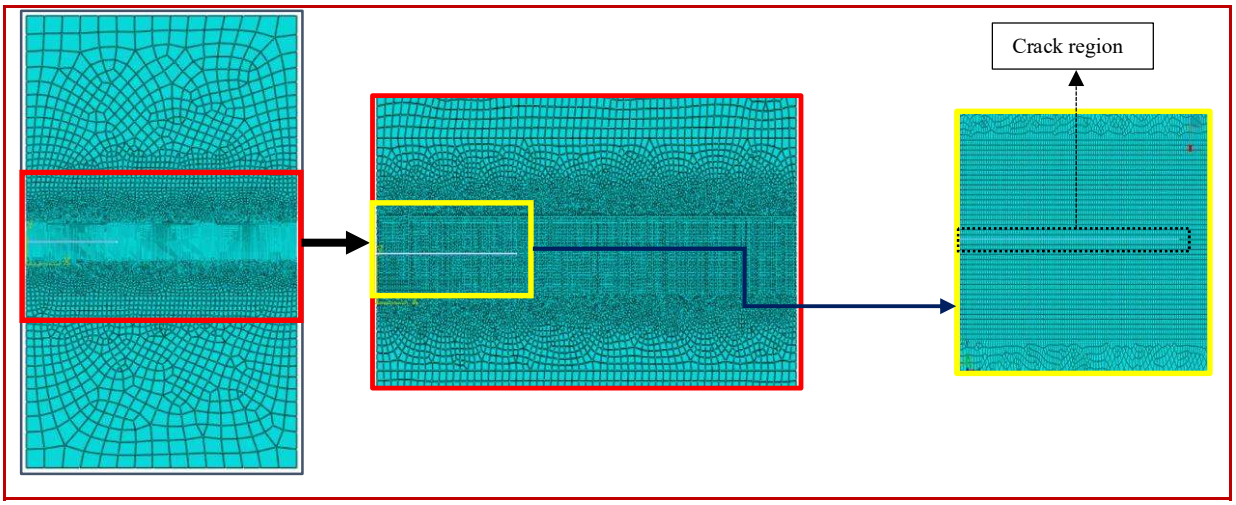

Figure 3-8. The structure of discretization of the model into finite elements

Convergence Study

The convergence analysis is needed for an accurate solution compared to the analytical solution of the problem by performing varying of the element size called mesh size. This study enables us to continue the next analysis using the parameters utilized for convergency analysis. The parameters are maybe the mesh size and the type of element in the element library of Abaqus software. In this study, the focus is on the mesh size convergency compared with the analytical formula as stated below. This is because the geometry of the problem is simple two-dimensional plate form so the mesh simply models the approximate solution by conveying the geometry of the sample so no need for the complexity of the type of element is needed.

Therefore, sufficient refined mesh is needed to confirm the output from finite element analysis is adequate. The mesh refinement level influences the exactness and convergence of the parameter results. The course meshes can surrender inaccurate output utilized for analysis in the explicit and implicit methods in Abaqus. Contradicting this, using the fine mesh or increasing the mesh density in numerical analysis tends near to the converged value. Beyond this mesh refinement will results in an insignificant change in solution, this mesh is said to be converged(Jeyakodi, 2016). The phenomena of this will give confidence in numerical simulations that produce accurate and reliable solution results.

The mesh convergency analysis can be done by performing the important parameter in the analysis. In this study, the stress fields are selected to perform their convergency with the analytical formula. The crack is modeled by XFEM in a different orientation such as center and inclined crack at the mid of the 2D dimensional plate geometry in different crack lengths.

The convergency has done compared with the analytical formula for the mode-I fracture by applying remote stress on single edge crack material modeling along collinear with the XFEM crack initiated, which means the coordinate of $\theta = 0$ and the radius r, $0.04 < r \leq 0.06$.

The Stress Fields Ahead of a Crack Tip for Mode I in a Linear Elastic, Isotropic Material for plane strain condition are(Zehnder, 2012): -

$$\sigma_{xx} = \frac{K_I}{\sqrt{2\pi r}} cos\left(\frac{\theta}{2}\right)\left[1 - sin\left(\frac{\theta}{2}\right) sin\left(\frac{3\theta}{2}\right)\right]$$
$$\sigma_{yy} = \frac{K_I}{\sqrt{2\pi r}} cos\left(\frac{\theta}{2}\right)\left[1 + sin\left(\frac{\theta}{2}\right) sin\left(\frac{3\theta}{2}\right)\right] \quad (3.13)$$
$$\tau_{xy} = \frac{K_I}{\sqrt{2\pi r}} cos\left(\frac{\theta}{2}\right) sin\left(\frac{\theta}{2}\right) sin\left(\frac{3\theta}{2}\right)$$

For the boundary condition of $\theta = 0$ and the radius r, this is needed for simplifying the comparison of the mathematical results with the numerical results, the stress fields reduced to: -

$$\sigma_{xx} = \frac{K_I}{\sqrt{2\pi r}} = \sigma_{yy} \; and \; \tau_{xy} = 0 \quad (3.14)$$

The stress intensity factor,

$$K_I = Y\sigma\sqrt{\pi a} \quad (3.15)$$

The shape factor for the single edge crack material is

$$Y = 1.12 - 0.23(a/w) + 10.55(a/w)^2 - 21.71(a/w)^3 + 30.38(a/w)^4 \quad (3.16)$$

For $a = 0.04m$ and $w = 0.1m$, the dimension confirms the standard for single edge crack materials as described in the previous section, the shape factor is

$$Y = 2.104288$$

For the applied remote stress at the upper boundary of the section $\sigma = 10MPa$ this value taken out of boundary but it is needed for checking the consistency of result with mesh size for numerical modeling, the stress intensity factor is,

$$K_I = Y\sigma\sqrt{\pi a}$$
$$K_I = 2.104288 \times 10MPa\sqrt{(\pi \times 0.04m)}$$
$$K_I = 7.79 \; MPa\sqrt{m} \quad (3.17)$$

Substituting the result into the above Equation (3.14 the stress field for the crack front line for different radius r can be calculated and depicted in the following graphs that compare both the numerical and the analytical methods. In numerical methods, different mesh size has implemented up to stable and appropriate result overcome in contrast with mathematical results. The following figure shows the stress filed along the crack front to the border of material for local mesh size between 0.05 and 0.00005 m.

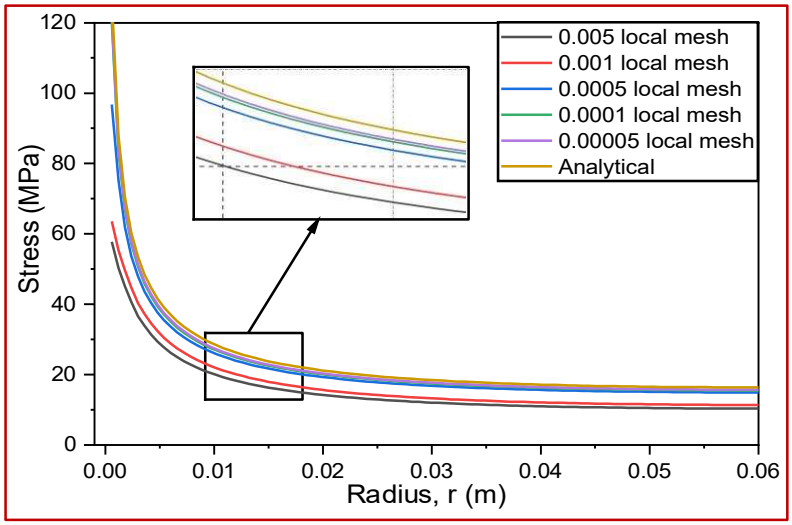

Figure 3-9. Convergence of mesh size relative to analytical method

The local mesh element size varied as a stable result sustained compared to the analytical result. This is done on the straight line for varied radius r. The type of element size is selected based on the error according to the mathematical result.

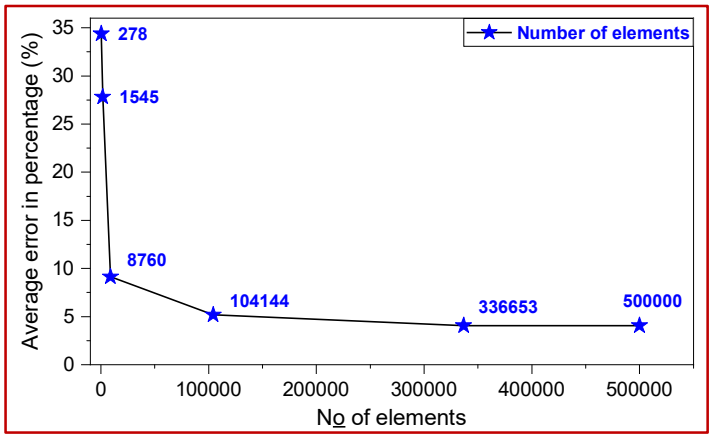

Figure 3-10. The error of numerical results compared to analytical for different mesh size

According to Figure 3-7, the mesh size (number of elements) affects the final result. When the fine mesh is used, it approaches the analytical one. In this study, coarse mesh size will result in much error around 34.5% while fine mesh size becomes an error of 4.23%. As shown in the figure

for elements of mesh that reaches 340,000 the result is sustained and no change happens on the results. So, 340,000 total elements of 0.00005 local mesh size are accepted for this analysis. The table below clarifies all the data in the numerical analysis used.

Table 3-6. Mesh property parameters used in convergence study

S. No	Local mesh size	Global mesh size	Total no of elements	Element statistics	
				Element type	No of elements
1	0.005	0.01, 0.05	278	CPE4R CPE3	267 11
2	0.001	0.01, 0.05	1545	CPE4R CPE3	1498 47
3	0.0005	0.01, 0.05	8760	CPE4R CPE3	8581 179
4	0.0001	0.02	104144	CPE4R CPE3	103217 927
5	0.00005	0.02	336653	CPE4R CPE3	334452 2201
6	0.00001	0.02	500000	CPE4R	500000

CPE4R stands for Four-node (4) Plain Strain (PE) with Reduced Integration(R) Continuum(C) element

The triangular element in the analysis is created due to the selection of the type of quadrilateral element that means when the quad-dominated element has been selected another type of element is incorporated but in the crack region structured quad material is implemented. Since XFEM crack allowed in structure configuration of mesh. All in all, the quad dominated allows for decreasing the number of elements simultaneously cost of time and processing of devices.

3.6.8 Post Processing

In the preprocessing i.e., part modeling, property module, meshing, etc. are the inputs for the analysis and lead for processing the analysis. All data is checked and submitted for a job in the job module for analysis to visualize the results in the real arena. The job module is used to analyze the part and allow for submit the analysis and visualize the progress along with the monitor.

After the work has been done, the Abaqus Standard is allowed for visualization of the result that has filled in step module for history output request and field output requests. The history request output can be collected from the data in the job monitor for the specific region of any parameters directly from the data record. Hence, in field output requests the parameters are visualized through different methods using contour, line, graphs, un-deformed and deformed shape, etc. which allowed for extracting results in any field of the module for each of the parameters requested before.

Chapter Four
4 Results and Discussion

4.1 Introduction

In this chapter different phenomena of the analysis including the effect of thermomechanical loading on the crack stress fields that accommodates all the parameters related to the fracture mechanics is investigated. Some of the fracture parameters are the crack length, the crack angle, the applied stress, and the temperature on the boundary of the model. The analysis is held in two main modes of fracture which are pure mode I and mixed-mode loading. The former one was analyzed in both edge crack and a center crack whereas the later analysis is using inclined center crack by applying the tensile remote mechanical stress at the top boundary of the model while fixing the bottom. This configuration of the stress on the top boundary of the model results in a mixed-mode fracture described in the section of mixed-mode loading below.

4.2 Pure Mode-I Loading

In this section, the mechanical stress applied to the surface of the model for crack orientation is perpendicular to the load. Upon this, the orientation of the crack and the direction of mechanical loading are perpendicular to each other. In the computation of the mechanical and thermal load, the boundary and loading conditions are taken from the literature and the basic fracture mechanics formulations stated in Equation from 3.1-3.6.

From section 3.2 of geometrical modeling, based on the standard of BS 8571, the parameters are taken from literature (Zhu, 2016) because the recommended dimension of the material is existed on it since the main standard document is limited to access. For plane strain condition assumption taking the depth as a unit the width of material $W = 100mm$ and height $H = 200mm$ and the crack ratio would be $a/w = 0.1\ to\ 0.5$ so $a = 0.01\ to\ 0.04m$ length is considered in this work. In addition, the limit load applied in the material has been calculated from Equation 3.2.

For different crack length configurations, the limit load and limit stress applied on the middle tension material for the case of this research would be specified in the table below.

Table 4-1. Remote stress required for applying load on the model

Crack Length	$a/w = 0.1$	$a/w = 0.2$	$a/w = 0.3$	$a/w = 0.4$	$a/w = 0.5$
Ligament Size	90 mm	80 mm	*70 mm*	*60 mm*	*50 mm*
Limit Load	42608 KN	37874 KN	*33139 KN*	*28405 KN*	*23671 KN*
Limit Stress	426 MPa	*379 MPa*	331 MPa	*284 MPa*	*236 MPa*

For the crack length ratio between 0.2-0.4, the value of the limit load and stress is between the two extremes so the applied load on the model can be taken below the value of 236 MPa. And the

edge crack consideration on the model is substituted by the middle crack in tension due to the symmetry so in this section the middle center crack under tension load is considered for both mechanical load and thermomechanical load simulations.

4.2.1 Center Crack

In this topic, only the material under pure mode I tension load with the center crack on the model under a different scenario of loading, crack size and varied mechanical stress is implemented as mentioned in the above section in which the material is capable to withstand according to the standard. The edge crack is not considered because of symmetry with middle crack under tension and also both edge and center crack are under tension loading no different result will come over. So, the remote stress applied on the upper boundary of the material applied is 20, 50 and 100 MPa. The boundary conditions and loading conditions on the material for the different scenarios can be simulated in a numerical modeling tool called Abaqus as input is depicted here below.

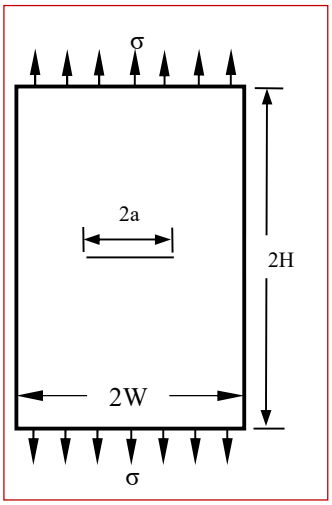

Figure 4-1. The loading and geometry condition of the model for pure mode I

In this analysis, the mechanical load was applied on the top surface using XFEM by increasing the crack ratio from 0.1 to 0.4 for the different loads to identify the variation of the stress field around the crack and crack tip. This enables to comparison and plots the change in the stress field with that of the thermo-mechanical stress field around the crack tip.

The graph depicted below on the table shows the mechanical stress distribution around the crack tip i.e., the Von Mises stress contour distribution around XFEM crack for different loading conditions and crack ratios.

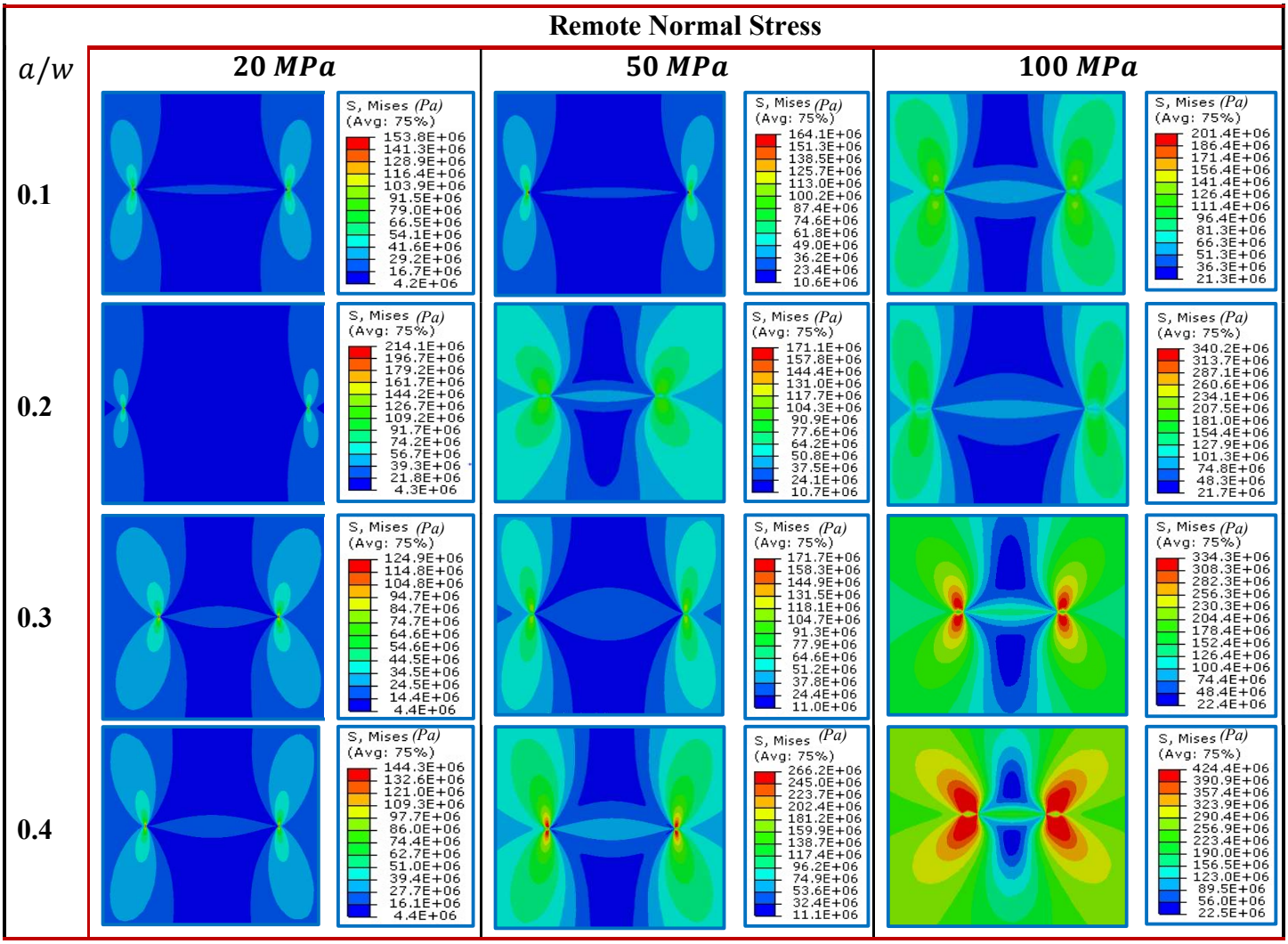

Figure 4-2. The contour map of Von Mises stress field at the crack tip for pure mode I loading

The contour map for different loading and crack length scenario show there is a change in the contour of stress distribution through the two cases. This change in contour also results in the change of the in-plane stress field around the crack tip. Furthermore, the in-plane stresses at the crack tip also vary according to the contour map as shown above. The mechanical stress in pure mode –I loading affects the stress contour around the crack tip as shown hereafter. For different crack ratios with the same remote stress yields a change in the mechanical stress field at the crack tip this is due to the direct relationships between the crack length and the stress field mathematically.

The graph of the contour plot stress versus angular position is extracted from the point value by creating the circular path on the vicinity of crack tip at some radian value. The point value i.e., stress components extracted from the nodal or elemental value in which interpolated from them.

The circumferential circular path created by specifying the location of three points on arc in which an appropriate point place specified in the figure below. The stress components extracted for 100 points in angular spacing of 3.6° surrounding crack tip. The procedure of evaluating values explained in the following graphical interpretation.

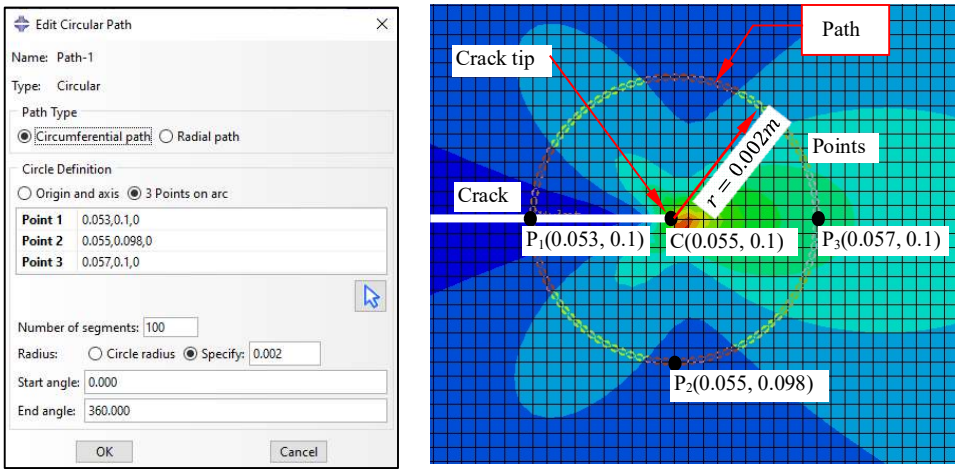

Figure 4-3. The procedure of extracting stress values from point surrounding crack tip

The figure above shows the value extraction process from the point which is incorporated on the Abaqus software. This procedure is utilized for all stress component extraction for different conditions depicted hereafter this section. The crack tip(center) is known from the whole model after that the location of three points inserted with the radian value and the points in which the stress value extracted is drawn. The point P_3 is the starting point in which it shows zero degree and from P_3 to P_1 through P_2 is clockwise and from P_3 to P_1 counter clock wise direction is considered throughout the document. Based on the above explanation, the stress fields for mode-I loading case explained here in the following graphs.

a)

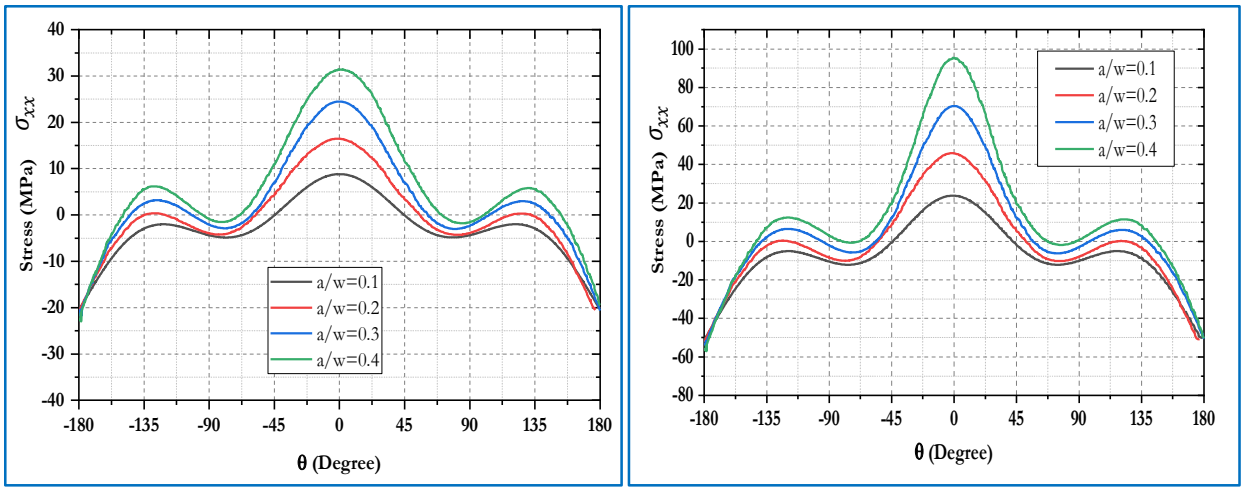

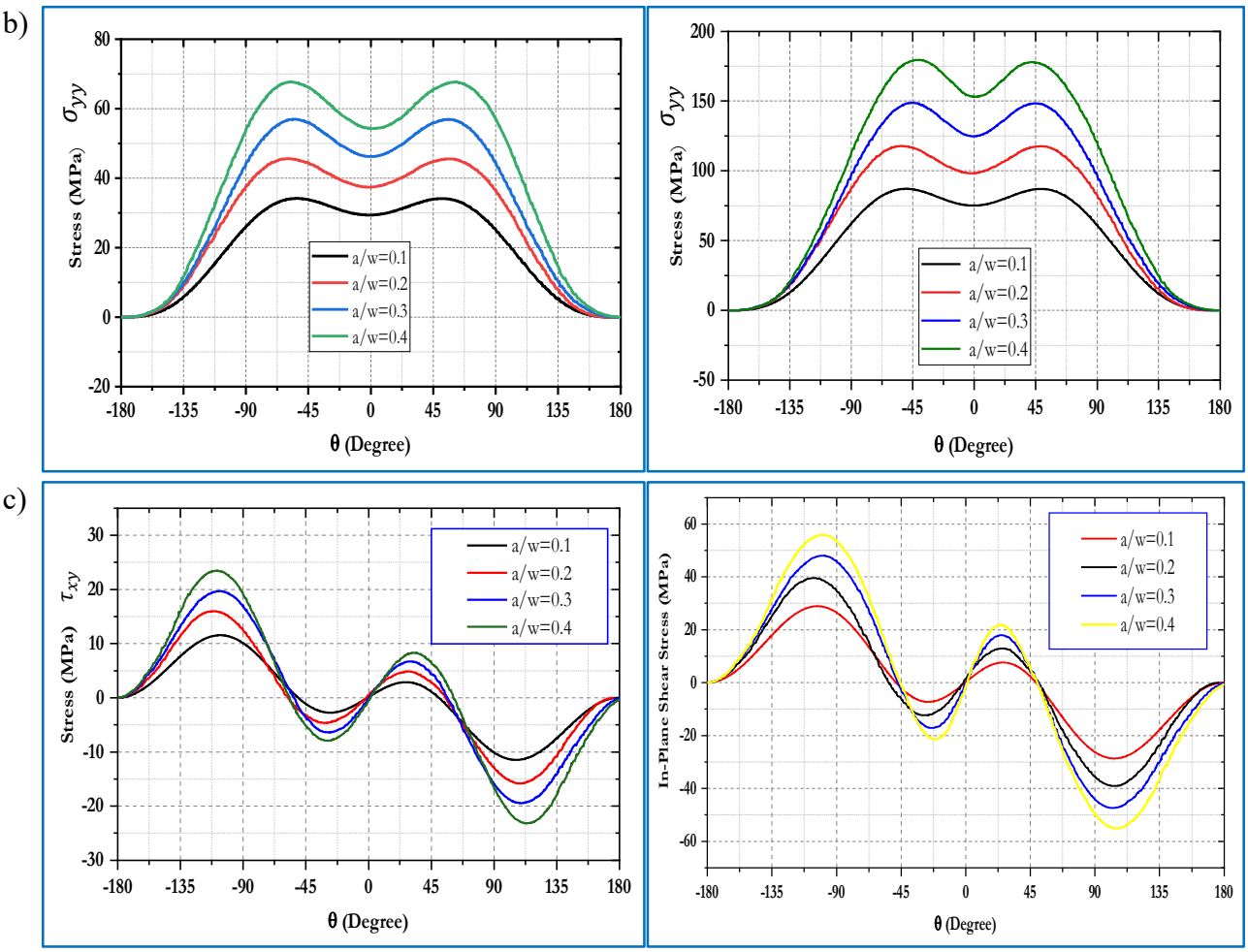

Figure 4-4. The mechanical pure mode-I in-plane stress fields for different crack ratios as a function of θ. Left: 20MPa Right: 50MPa. a). σ_{xx}, b). σ_{yy} and c). τ_{xy}

As shown above, Figure 4-4 depicts the mechanical in-plane stress field around the crack tip for a varying crack ratio of constant applied remote stress. And it is showed the change in the magnitude of stress fields as crack ratio vary. The in-plane stress σ_{xx} as shown in Figure 4-4 (a) has three maximums. Two local maximums are around $\pm 130°$ and the global maximum is at $\theta = 0°$. These two maxima are same for different crack ratios despite their magnitude of the stress. In addition, the contour plot of the stress field is similar horizontally and vertically stands for remote stress and crack ratio respectively. But for the case of change in the applied remote stress, the contour plot is steeper when it increased as shown in Figure 4-5(a) for a particular crack ratio for showing the change. The mechanical in-plane stress σ_{yy} depicted in Figure 4-4 (b) has similar condition with that of in-plane stress σ_{xx} by pattern of contour in both crack ratio and remote stress increase. The local maximums are equal in magnitude and they occur around $\theta = \pm 65°$ for remote stress of 20MPa. But these local maximums shifted to $\theta = \pm 45°$ for 50MPa remote stress in

addition to change in magnitude of maximum. The mechanical in-plane shear stress τ_{xy} as presented in Figure 4-4 (c) has two local maximums and two local minimums. And the shear stress is null at $\theta = 0°$ and local maximums are at $\theta = -115°$ and $\theta = 30°$ in addition the local minimums are at $\theta = -30°$ and $\theta = 112.5°$. These maximums and minimums varied when the remote stress changes with shift in angular location. These variation of the local maximum and minimums due to change in applied remote stress for particular crack ratio are depicted as shown in below Figure 4-5(b).

a) b)

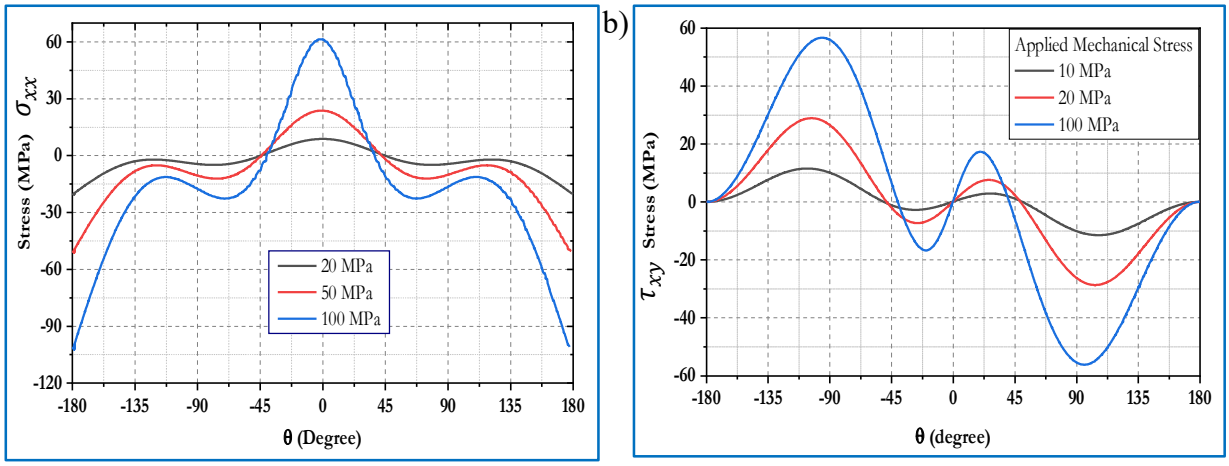

Figure 4-5. Variation of stress field for variation of remote stress for the crack ratio of $a/w = 0.1$ (a) In plane stress, σ_{xx} and (b) In-plane stress, τ_{xy}

The figure above shows a change in the magnitude of the mechanical stress field near to crack tip as remote stress increased. The magnitude of the maximums and minimums are increased simultaneously with remote stress and shifts in the position of the two extremes observed for the in-plane shear stress field.

Figure 4-6 shows the mechanical stress fields around the crack tip for particular remote stress and crack ratio of 100MPa and 0.1 respectively. The figure tells that the in-plane stress fields vary for certain radius away from the crack tip and has different maximums and minimums with the varying position.

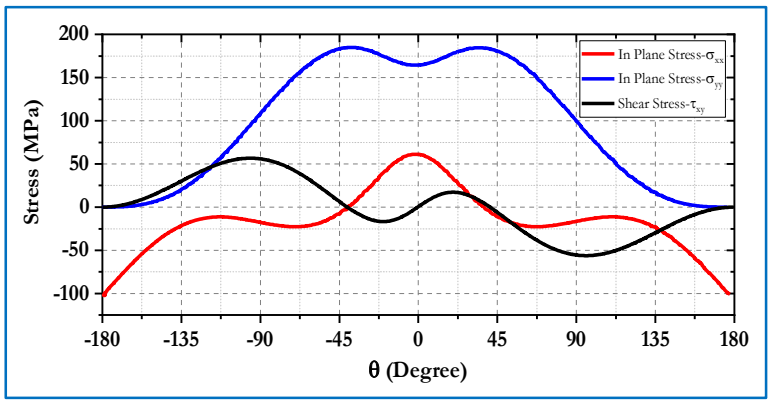

Figure 4-6. The In-plane stress fields around the crack tip as a function of θ

Generally, from the Figure 4-4 and Figure 4-5 the change in magnitude of the stress field happen when the crack ratio increases for any of stress components i.e., σ_{xx}, σ_{yy} and τ_{xy}. This is because of the direct relationship between the stress fields with the applied remote stress and the crack length. The result match with the theoretical hypothesis i.e., "linear elastic bodies must undergo proportional stressing, i.e., all the stress components at all locations increase in proportion to the remotely applied forces. Thus, the crack-tip stresses must be proportional to the remote stress, and $K_I \propto \sigma$"(Anderson, 1995).

4.2.1.1 Thermo-Mechanical Stress Field

The Thermo-Mechanical loading analysis performed by Abaqus executes the stress field near the crack tip for different loading and parametric conditions. This was by utilizing the heat transfer analysis for temperature field distribution on the body and then performing the static general analysis using the temperature field as a predefined field for the combined loading effect on the crack tip stress field.

In the above section, only the effect of mechanical loading and crack ratio on the crack tip stress fields was investigated. Since one of the objectives of the research is to investigate the thermal effect on the stress field, the crack is considered as thermally insulated in the model in which is adiabatic crack. Mean that the displacement field and temperature field are discontinuous along the crack. The XFEM method allows discontinuity by using additional functions as described in the literature review. The temperature across the crack is discontinuous and heat flux is singular at the crack tip. And the XFEM method used the same analogy for the temperature field equation as of displacement field. The temperature field distribution can be modeled by Abaqus/CAE using the heat transfer procedure. Later the output from the analysis can be the input for the thermo-mechanical modeling in the static general procedure.

The boundary condition and the temperature field distribution for the center adiabatic crack plate are shown in Figure 4-6 below. Even though, the change in temperature field is observed while changing the boundary condition but the contour of the field is not changed. For thermo-mechanical simulation, three temperature gradients are utilized to show the change in stress fields nominated as ΔT_1, ΔT_2 and ΔT_3 which represents the temperature field of the model for the boundary conditions on the upper and lower edge of the plate as shown below.

ΔT_1-stands for temperature field distribution for $\pm T = \pm 293K$

ΔT_2-stands for temperature field distribution for $\pm T = \pm 323K$

ΔT_3-stands for temperature field distribution for $\pm T = \pm 362K$

This temperature variation was selected because it is assumed that the temperature field generated near to crack tip results in elastic deformation in the vicinity of the crack tip(Kidane *et al*., 2010).

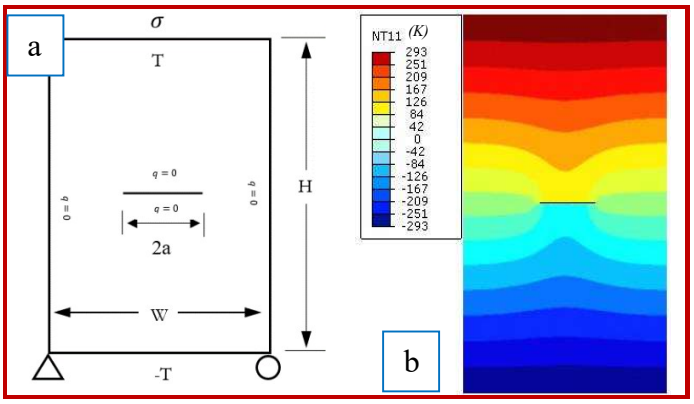

Figure 4-7. The boundary and loading condition (a) temperature field distribution (b)

4.2.1.2 Varying Temperature

In this section, the effect of temperature change on the stress fields is investigated and shown hereafter. The stress components are extracted for radius r of 0.002m from the crack tip which is based on *(*Kidane *et al*., 2010). The contour map of the Von Mises stress distribution at crack tip for different thermal boundary conditions i.e., temperature field distribution (ΔT_1, ΔT_2 and ΔT_3) for 50MPa and crack ratio of a/w=0.1 is shown in Figure 4-8 below to distinguish the change in the stress field of the mechanical and thermo-mechanical loading cases.

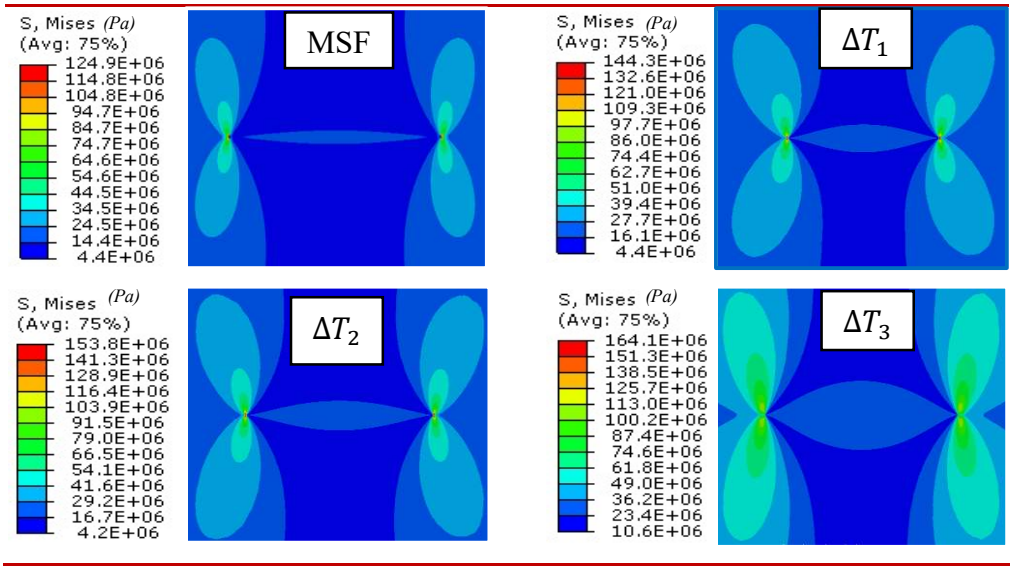

Figure 4-8. The contour map of mechanical and thermo-mechanical stress field around the crack tip for 50MPa and a/w=0.1

From Figure 4-8 as shown above, it is observed that there is a change in the contour of stress fields around the crack tip for the same loading with different thermo-mechanical loading figure out by the value of Von Mises stress. This becomes due to the temperature change in the vicinity of the crack tip. For more elaboration to consider all parameters undertaken in this research the following graphical interpretation shows the change in phenomena around the crack tip.

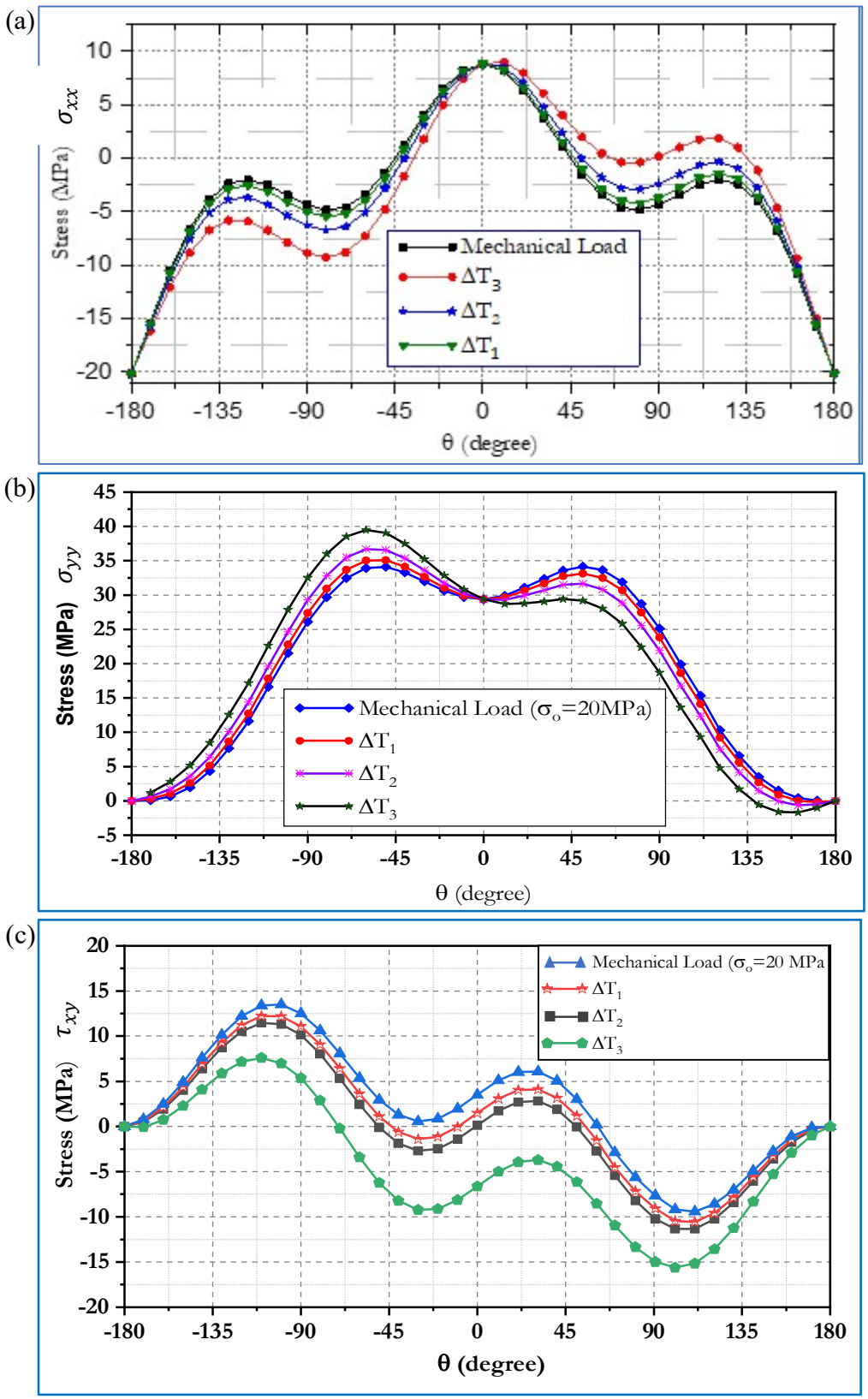

Figure 4-9. The combined In-plane stress fields as a function of θ around crack tip for $\sigma_o = 20MPa$ and $a/w = 0.1$ a). σ_{xx}, b). σ_{yy} and c). τ_{xy}

In the above Figure 4-9(a-c) showed the variation of the stress fields in the vicinity of the crack tip as a function of angular position θ with the variation of tempreture gradient varied from the boundary of the model to crack surface for specific applied remote stress and crack ratio. For in-plane stress σ_{xx} in Figure 4-9(a) the thermo-mechanical stress field varied with a change in the temperature gradient. As the temperature gradient increased the thermo-mechanical stress field decreased in a clockwise direction between $-180° < \theta < 0°$ whereas thermo-mechanical stress field σ_{xx} increased or above the mechanical stress field in between the angular position $0° < \theta < 180°$ for anti-clockwise direction. In this graph shown also the local maximum magnitude locations are around $\pm 120°$ and the global maximum is at the head of the crack tip for $r = 0.002m$ around $\theta = 0°$ which is constant for all cases and local maximum magnitude varies at $-120°$ and $120°$ relative to consecutive temperature gradient variation.

For in-plane stress σ_{yy} shown in Figure 4-9(b), the trend of the stress field for each temperature gradient differs as compared to σ_{xx}. The stress increased as temperature gradient increased for clockwise direction as θ between $-180°$ and $0°$ while the stress fields decreased as temperature gradient increased for the anti-clockwise direction of θ in between $0°$ and $180°$. As observed in this stress field has local maximums around $\pm 60°$ for the mechanical stress field. This local maximum increased in magnitude as the temperature gradient increased for θ is around $-60°$ whereas the local maximum decreased as the temperature gradient increased for θ is around $60°$. The thermo-mechanical in-plane stress fields shifted from increasing to decreasing at an angular position of θ is at $0°$ that is a head of the crack tip.

The shear thermomechanical stress fields τ_{xy} as shown in Figure 4-9(c) has a different profile of decreasing and increasing phenomena as of σ_{xx} and σ_{yy}. This in-plane stress field decreased as the temperature gradient increased and has two different maximum and minimum values around $-120°$ and $20°$. These maximum and minimum values decrease as the temperature gradient decreases and the profile of the stress field for a certain radius is similar to temperature variation.

4.2.1.3 Varying Remote Stress

In this section, the remote stress variation implemented in the model while the temperature field and crack ratio keep to constant and the mechanical stress field and the thermo-mechanical stress fields are compared.

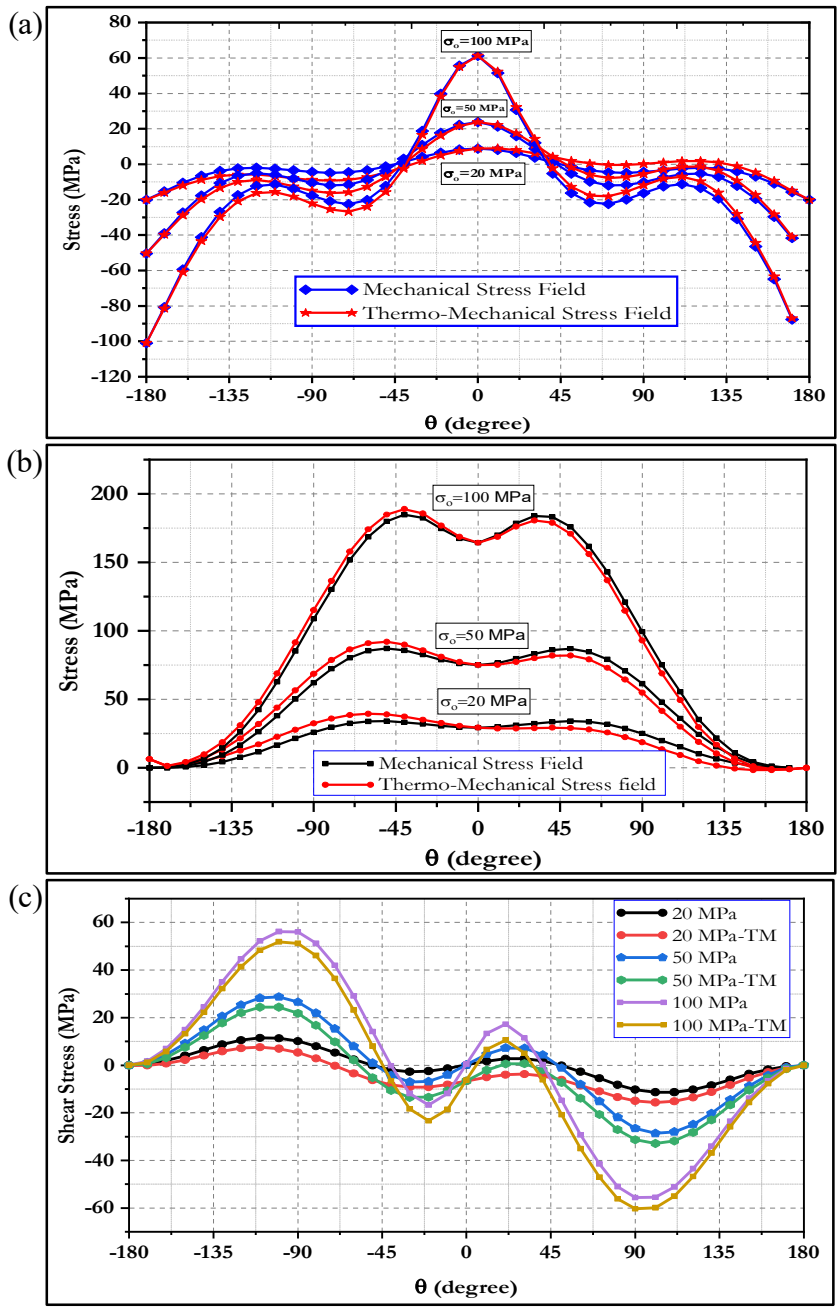

Figure 4-10. The In-plane stress fields as a function of θ around crack tip under varying remote stress for $a/w = 0.1$ and ΔT_3. a). σ_{xx}, b). σ_{yy} and c). σ_{xy}

This figure shows that the mechanical stress field and the thermo-mechanical stress fields have the same pattern of the profile except for the magnitude difference. As observed in Figure 4-10(a), the in-plane stress σ_{xx} for mechanical and thermo mechanical loading cases has the same profile except for their magnitude but for varying the mechanical load applied on the plate the magnitude of the contour changes to the load. However, the maximum and local maximums are set to constant while a change in load. In another in-plane stress σ_{yy} in Figure 4-10(b) the change in magnitude

of both the thermo-mechanical and mechanical stress field is observed and this is because of the change in load and the profile of the stress field is explained in the previous section. But it is observed that a shift of maximum to another angular position when the load increased i.e., the local maximum shifted from around $\theta = \pm 115°$ to $\theta = \pm 45°$ for the load increased from $\sigma_o = 20MPa$ to $\sigma_o = 100MPa$. For the in-plane shear stress τ_{xy} shown in Figure 4-10(c) the same type of profile of the stress field observed for different loading cases except for the change in the absolute magnitude of the result.

4.2.1.4 Varying Crack Ratio

The thermomechanical stress fields for the different crack ratio are depicted below for the 50MPa remote stress and the temperature gradient of ΔT_2 as follow.

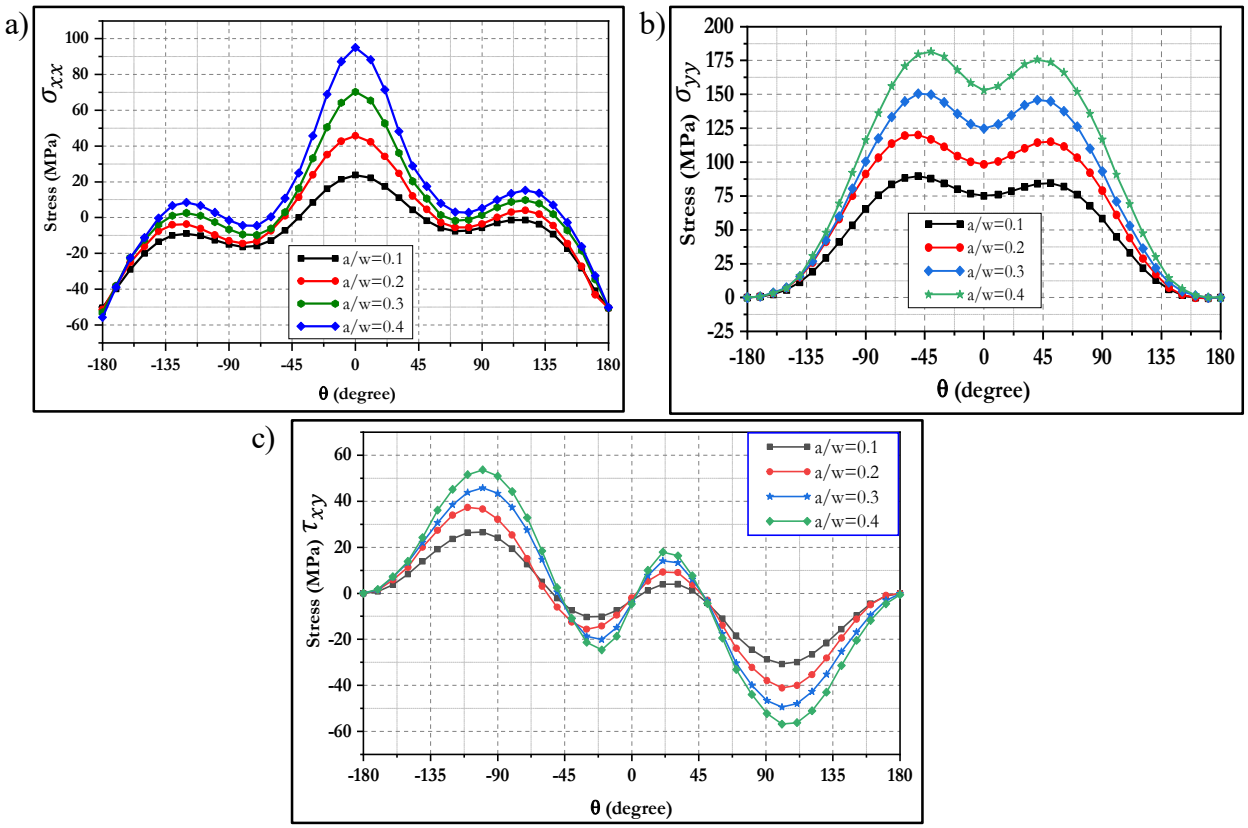

Figure 4-11. The in-plane thermo-mechanical stress fields for the varying crack ratio of $\sigma_o = 50MPa$ and ΔT_2. a). σ_{xx}, b). σ_{yy} and c). τ_{xy}

In all phenomena, in the above figure, the thermomechanical stress fields have the same contour as of mechanical stress field rather than the change in magnitude observed in Figure 4-9. As for the mechanical stress field, the change in the thermomechanical stress field varies with the crack ratio superimposed with the mechanical load. This behavior of stress field is for all in-plane stresses σ_{xx}, σ_{yy} and τ_{xy}.

4.3 Mixed Mode Loading

Similar to the previous loading type, in this section, the mechanical loading is the same with the pure mode–I while the plate is initiated with an inclined center crack with angle α of 15°, 30°, 45° and 60°. This configuration experienced the crack as a combined Mode I and Mode II loading by redefining the coordinate of the crack align with the global coordinate as shown in Figure 4-12 below. The applied remote stress could be resolved into shear and normal components this results in Mode II and pure Mode I loading to the crack respectively. The numerical analysis was held by tension load applied on the upper boundary in Abaqus software and the stress fields extracted from inclined configuration and converted to global rectangular coordinate by using the following Equation (4.1.

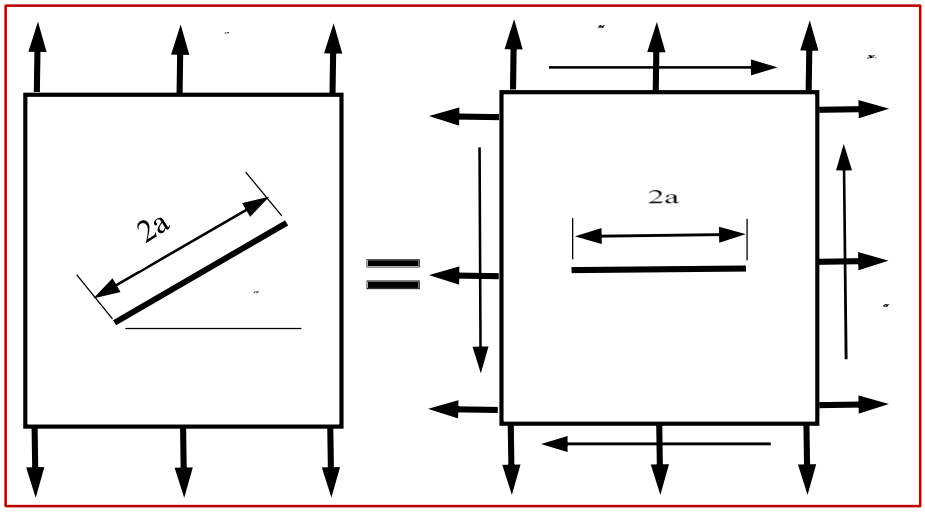

Figure 4-12. Mixed Mode loading configuration

$$\sigma_{x'} = \sigma\, sin^2(\alpha)$$
$$\sigma_{y'} = \sigma\, cos^2(\alpha) \qquad (4.1)$$
$$\tau_{xy'} = \sigma\ \sin(\alpha)\cos(\alpha)$$

Using the above relationship, the stress field around the crack tip is extracted and converted to a global rectangular coordinate for both mechanical and thermo-mechanical stress fields. The figure below shows the contour map of stress distribution around the crack face for different crack configurations and remote stress on the boundary.

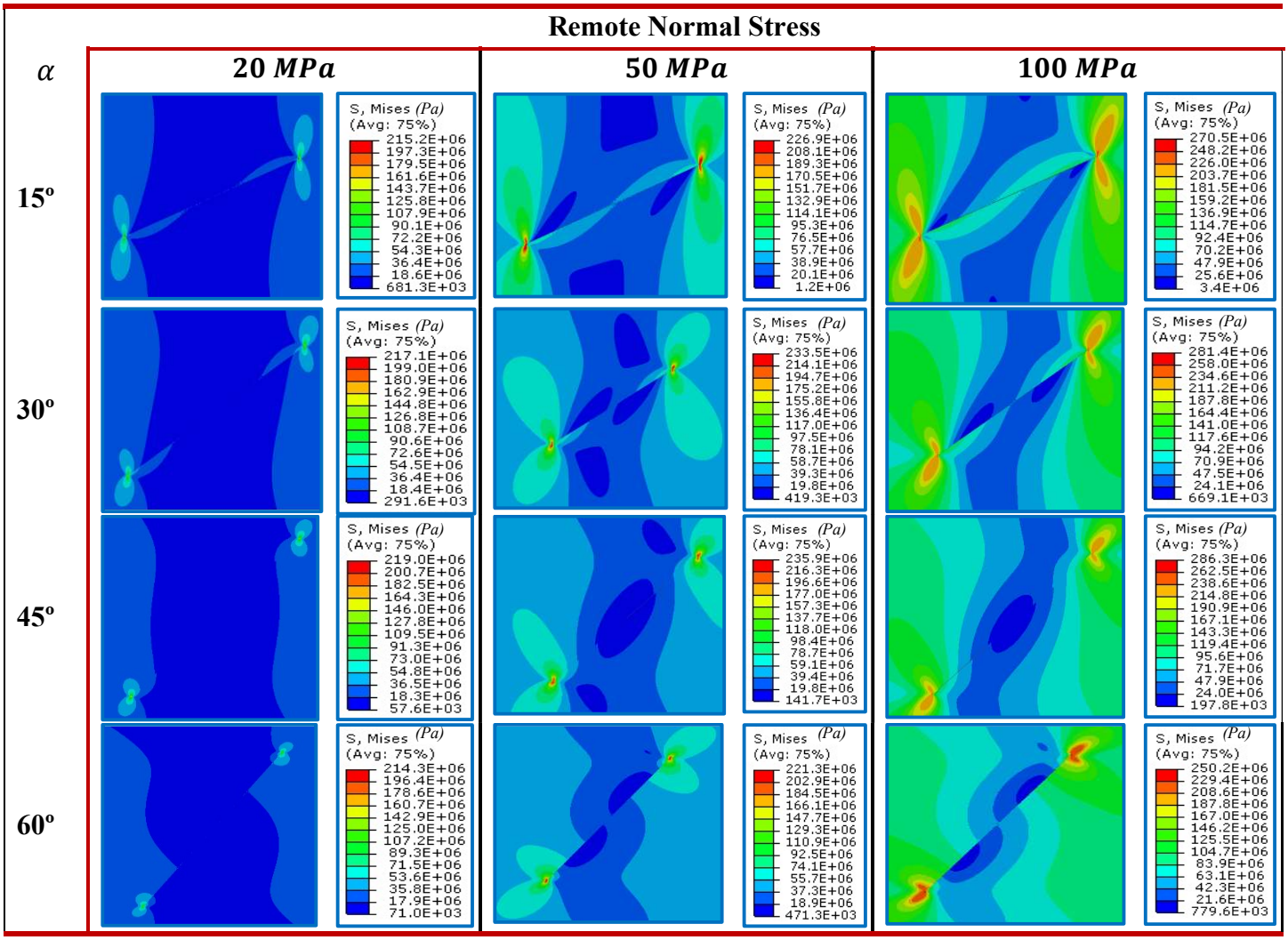

Figure 4-13. The contour map of mechanical stress field at the crack tip for Mixed Mode loading

The figure above shows there is a change in the contour map for different loading cases and this showed by the Von Mises stress column figure out near to the contour map. The mechanical stress field with no temperature effect was extracted for comparison with the thermo-mechanical stress fields and shown hereafter for particular loading case and crack angle configuration. The values of the stress fields extracted for certain radius $r = 0.002m$ as a function of angular position θ from the crack tip(Kidane *et al*., 2010).

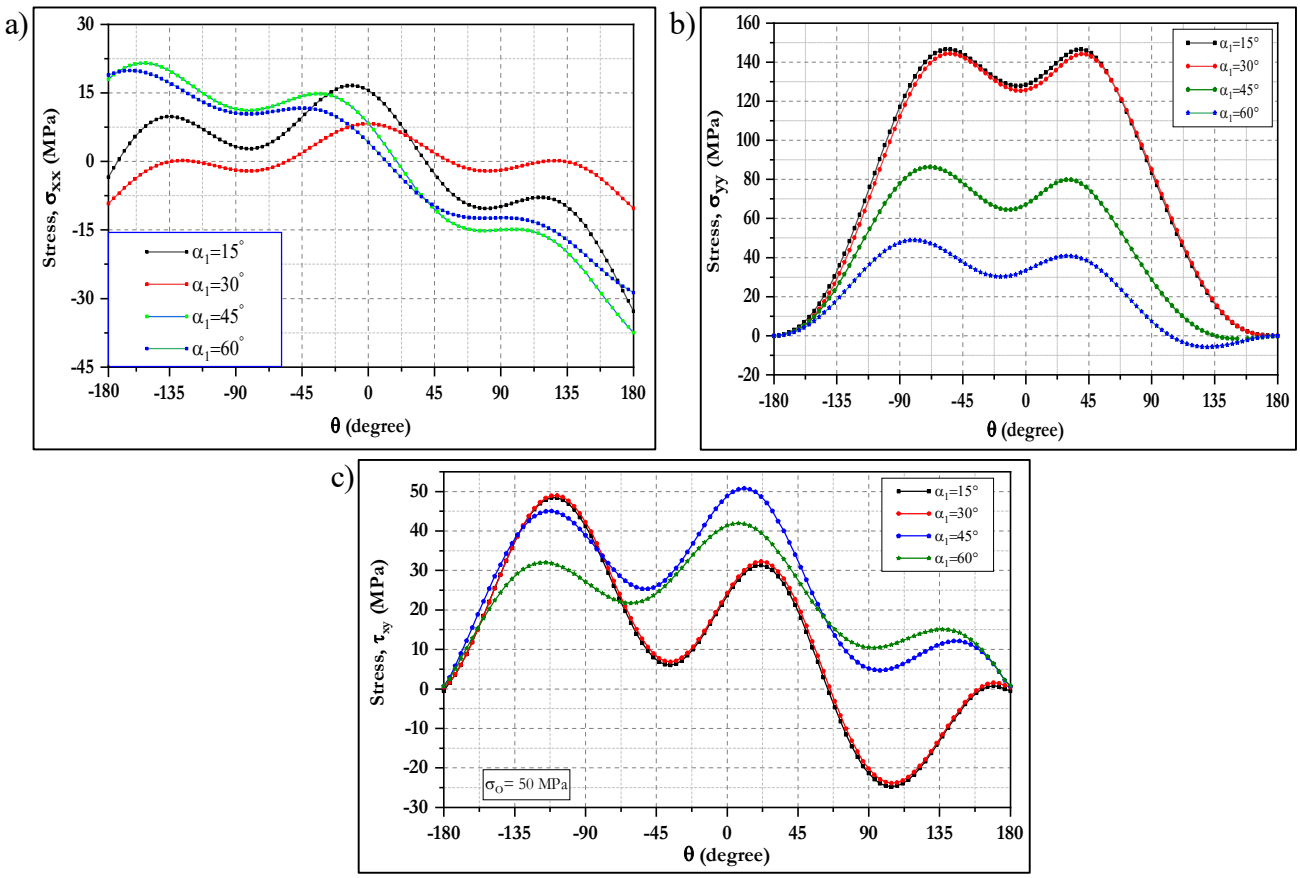

Figure 4-14. The Mixed Mode in-plane mechanical stress field for varying crack angle, a). σ_{xx}, b). σ_{yy} and c). τ_{xy}

As shown in the above figure the profile of the mechanical stress fields for all cases are different from the former pure Mode I mechanical stress fields. This is because of the combined effect of both Mode I and Mode II fracture. Upon this, the profile of the stress field for different crack angles showed us differently. Considering Figure 4-14(a) shows the mixed-mode in-plane mechanical stress field σ_{xx} for different crack angle in which the remote stress is 20MPa. The contour for all crack orientations is varied by profile, peaks and valleys, and maximum and minimums angular position. In all cases, the maximum and local maximums are three in number and constant. In all in-plane stress fields, the shift of maximums angular position is observed. For in-plane stress field in y-direction two maximum and two minimum values for a different angular position to crack angle. This became different from the mode-I loading case. For mixed-mode in-plane shear stress Figure 4-14(c) the local maximums and maximum values shifted according to the crack orientation, in addition, the profile of the contour converted from decreasing to increasing in negative stress for $\alpha = 15°$ and $\alpha = 30°$ from $\theta = 110°$ to $\theta = 180°$. The fluctuation of stress

plot for mixed mode case is due to dominancy. For instance, the crack angle $\alpha = 0°$ mode -I is dominant whereas the mode-II maximum at $\alpha = 45°$ in which τ_{xy} is maximum.

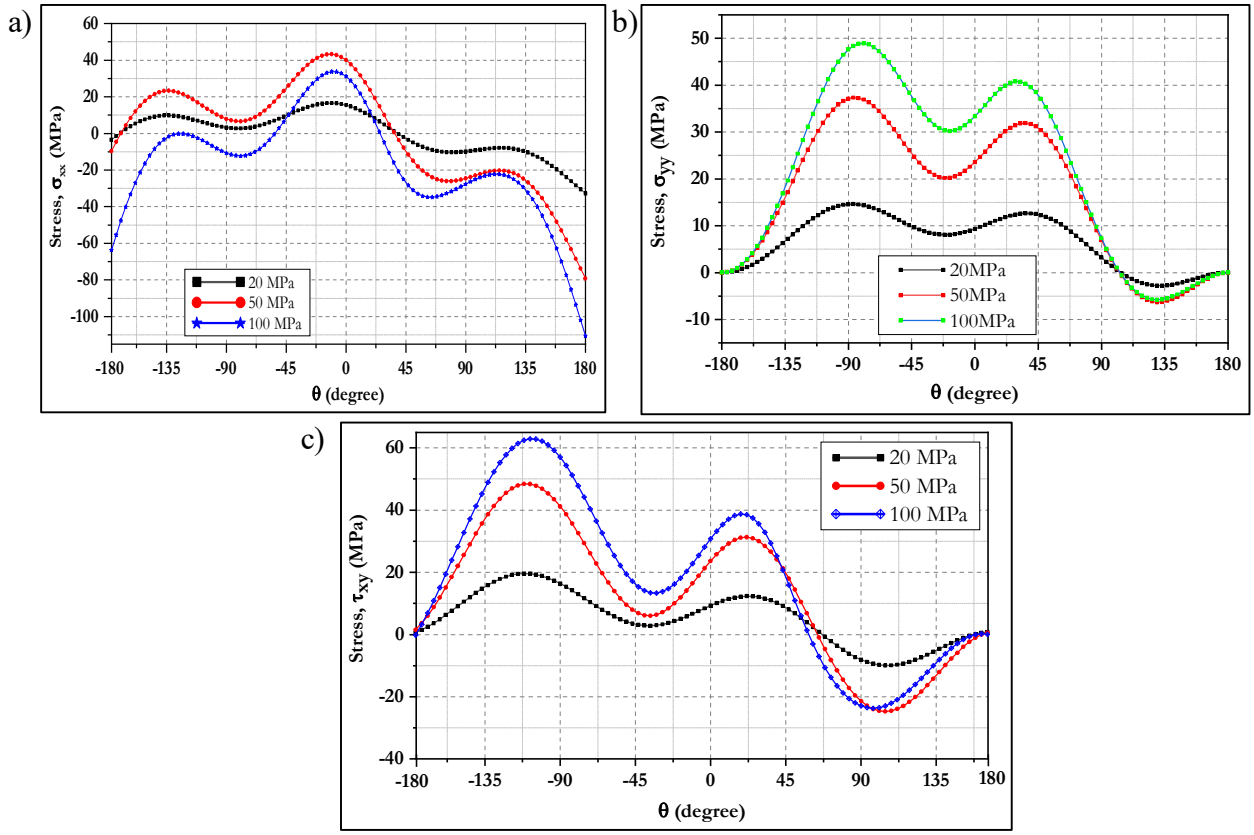

Figure 4-15. The Mixed Mode in-plane mechanical stress fields for varying remote stress, a). σ_{xx}, b). σ_{yy} and c). τ_{xy}

Figure 4-15 shows the variation of the contour plot of the in-plane stress fields σ_{xx}, σ_{yy} and τ_{xy} with respect to varying remote stress applied uniaxially for inclined crack that belongs to a mixed-mode fracture for constant crack angle in all stress fields. The maximums and minimums in all cases are shifted per the remote stress. So, the maximums and minimums depend on the applied load for constant crack orientation. These extremes are also magnified around the location of angular positions. For in plane-stress σ_{xx}, the maximum value located around θ value of $25°$ and local minimums around $-150°$ and $120°$ for 20MPa remote stress. These values shifted to $-30°$ for maximum and around $\pm 115°$ for local maximums for remote stress of 50MPa. Considering in-plane stress σ_{yy} in Figure 4-15(b) the maximum and local maximums are increased with remote stress for tensile stress but decreased in compression stress case for angular location between θ value of $105°$ and $180°$. The phenomena of the maximums in shear stress fields τ_{xy}

same with that of σ_{yy} stress field as shown in Figure 4-15(c) despite the angular location of this maxima.

4.3.1 Thermo-Mechanical Stress Fields

For the Mixed Mode fracture loading case the crack is oriented to a certain degree from horizontal and the Thermo-Mechanical loading analysis performed by Abaqus executes the stress field near to the crack tip for different loading and parametric conditions. The temperature at discretized element node obtained from the steady-state heat transfer analysis from the Abaqus heat transfer procedure and then utilized as an input for general static procedure as a predefined ODB file to obtain the combined loading effect on the crack tip stress field across the plate.

In the above section, only the mechanical mixed-mode stress field with the different scenarios is investigated. Since one of the objectives of the research is to investigate the thermal effect on the stress field, the crack is considered as thermally insulated and inclined a certain degree from horizontal in the model in which it is an adiabatic crack. The same analogy of thermal and mechanical boundary conditions as the Mode-I case is utilized in this section. So, the boundary condition and the temperature field distribution for the inclined adiabatic crack plate are shown in Figure 4-16 below. Even though, the change in temperature field was observed while changing the boundary condition but the contour of the temperature field is not changed for the different temperatures at the boundary of the left and right edge of the plate. The value of boundary conditions and load is similar with above Section 4.2.1.1

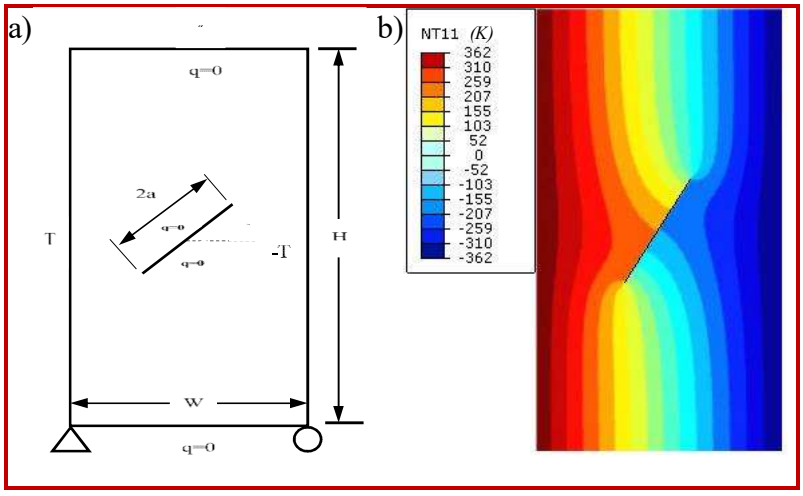

Figure 4-16. Thermo-mechanical conditions. (a) The boundary and loading conditions (b) The temperature field distribution

4.3.2 Varying Temperature

The temperature change at the right and left edge of the plate as shown in Figure 4-16 the temperature field is discontinuous across the crack and same for displacement field for adiabatic crack. This temperature distribution is employed as an input for general stress analysis in Abaqus to obtain the stress fields around the crack. The contour map of the Von Mises stress distribution at crack tip for different thermal boundary conditions i.e., temperature field distribution (ΔT_1, ΔT_2 and ΔT_3) for 100 MPa and crack angle of $\alpha = 30°$ is shown in Figure 4-17 below to distinguish the change in the stress field of the mixed-mode mechanical and thermo-mechanical loading cases. The effect of temperature change on the stress fields is investigated and shown hereafter. The stress components are extracted for radius r of 0.002m from the crack tip.

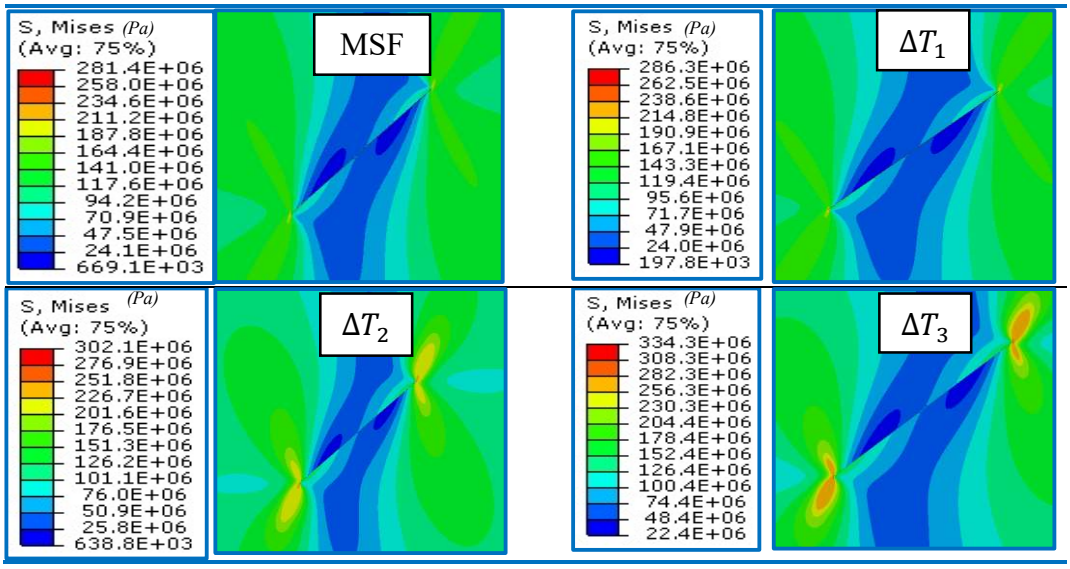

Figure 4-17. The contour map of mixed-mode mechanical and thermo-mechanical stress field around the crack tip for 100MPa and $\alpha = 30°$

From Figure 4-17 as shown above, it is observed that there is a change in the contour of stress fields around the crack tip as of Section 4.2.1.2 for the same loading with different thermo-mechanical loading figure out by the value of Von Mises stress. The extracted thermo-mechanical stress fields from the contour are shown in Figure 4-18 below. This change is due to the temperature change in the vicinity of the crack tip. For more elaboration to consider all parameters undertaken in this work the following graphical interpretation shows the change in phenomena around the crack tip.

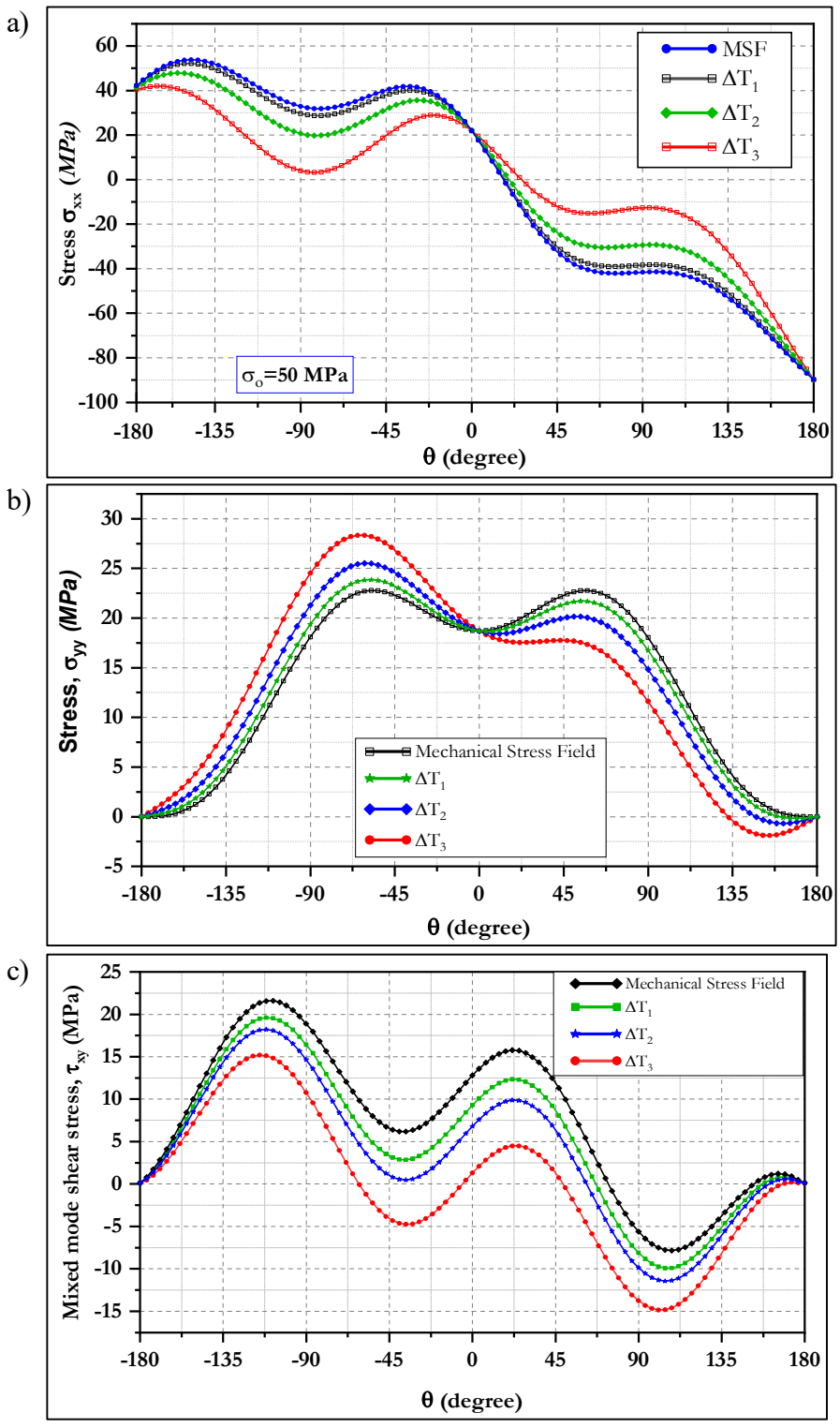

Figure 4-18. The Mixed Mode In-plane stress fields as a function of θ around crack tip with and without temperature gradient for same crack orientation and load. a). σ_{xx}, b). σ_{yy} and c). τ_{xy}

The figure showed that the stress field near the crack tip varied due to the effect of temperature upon the modeling of such Thermal-Stress analysis numerically by Abaqus software. The in-plane

stress σ_{xx} shown in Figure 4-18(a) has a maximum value around the open space created by a crack at about $\theta = -150°$ counting in clock wise direction from ahead of the crack tip and a local maximum around $\theta = -25°$ and $\theta = 100°$ for mechanical stress field as shown in the figure. These maximums decrease in magnitude in between the angular position θ between $\theta = -180°$ and $\theta = 0°$ as of temperature gradient increase. Despite this, the maximum values in angular position of $0° < \theta < 180°$ increase with increase in a temperature gradient. These phenomena of maximums and the contour of the stress field same for different remote stress. The in-plane stress σ_{xx} at $\theta = 0°$ is constant (crossed to each other) for all stress fields because temperature distribution becomes isothermal means no variation of temperature compared to the initial temperature of the plate and aligns with the mechanical stress fields. At $\theta = \pm 180°$ also the in-plane stress σ_{xx} start and ended with same value because of the adiabatic crack no temperature across the crack. The contour plot for mixed-mode is completely different from in pure mode I case described in the previous section.

For the in-plane stress in the y-direction σ_{yy} shown in Figure 4-18(b) contour plot is the vice versa of the in-plane stress σ_{xx} in magnitude of clockwise and anticlockwise direction. This stress field has a maximum value around $\theta = \pm 50°$ for mechanical stress field, this maximum value increase with an increasing temperature gradient in between the angular position of $-180° < \theta < 0°$ for clockwise direction but it decreases for the anticlockwise direction of $0° < \theta < 180°$ i.e., beyond $\theta = 0°$ that is below the mechanical stress field. The thermo-mechanical stress field for y-direction generates extra minimum values as the temperature gradient increased that approach to $\theta = 180°$. The value of the thermomechanical stress field follows the contour plot of the mechanical stress field but the maximums angular position varies accordingly shown in the last section of this chapter. As of θ value increase in clock wise direction, the value of σ_{yy} increased reached to its maximum beyond that decreasing including in anticlockwise direction until the local minimum value reached. After that increases θ approach to $180°$ for anticlock wise direction.

For the in-plane shear stress τ_{xy} shown in Figure 4-18(c), the contour of the stress field decreasing with an increase of the temperature gradient at the boundary of the crack. It has two maximum and minimums. These maximums and minimums are decreasing for the angular position of run from $\theta = -180°$ to $\theta = 180°$. This stress ended with zero stress at the crack open surface ($\theta = \pm 180°$) for thermo mechanical stress fields this is because of the distribution temperature around the crack surface. Generally, the stress fields are ended with the same stress value at $\theta =$

$\pm 180°$ this is because of the temperature near to the crack is null that makes the stress equitable with the mechanical stress.

4.3.3 Varying Crack Angle

The thermo-mechanical stress fields for the different crack ratio are depicted below for the constant remote stress and the temperature gradient as follow.

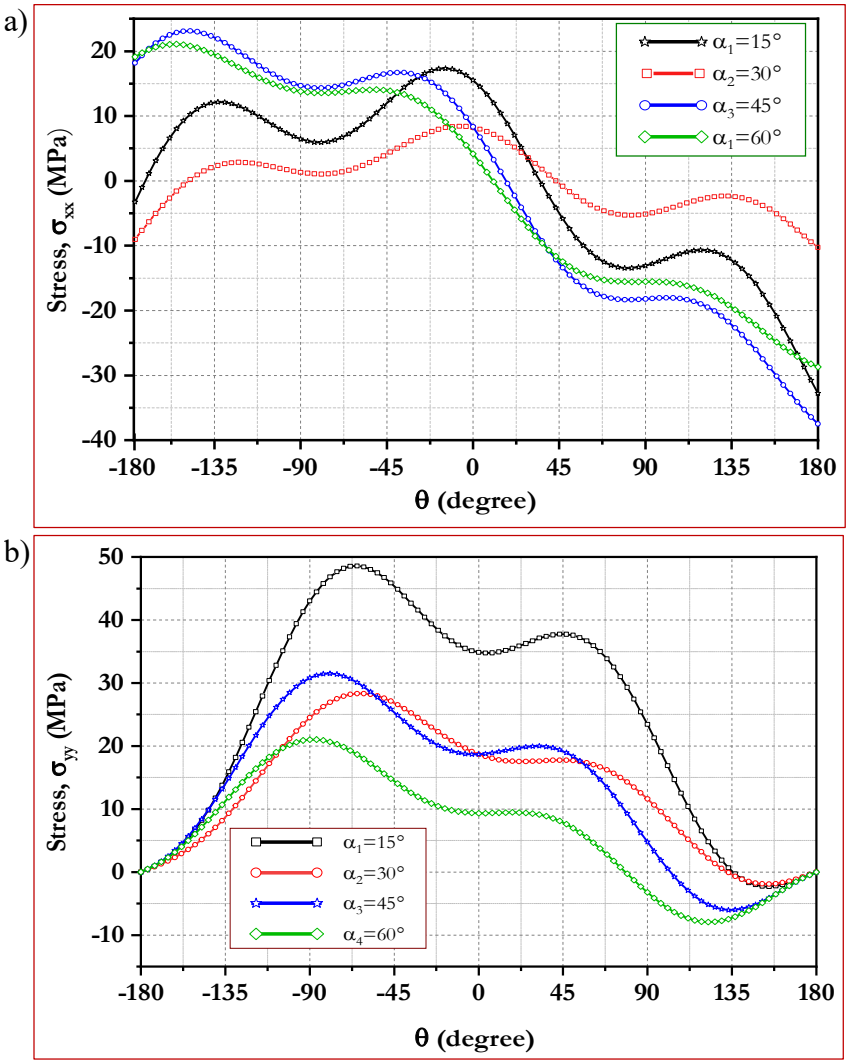

Figure 4-19. Mixed-mode thermo-mechanical stress fields for a varying crack angle for constant temperature gradient (ΔT_2). a). in-plane stress σ_{xx}, and b). in-plane stress σ_{yy}

In all phenomena in Figure 4-19 shown above the thermomechanical stress fields has the same contour as mechanical stress fields as shown in Figure 4-14 rather than the change in magnitude of the values of stress along with the angular position. As for the mechanical stress field, the change in the thermomechanical stress field varies with the crack angle superimposed with the mechanical load. This behavior of the stress field is shown for all in-plane stresses σ_{xx}, σ_{yy} and τ_{xy}. The

details of the maximums and minimums with their angular positions are depicted in the summary of this chapter.

4.3.4 Varying Remote Stress

In this section, the remote stress variation is implemented in the model while the temperature field and crack angle seize to constant and the mixed-mode mechanical and the thermo-mechanical stress fields are compared.

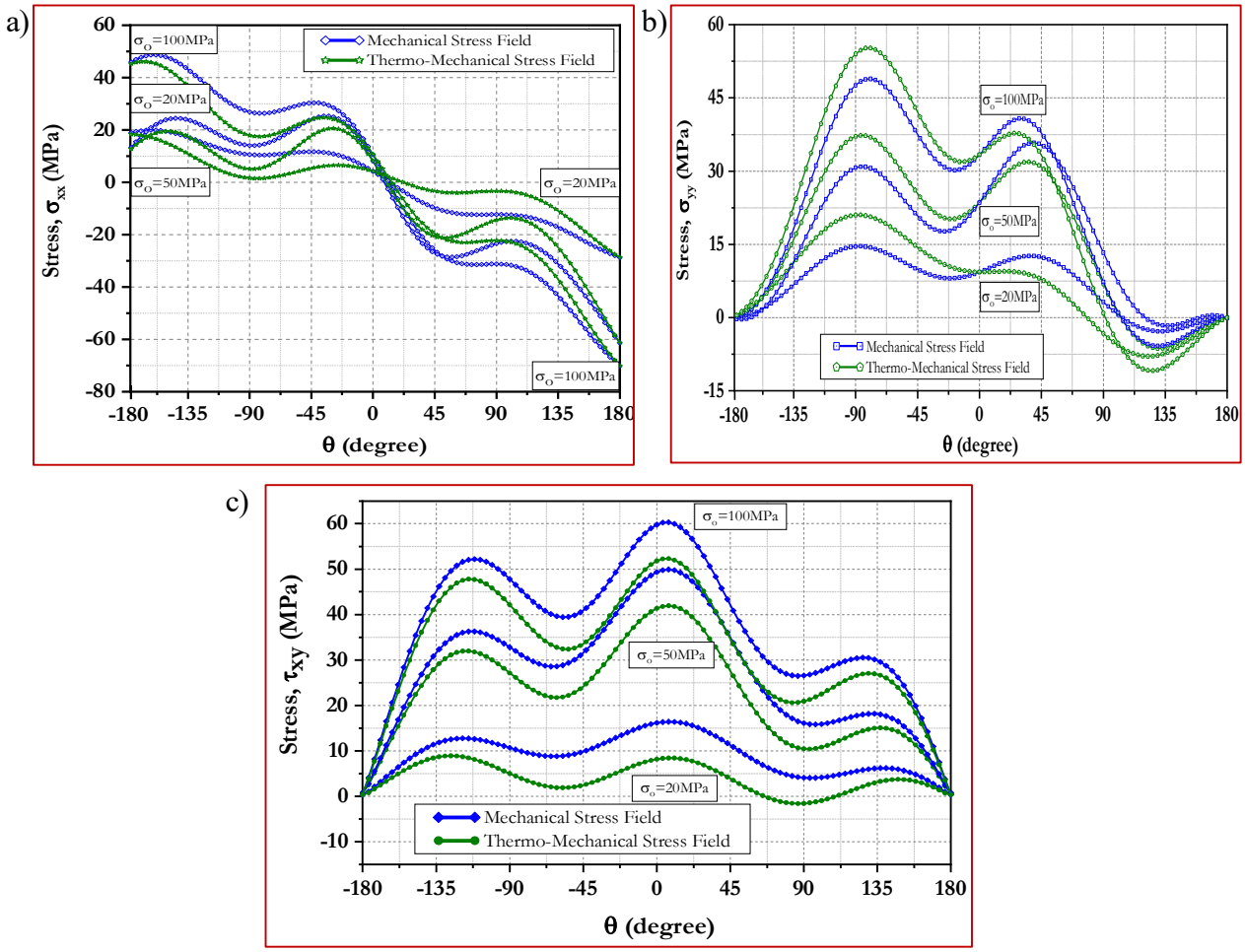

Figure 4-20. The mixed-mode in-plane stress fields as a function of θ around crack tip under varying remote stress for $\alpha = 60°$ and ΔT_3. a). σ_{xx}, b). σ_{yy} and c). σ_{xy}

In this Figure 4-20 shown above that the mechanical stress field and the thermo-mechanical stress fields have different stress values and any angular position except at $\theta = \pm 180°$ for tempreture gradient of ΔT_3. These phenomena of the stress field are also similar to the temperature gradient of ΔT_1 and ΔT_2 but the value is differed as shown in Figure 4-18(a-c). And the pattern of the contour for all cases of parametric conditions is the same despite its magnitude difference. As observed in Figure 4-20(a), the in-plane stress σ_{xx} for mixed mode mechanical and thermo

mechanical loading cases has same profile except for their magnitude but for varying the mechanical load applied on the plate the magnitude of the contour changes with the load i.e., increases as remote stress increase. However, the maximum and local maximum values are shifted upward with a change in load for angular position θ value in between $-180°$ and $0°$ for clock wise direction but these maximums shifted downward when the θ value in between $0°$ and $180°$ for anticlock wise direction from crack tip. For another in-plane stress σ_{yy} shown in Figure 4-20(c) the mixed mode stress fields for mechanical and thermo-mechanical cases seizes the same phenomena for each loading as shown in Figure 4-18(c). The stress field magnitude increases as of loading increase including the peaks and valleys. In all cases of loading the thermo-mechanical stress field beyond the mechanical stress field in an anti-clockwise direction for θ value in between $0°$ and $180°$ and above mechanical stress field for θ value in between $-180°$ and $0°$ in clock wise direction. But it is observed that a shift of maximum value to another angular position when the load increased i.e., the maximum value shifted from around $\theta = -90°$ to $\theta = -70°$ and the local maximum value shifted from around $\theta = 45°$ to $\theta = 20°$ for the load increased from $\sigma_o = 20MPa$ to $\sigma_o = 100MPa$. For the inplane shear stress τ_{xy} shown in Figure 4-20(c) the same type of profile of the stress field observed for different loading case except the change in the absolute magnitude of the result for both mixed-mode mechanical and thermo-mechanical stress fields. For all cases the thermo-mechanical stress field aligned with mechanical stress field at the crack open face this is because of thermally insulted crack considered in the analysis.

4.4 Summary

In this section, the effect of temperature gradient on the stress fields is summarized by investigating the maximum and minimum stress values under different conditions which are the remote stress, crack angle, crack ratio, different temperature gradient for comparison of the mechanical and thermo-mechanical stress fields for pure mode–I and mixed-mode cases as discussed in the above section. The former Table 4-2 shows the maximum and local minimum values of the mode-I mechanical and thermomechanical stress fields with their angular position from the crack tip for a constant crack length of all conditions depicted. The later Table 4-3 also shows the extreme mixed-mode mechanical and thermomechanical stress field values with their angular position from the crack tip for constant crack angle orientation of all conditions depicted.

Table 4-2. The effect of temperature on mode-I stress fields and its angular position on extreme values for the constant crack ratio

σ_o (MPa)	Mechanical Stress Fields (MPa)			Thermo-Mechanical Stress Fields (MPa)								
				ΔT_1			ΔT_2			ΔT_3		
(MPa)	σ_{xx}	σ_{yy}	τ_{xy}	σ_{xx}	σ_{yy}	τ_{xy}	σ_{xx}	σ_{yy}	τ_{xy}	σ_{xx}	σ_{yy}	τ_{xy}
Maximum Values (MPa)												
20	16.48	45.59	15.98	16.5	46.71	16.74	16.48	48.39	14.1	16.59	51.23	12.26
50	45.83	117.72	39.54	45.81	118.8	40.35	45.8	120.31	37.52	45.8	122.9	35.52
100	161.11	290.43	70.861	161.1	290.5	71.8	161.1	290.49	68.55	161.1	290.6	66.24
	Angular Position (degree)											
20	0	-60.12	-112.3	0	-60.48	-109.4	0	-62.28	-112.3	0	-62.28	-115.6
50	0	-53.64	-106.5	0	-53.64	-104.4	0	-53.64	-107.2	0	-54.36	-107.3
100	0	-1.08	-93.6	0	-56.88	-92.88	0	-1.08	-93.6	0	-1.08	-93.96
Local Minimum Values (MPa)												
20	-21	37.42	-15.82	-20.97	37.42	-15.04	-21.01	37.42	-17.82	-21.07	-1.611	-19.84
50	-52.41	98.32	-39.13	-52.42	98.32	-38.3	-52.45	98.32	-41.24	-52.52	-1.430	-43.35
100	-104.5	290	-70.30	-104.6	290	-69.4	-104.6	289.91	-72.64	-104.7	-1.29	-75
	Angular Position (degree)											
20	$\pm$180	0	109.44	$\pm$180	0	109.4	$\pm$180	0	106.6	$\pm$180	160.2	106.6
50	$\pm$180	0	104.4	$\pm$180	0	104.4	$\pm$180	0	102.3	$\pm$180	163.1	102.3
100	$\pm$180	0	92.52	$\pm$180	0	92.88	$\pm$180	0	92.52	$\pm$180	164.2	92.52

In this table the extreme values of the in-plane stress σ_{xx} for both mechanical and thermomechanical stress fields coincide the same value with their angular position but the profile of the contours of them are different. For in-plane stress σ_{yy} the maximum values of the stress field increase horizontally from left to right and vertically top to downward. The angular position of maximum value approach to $\theta = 0°$ vertically and horizontally a small angle shift of angular position observed for temperature gradient increase. The local minimum value decreases horizontally i.e., temperature gradient increases and the angular position of this extreme shift from $\theta = 0°$ to around $\theta = 160°$ and vertically increase to $\theta = 164.2°$ from top to down. The maximum value of in-plane shear stress τ_{xy} increases vertically from top to down that is with applied stress and horizontally decreases from right to left as temperature gradient increases. The angular position of this stress increases vertically in negative value but horizontally a little shift in angle is observed but it is almost the same. The local minimum value of in-plane shear stress τ_{xy} decreases both vertically and horizontally in negative value. The angular position of this local minimum decreases vertically from to down as of the applied increase but horizontally approaches to the same angle.

Table 4-3. The effect of temperature on mixed-mode stress fields and its angular position on extreme values for same crack orientation

σ_o (MPa)	Mechanical Stress Fields (MPa)			Thermo-Mechanical Stress Fields (MPa)								
				ΔT_1			ΔT_2			ΔT_3		
	σ_{xx}	σ_{yy}	τ_{xy}	σ_{xx}	σ_{yy}	τ_{xy}	σ_{xx}	σ_{yy}	τ_{xy}	σ_{xx}	σ_{yy}	τ_{xy}
Maximum Values (MPa)												
20	8.24	22.79	7.98	9.71	23.87	3.56	24	25.53	5.994	84.25	28.34	6.56
50	43.75	108.2	49	42.2	109.32	44.423	40.7	111.01	46.96	44.35	113.83	47.53
100	35.9	144.43	66.55	34.76	145.46	61.65	33.9	147.02	64.4	36.35	149.62	65.02
	Angular Position (degree)											
20	0	-64.3	-108	18	-64.25	-115.2	100.8	-64.5	-111.6	-7.2	-64.86	-111.6
50	-10.8	-61.2	-108	-7.2	-61.2	-111.6	0	-61.2	-111.6	-10.8	-61.2	-108
100	-7.2	-54	-104.4	-7.2	-54	-104.4	0	-54	-104.4	-10.8	-54	-104.4
Local Minimum Values (MPa)												
20	-10.26	0	-7.91	-11.02	-1.66	-12.73	-27.7	-6.72	-9.97	-10.26	-1.9	-9.38
50	-79.14	0	-23.842	-79.14	-2.83	-28.75	-79.14	-7.12	-26	-79.14	-1.61	-25.38
100	-110.08	0	-19.8	-110.8	-0.93	-24.97	-110.8	-3.452	-23	-110.8	-0.97	-21.4
	Angular Position (degree)											
20	180	180	108	-82.8	169.2	100.8	-86.4	162	104.4	180	154.8	108
50	180	180	104.4	180	170	104.4	180	165.6	104.4	180	162	104.4
100	180	180	100.8	180	172.8	97.2	180	169.2	100.8	180	165.6	100.8

In this table, the mixed-mode extreme values of the mechanical stress fields and thermomechanical stress fields are extracted. For in-plane stress σ_{xx} the maximum value changes relative to the remote stress but horizontally it increases as the temperature gradient increase for all applied stress used in this work. The angular position of this maximum value shifts relative to each other as remote stress varies vertically and horizontally a shift in angular position observed for temperature gradient vary. The local minimum value of in-plane stress σ_{xx} decrease vertically as remote stress increase in negative value and is observed for all conditions but horizontally same value observed what if temperature gradient happens. No shift of the angular position of this minimum value was observed vertically as of remote stress increase and horizontally also no change in angular position except for 20MPa.

The maximum values of in-plane stress σ_{yy} increases vertically as of remote stress increase for mechanical and thermomechanical stress field case and also increases horizontally for all remote stress as temperature gradient increases. The angular position of this maximum value varies from around $\theta = -64°$ to $\theta = -54°$ for all cases vertically and horizontally no change in angular position observed. The local minimum value of this in-plane stress σ_{yy} fluctuates vertically for all cases but it decreases horizontally when the temperature gradient increase from ΔT_1 to ΔT_3 in the negative value. The angular position of this minimum value increases vertically for the

thermomechanical stress field but $\theta = 180°$ for the mechanical stress field and decreases as the temperature gradient increases horizontally. For in-plane shear stress τ_{xy}, the maximum value increases with remote stress increase vertically for all cases and decreases with temperature gradient increase. The angular position of the maximum value decreases as remote stress increase vertically but a little shift in angular position is observed, horizontally for temperature gradient increase but almost constant. The local minimum of this in-plane stress τ_{xy} varies as remote stress increase vertically and also varies with temperature gradient increase horizontally. The angular position this local minimum value decrease with increase in remote stress but a little difference observed horizontally as temperature gradient increase but considered as no shift in angular position.

4.5 Discussion

Based on the results the change in stress fields for a certain radian value (0.002m) from crack tip is observed for mode I as well as mixed mode fracture loading cases using different temperature boundary conditions at the edges of the plate. According to the result shown in both Sections 4.2 and 4.3 a change in mechanical stress fields observed for varying crack ratio, remote stress and crack angle. This is due to mathematical relation of the stress fields with crack length and remote stress. But for mixed mode case the change in stress fields vary accordingly because of the fracture mode I and mode -II domination for varying crack angle observed.

For thermo-mechanical stress fields, for all conditions the stress field at the crack surface seizes to constant as shown in Figure 4-9 and Figure 4-18 at the angular position of $\theta = 180°$ and $\theta = -180°$ because no temperature variation across the crack that develops thermal stress and the crack is adiabatic (thermally insulated). In addition, the thermo-mechanical stress fields alongside of the crack tip at angular position of $\theta = 0°$, the stress components σ_{xx} and σ_{yy} are preserves to constant due to the temperature distribution is settled to zero according to the temperature distribution shown in Figure 4-7 and Figure 4-16 for mode I and mixed mode loading cases respectively. The increment and decrement of the plot of thermo-mechanical stress fields with temperature gradient is observed because of the compressive and tensile thermal stress develops with respect to the sign of temperature with their respective magnitude. The rise and fall of the maximum and minimum values with respect to the mechanical stress is calculated as follow.

$$Percentage\ Change(\%) = \frac{Increase/Decrease}{Original(Reference)\ Number} \times 100$$

For the case of this research: -

In case of Maximum values

$$Percentage\ Change(\%) = \frac{(Max.\ Thermo - Mechanical\ ) - (Max.\ Mechanical\ )}{Max.\ Me\ \ hanical\ Stres} \times 100$$

In case of Minimum values

$$Percentage\ Change(\%) = \frac{(Mi\ \ .\ Thermo - Mechanical\ ) - (Min.\ Me\ \ hanical\ )}{Min.\ Mechanical\ Stress} \times 100$$

Based on the above percentage increase or decrease calculation the rise and falling of the stress values for the case of pure mode-I and mixed mode cases depicted as shown in the figure below.

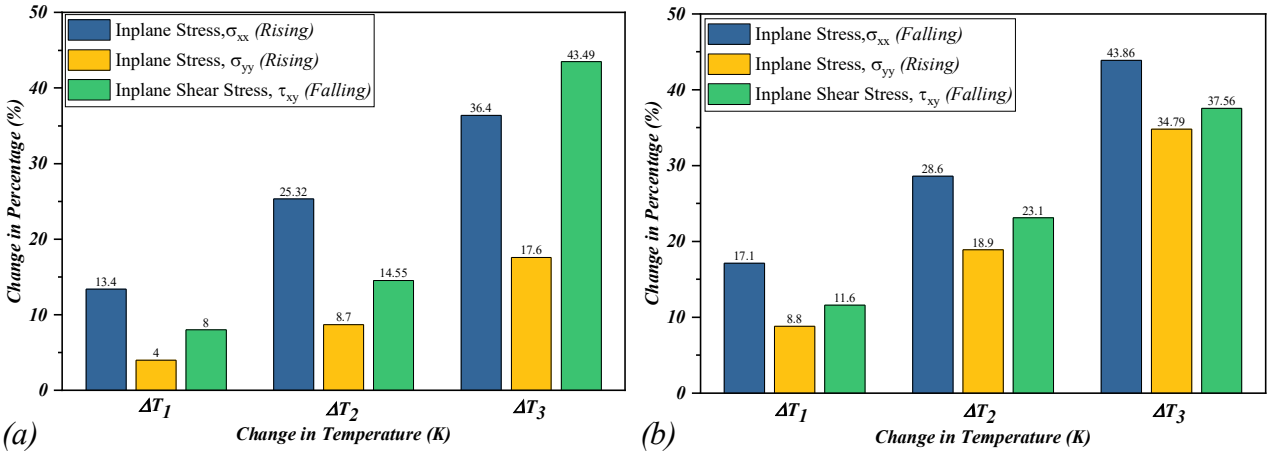

Figure 4-21. The percentage change in extreme stress values for Pure Mode-I case. (a) Maximum and (b). Minimum values

The above figure shows that the rising and falling of the extreme values relative to the mechanical extreme values. Generally, there is a change in stress values at the point of maximum or minimum values with respect to the temperature change for the case of Pure Mode- I loading. The in-plane stresses (σ_{xx} and σ_{yy}) are rising from 13.4 to 36.39% and 4 to 17.6% respectively while the in-plane stress τ_{xy} falling by 8 to 43.49% in rising of temperature change ΔT_1 to ΔT_3 in case of considering the maximum values. However, in case of considering the minimum values the in-plane stresses (σ_{xx} and τ_{xy}) are falling by 17.1 to 43.86% and 11.6 to 37.56% respectively while the in-plane stress σ_{yy} increasing by 8.8 to 34.79% in rising of temperature change ΔT_1 to ΔT_3 for the pure mode-I thermo-mechanical loading.

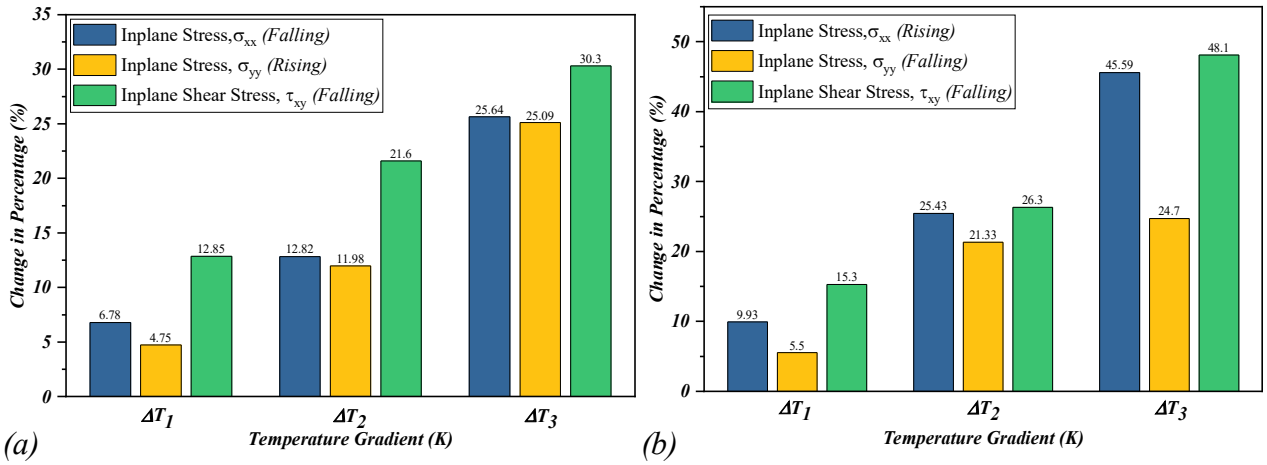

Figure 4-22. The percentage change in extreme stress values for Mixed Mode case. (a) Maximum and (b). Minimum values

The phenomenon of the extreme values for the case of mixed and pure mode-I loading cases are differ each other. These has shown in the above figures and in summery section of the paper. Based on this, the above figure shows that the rising and falling of the extreme values relative to the mechanical extreme values. Generally, there is a change in stress values at the point of maximum or minimum values with respect to the temperature change for the case of Mixed Mode loading. The in-plane stresses (σ_{xx} and τ_{xy}) are falling from 6.78 to 25.64% and 12.85 to 30.3% respectively while the in-plane stress σ_{yy} rising by 4.75 to 25.09% in rising of temperature change ΔT_1 to ΔT_3 in case of considering the maximum values. However, in case of considering the minimum values the in-plane stresses (σ_{yy} and τ_{xy}) are falling by 5.5 to 24.7% and 15.3 to 48.1% respectively while the in-plane stress σ_{xx} increased by 9.93 to 45.59% in rising of temperature change ΔT_1 to ΔT_3 for the mixed mode thermo-mechanical loading. All in all, the shear stress maximum values are falling whereas the variation of extreme values for other in plane stresses are observed.

4.6 Validation Using the Analytical Results

In this section, the outputs of the numerical result which is by numerical method and by the analytical method for thermo mechanical stress field contour plot for mixed mode loading case is presented. Validation is performed by using the paper Kidane, Chalivendra, & Shukla, 2010 since this work also the continuation of it except for stationary crack and considering mode-I loading condition. For the case of analytical methodology of capturing the stress field, the developed formula considers a moving crack (propagating crack) at constant speed along $x-$ direction and the plot of stress fields are normalized. So, here in this paper it is used to validate the contour map

of the stress shapes not the direct results. Figure 4-23 represents the normalized mixed-mode in-plane stress fields as functions of θ around the crack tip for different temperature fields taken from (Kidane et al., 2010).

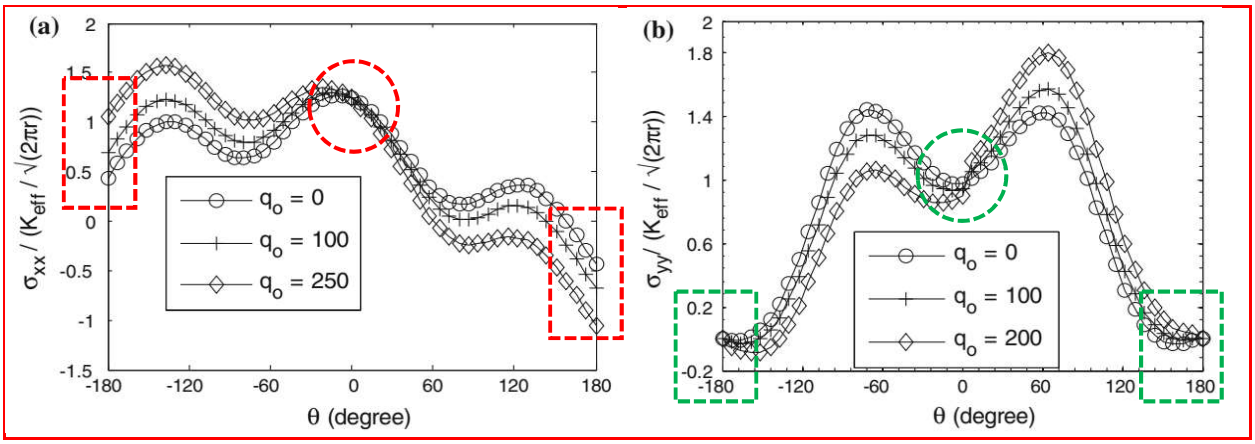

Figure 4-23. The analytical normalized mixed-mode in-plane stress fields as functions of θ around the crack tip for different temperature fields. a). σ_{xx} and b). σ_{yy}(Kidane et al., 2010)

The Figure 4-23 above shows there is a change in thermomechanical stress field based on the change in temperature field where q_0 stands for temperature coefficient (real constant) analytically. For comparison the numerical result for mixed mode fracture is depicted as follow.

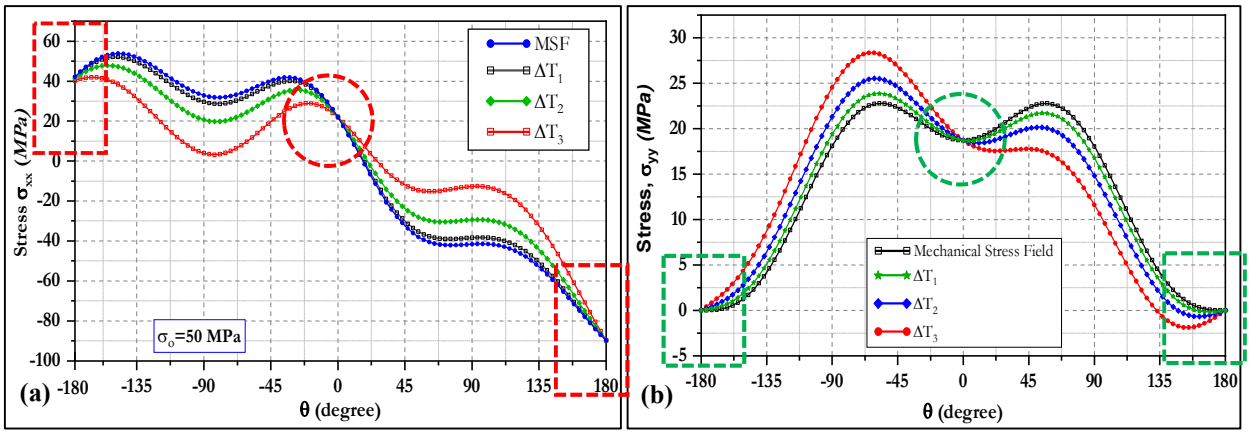

Figure 4-24. The numerical mixed mode in-plane stress fields as a function of θ around crack tip with temperature gradient for same crack orientation and load. a). σ_{xx}, b). σ_{yy}

The two figure above shows the change in stress fields observed for both analytical and numerical method. The corresponding validation of the result is between Figure 4-23(a) and Figure 4-24(a) which is the in-plane stress along $x-$direction and between Figure 4-23(b) and Figure 4-24(b) which is in plane stress along $y-$direction. Considering the in-plane stress σ_{xx}, the corresponding a high change in the stress with thermal load at angular position of $\theta = \pm 180°$ for analytical one (Figure 4-23(a)) is because of the in plane stress depends on both the propagation

of the crack along x −direction allowed to propagate by a constant speed but not y −direction and the change in thermal load according to the analytically developed equation(the reference coordinate transformed to crack-tip coordinates) whereas the corresponding numerical results (Figure 4-24(a)) shows no change in stress at $\theta = \pm 180°$ since the crack is adiabatic and also stationary i.e. propagating of crack is not allowed as well as no temperature variation at the heads of crack tip based on Figure 4-7 as the red dotted rectangular plot represents in both figures. For the case of $\theta = 0°$ both numerical and analytical values coincide to same stress value as represented by red dotted circle plot on figure.

Considering the in-plane stress σ_{yy}, the change in the stress at angular position of $\theta = \pm 180°$ like for in-plane stress σ_{xx} is not observed for both analytical and numerical result shown in Figure 4-23 and Figure 4-24(b) this is because of propagation is allowed only along x −direction for analytical result and for numerical it is stationary as represented in green dotted rectangle plot in corresponding figures. At a head of crack tip for certain radian value i.e., at $\theta = 0°$ both numerical and analytical values coincide to same stress value as represented by green dotted circle plot on figures. The flip of change in increment and decrement in contour map of stress components observed in Figure 4-23 and Figure 4-24 due to the temperature field distribution change. The temperature field distribution change as shown in Figure 4-7 is directly linked with the boundary conditions given in the problem. This variation of the boundary condition affects the phenomenon of the stresses. These situation results for the variation of stress plot from $0°$ to $180°$ and $0°$ to $-180°$ for analytical and numerical cases shown in Figure 4-23 and Figure 4-24. These all phenomena of the result showed the reliability of the numerical result with that of analytically developed results.

Chapter Five
5 Conclusion and Recommendation

5.1 Conclusion

The thesis goes through finding the thermomechanical stress field around crack tip away from for radius of 0.002m numerically by Abaqus software modeling the crack using Extended Finite Element Method (XFEM). It checks the effect of temperature field distribution on the two-dimensional plate for mode-I and mixed-mode fracture cases by considering the crack thermally insulated or adiabatic crack. The problem was simulated by utilizing the heat transfer for temperature field distribution and the Thermal-Stress procedure for thermomechanical stress distribution in Abaqus software. Upon this, the following points are observed based on numerical mechanical and thermo-mechanical stress field contour plot developed in the previous chapter:

- The temperature field distribution in the material has an impact on the stress field in the vicinity of the crack tip this may lead to unexpected failure of material that not considers the temperature effect during designing.
- When the temperature gradient increases the absolute magnitude of the stress field σ_{xx} and σ_{yy} increase for $0° \leq \theta \leq 180° and \quad -180° \leq \theta \leq 0°$ respectively but decreases vice versa in addition the shear stress τ_{xy} decreases for $-180° \leq \theta \leq 180°$.
- The stress field for thermo-mechanical loading cases preserves the profile of the mechanical stress field but the value differs from it.
- The contour plot of the stress field in the vicinity of the crack tip varies in mode-I and mixed-mode loading cases for both mechanical and thermomechanical stress fields.
- A shift in angular positions of the in-plane thermo-mechanical stress maximum and minimum values was observed.

5.2 Recommendation and Future Works

This research is intended for finding the crack tip stress field around crack for Mode–I and Mixed Mode fracture and investigates the thermal effect around the crack tip. Based on the result, the temperature affects the stress field around the crack tip that tends to make overstressed on surrounding crack for all components of in-plane stresses. Upon the way of this thesis work, the following recommendation points are drawn for the precondition of material design and selection for a certain purpose. Since the overstressed on surrounding of the crack by thermo-mechanical loading leads to a precondition for designers and material personnel to consider the thermal effect.

Upon doing this research work, numerical modeling of the stress field around the crack tip for homogeneous materials some gabs observed and recommended to fill in the next researches. So, the following points are recommended that needs further study: -

- Considering the crack as thermally conductive, isothermal crack and study the thermomechanical stress field around the crack tip.
- Modelling of the thermomechanical stress field for another type of materials that has different thermal and mechanical properties i.e., inhomogeneous materials, FGMs, etc.
- Studying the thermal effect on the fracture parameters such as stress intensity factor, strain energy rate.
- The effect of temperature or heat flux on the crack propagation direction compared with analytically developed formula.
- Expanding this thesis work methodology for certain engineering component applications.

References

Abaqus Documentation 6.12, A. (2016). *Analysis User's Manual Volume II: Analysis*.

Abotula, S., Kidane, A., Chalivendra, V. B., & Shukla, A. (2012). Dynamic Curving Cracks in Functionally Graded Materials Under Thermo-Mechanical Loading. *International Journal of Solids and Structures*, *49*(13), 1637–1655. https://doi.org/10.1016/j.ijsolstr.2012.03.010

Aglan, H., Qian, Z., & Mitra-Majumdar, D. (1992). The Effect of Temperature on the Critical Failure Properties of Advanced Polymer Composites. *Polymer Testing*, *11*, 169–184. https://doi.org/10.1016/0142-9418(92)90048-G

Ai, W. (2018). *Computational Fracture Modelling by an Adaptive Cracking Particle Method*. Durham University.

Anderson, D. D. (2002). *Experimental Investigation of Quasistatic and Dynamic Fracture Properties of Titanium Alloys* [California Institute of Technology]. https://doi.org/10.7907/NHZS-D271

Anderson, T. L. (1995). *Fracture Mechanics: Fundamentals and Applications* (Second Edi). CRC Press.

Bäker, M., Reese, S., & Silberschmidt, V. V. (2019). Simulation of Crack Propagation Under Mixed-Mode Loading. In *Handbook of Mechanics of Materials*. Springer Nature Singapore Pte Ltd.

Bathini, U., Srivatsan, T. S., Patnaik, A., & Quick, T. (2010). A Study of the Tensile Deformation and Fracture Behavior of Commercially Pure Titanium and Titanium Alloy : Influence of Orientation and Microstructure. *Journal of Materials Engineering and Performance*, *19*(8), 1172–1182. https://doi.org/10.1007/s11665-010-9613-5

Bordas, S., & Duflot, M. (2007). Derivative Recovery and A Posteriori Error Estimate for Extended Finite Elements. *Computer Methods in Applied Mechanics and Engineering*, *196*(35–39), 3381–3399. https://doi.org/10.1016/j.cma.2007.03.011

Bostanci, S. M. (2019). *Finite Element Modelling of TBC Failure Mechanisms by Using Extended Finite Element Method and Cohesive Zone Method*. Middle East Technical University.

Bouhala, L., Makradi, A., & Belouettar, S. (2012). Thermal and Thermo-Mechanical Influence on Crack Propagation Using an Extended Mesh Free Method. *Engineering Fracture Mechanics*, *88*, 35–48. https://doi.org/10.1016/j.engfracmech.2012.04.001

Boutabout, B., Chamaa, M., Bouiadjra, B. A. B., Serier, B., & Lousdad, A. (2009). Effect of Thermomechanical Loads on the Propagation of Crack Near the Interface Brittle/Ductile.

Computational Materials Science, *46*(4), 906–911. https://doi.org/10.1016/j.commatsci.2009.04.039

Broek, D. (1986). *Elementary Engineering Fracture Mechanics* (Fourth edi). Martinus Nijhoff Publishers (1986). https://doi.org/10.1007/978-94-009-4333-9

Carla, M., Rodrigues, M., Santos, L. D. A., Engenharia, E. De, & Horizonte, B. (2017). Influence of Temperature on Mechanical Properties , Fracture Morphology and Strain Hardening Behavior of a 304 Stainless Steel. *Materials Research*, *20*, 141–151. https://doi.org/10.1590/1980-5373-mr-2016-0932

Chen, H., Wang, Q., Liu, G. R., Wang, Y., & Sun, J. (2016). Simulation of thermoelastic Crack Problems Using Singular Edge-Based Smoothed Finite Element Method. *International Journal of Mechanical Sciences*, *115*, 123–134. https://doi.org/10.1016/j.ijmecsci.2016.06.012

Duan, C., Chen, X., & Li, R. (2020). The Numerical Simulation of Fatigue Crack Propagation in Inconel 718 Alloy at Different Temperatures. *Aerospace Systems*, *3*, 87–95. https://doi.org/10.1007/s42401-020-00044-z

Duflot, M. (2008). The Extended Finite Element Method in Thermoelastic Fracture Mechanics. *International Journal for Numerical Methods in Engineering*, *74*(5), 827–847. https://doi.org/10.1002/nme

Esmati, V., Nazari, M. B., & Mahdizadeh, M. (2018). Implementation of XFEM for Dynamic Thermoelastic Crack Analysis Under Non-Classic Thermal Shock. *Theoretical and Applied Fracture Mechanics*, *95*, 42–58. https://doi.org/10.1016/j.tafmec.2018.02.007

Fries, T. (2018). Extended Finite Element Methods (XFEM). *Encyclopedia of Continuum Mechanics*, 1–10. https://doi.org/10.1007/978-3-662-53605-6 17-1

Fu, Y., Wang, Z., Ren, F., & Wang, D. (2017). Numerical Model of Thermo-Mechanical Coupling for the Tensile Failure Process of Brittle Materials. *AIP Advances*, *10*(10), 105023–17. https://doi.org/10.1063/1.4977701

Goli, E., Bayesteh, H., & Mohammadi, S. (2014). Mixed Mode Fracture Analysis of Adiabatic Cracks in Homogeneous and Non-Homogeneous Materials in the Framework of Partition of Unity and the Path-Independent Interaction Integral. *Engineering Fracture Mechanics*, *131*, 100–127. https://doi.org/10.1016/j.engfracmech.2014.07.013

Grégoire, D., H. Maigre, Réthoré, J., & Combescure, A. (2007). Dynamic Crack Propagation Under Mixed-Mode Loading – Comparison Between Experiments and X-FEM Simulations.

International Journal of Solids and Structures, *44*(20), 6517–6534. https://doi.org/10.1016/j.ijsolstr.2007.02.044

Guo, W. G., & Cheng, J. Y. (1999). MECHANICAL PROPERTIES AND DEFORMATION MECHANISMS OF A COMMERCIALLY PURE TITANIUM. *Acta Materials*, *47*(13), 3705–3720.

Habib, F., Sorelli, L., & Fafard, M. (2018). Full Thermo-Mechanical Coupling Using Extended Finite Element Method in Quasi-Transient Crack Propagation. *Advanced Modeling and Simulation in Engineering Sciences*, *5*(1), 1–18. https://doi.org/10.1186/s40323-018-0112-9

Hosseini, S. S., Bayesteh, H., & Mohammadi, S. (2013). Thermo-mechanical XFEM crack propagation analysis of functionally graded materials. *Materials Science & Engineering A*, *561*, 285–302. https://doi.org/10.1016/j.msea.2012.10.043

Jeyakodi, G. K. (2016). *Finite Element Simulation of the In - Situ AFP process for Thermoplastic Composites using Abaqus*. Delft University of Technology.

Kanninen, M. F., & Popelar, C. H. (1985). *Advanced Fracture Mechanics* (First Edit). Oxford University Press.

Khoei, A. R. (2015). *EXTENDED FINITE ELEMENT METHOD: THEORY AND APPLICATIONS*. John Wiley & Sons.

Kidane, A., Chalivendra, V. B., & Shukla, A. (2010). Thermo-mechanical stress fields and strain energy associated with a mixed-mode propagating crack. *Acta Mechanica*, *215*(1), 57–69. https://doi.org/10.1007/s00707-010-0305-x

Kidane, A., Chalivendra, V. B., Shukla, A., & Chona, R. (2010). Mixed-Mode Dynamic Crack Propagation in Graded Materials Under Thermo-Mechanical Loading. *Engineering Fracture Mechanics*, *77*(14), 2864–2880. https://doi.org/10.1016/j.engfracmech.2010.07.004

Kotousov, A. G. (2002). On a thermo-mechanical effect and criterion of crack propagation. *International Journal of Fracture*, *114*(4), 349–358.

Kumar, S., Singh, I. V, Mishra, B. K., & Singh, A. (2016). New Enrichments in XFEM to Model Dynamic Crack Response of 2-D Elastic Solids. *International Journal of Impact Engineering*, *87*, 198–211. https://doi.org/10.1016/j.ijimpeng.2015.03.005

Lee, K. H., Chalivendra, V. B., & Shukla, A. (2008). Dynamic Crack-Tip Stress and Displacement Fields Under Thermomechanical Loading in Functionally Graded Materials. *Journal of Applied Mechanics*, *75*(5), 1–7. https://doi.org/10.1115/1.2932093

Liu, X. Y., Xiao, Q. Z., & Karihaloo, B. L. (2004). XFEM for Direct Evaluation of Mixed Mode

SIFs in Homogeneous and Bi-Materials. *International Journal for Numerical Methods in Engineering*, *59*(8), 1103–1118. https://doi.org/10.1002/nme.906

Menouillard, T., Song, J., Duan, Q., & Belytschko, T. (2010). Time Dependent Crack Tip Enrichment for Dynamic Crack Propagation. *International Journal of Fracture*, *162*(1–2), 33–49. https://doi.org/10.1007/s10704-009-9405-9

Moës, N., Dolbow, J. E., & Sukumar, N. (2017). Extended Finite Element Methods. *Encyclopedia of Computational Mechanics*. https://doi.org/10.1002/9781119176817.ecm2111

Nguyen, M. N., Bui, T. Q., Nguyen, N. T., Truong, T. T., & Lich, L. Van. (2017). Simulation of Dynamic and Static Thermoelastic Fracture Problems by Extended Nodal Gradient Finite Elements. *International Journal of Mechanical Sciences*, *134*, 370–386. https://doi.org/10.1016/j.ijmecsci.2017.10.022

Nishioka, T. (1994). The State of the Art in Computational Dynamic Fracture Mechanics. *JSME International Journal*, *37*(4), 313–333. https://doi.org/10.1299/jsmea1993.37.4_313

Nishioka, T. (2003). Computational Aspects of Dynamic Fracture. *Comprehensive Structural Integrity*, *3*, 211–254.

Owen, D. R. J., & Fawkes, A. J. (1983). *Enigineering Fracture Mechanics: Numerical Methods and Applications*. Pineridge Press Ltd.

Pant, M., Singh, I. V, & Mishra, B. K. (2010). Numerical Simulation of Thermo-Elastic Fracture Problems Using Element Free Galerkin Method. *International Journal of Mechanical Sciences*, *52*(12), 1745–1755. https://doi.org/10.1016/j.ijmecsci.2010.09.008

Pant, M., Singh, I. V, & Mishra, B. K. (2011). A Numerical Study of Crack Interactions Under Thermo-Mechanical Load Using EFGM. *Journal of Mechanical Science and Technology*, *25*(2), 403–413. https://doi.org/10.1007/s12206-010-1217-3

Parameswaran, V., & Shukla, A. (1999). Crack-tip Stress Fields for Dynamic Fracture in Functionally Gradient Materials. *Mechanics of Materials*, *31*(9), 579–596. https://doi.org/10.1016/S0167-6636(99)00025-3

Parkus, H. (1976). *Thermoelastlclty* (S. Edition (ed.)). Springer-Verlag. https://doi.org/10.1007/978-3-7091-8447-

Sepehri, J. (2014). *Application of Extended Finite Element Method (XFEM) to Simulate Hydraulic Fracture Propagation from Oriented Perforations*. Texas Tech University.

Sheng, A. (2018). *Modeling Brittle Fracture Under Thermo-Mechanical Loading with Discrete Volterra Dislocation Arrays*. UNIVERSITY OF CALIFORNIA.

Sih, G. C. (1962). On the Singular Character of Thermal Stresses Near a Crack Tip. *Journal of Applied Mechanics*, *29*(3), 587–589.

Simachew, H., & Kidane, A. (2020). *Mathematical Modeling for Thermo-Mechanical Stress Field Associated with A Propagating Crack in Homogenous Isotropic Materials*. Addis Ababa University.

T.L. Anderson. (2005). *Fracture Mechanics: Fundamentals and Applications* (Third Edit). Taylor & Francis Group, LLC.

William D. Callister, J. (2001). *Fundamentals of Materials Science and Engineering*. John Wiley & Sons, Inc.

Yadav, A., Patil, R. U., Singh, S. K., Godara, R. K., & Bhardwaj, G. (2020). A thermo-Mechanical Fracture Analysis of Linear Elastic Materials Using XIGA. *Mechanics of Advanced Materials and Structures*, 1–26. https://doi.org/10.1080/15376494.2020.1838006

Ye, J., Wang, Y., Li, Z., Saafi, M., Jia, F., Huang, B., & Ye, J. (2020). Failure Analysis of Fiber-Reinforced Composites Subjected to Coupled Thermo- Mechanical Loading. *Composite Structures*, *235*, 111756. https://doi.org/10.1016/j.compstruct.2019.111756

Zamani, A., & Eslami, M. R. (2010). Implementation of the Extended Finite Element Method for Dynamic Thermoelastic Fracture Initiation. *International Journal of Solids and Structures*, *47*(10), 1392–1404. https://doi.org/10.1016/j.ijsolstr.2010.01.024

Zamani, A., Gracie, R., & Eslami, M. R. (2010). Higher Order Tip Enrichment of eXtended Finite Element Method in Thermoelasticity. *Computational Mechanics*, *46*(6), 851–866. https://doi.org/10.1007/s00466-010-0520-2

Zehnder, A. T. (2012). *Fracture Mechanics* (Vol. 62). Springer Netherlands.

Zehnder, A. T., & Rosakis, A. J. (1991). On the Temperature Distribution at the Vicinity of Dynamically Propagating Cracks in 4340 Steel. *Journal of the Mechanics and Physics of Solids*, *39*(3), 385–415.

Zen, F. (2013). *Crack Modelling with the eXtended Finite Element Method*.

Zhu, X. K. (2016). Corrected Stress Intensity Factor Solution for A British Standard Single Edge Notched Tension (SENT) Specimen. *Fatigue and Fracture of Engineering Materials and Structures*, *39*(1), 120–131. https://doi.org/10.1111/ffe.12351

Appendix-A

The material property of the commercial pure Titanium material property that depends on the temperature extracted from the experimental work of (Guo & Cheng, 1999) for constant strain rate $(0.1/s)$ and digitized to numeric data is depicted as follows.

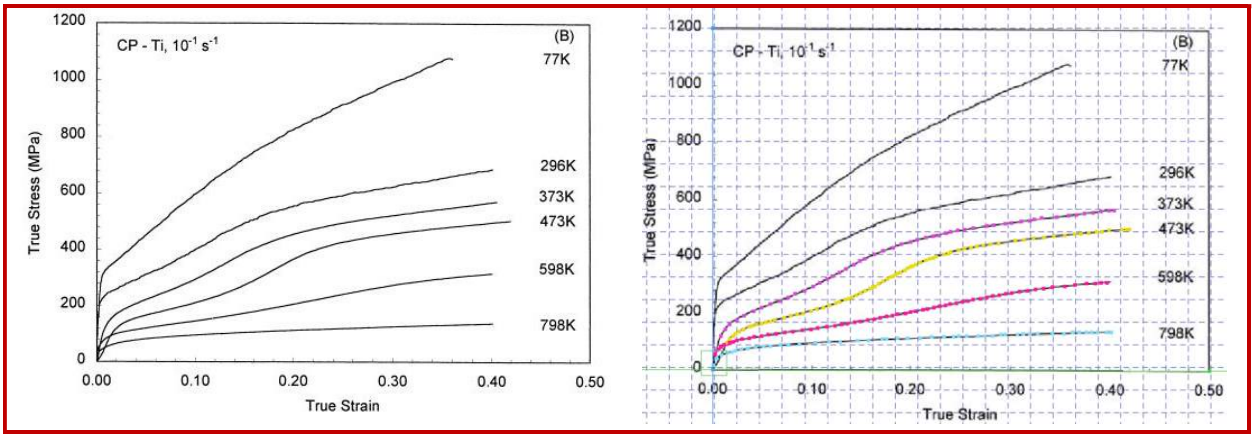

Figure A-0-1. The raw data (a) and the digitized data (b) (Guo & Cheng, 1999)

After extraction of the data, the yield stress (MPa) and plastic strain(mm/mm) can be tabulated as follow.

Table A-1. The extracted plastic property of Titanium for different temperature

$T = 296\ K$		$T = 373\ K$		$T=473\ K$		$T=598\ K$		$T=798\ K$	
$E = 6.3\ GPa$		$E = 15\ GPa$		$E = 6.2\ GPa$		$E = 12.5\ GPa$		$E = 11.6\ GPa$	
Yield Stress	Plastic Strain	Yield Stress	Plastic Strain	Yield Stress	Plastic Strain	Yield Stress	Plastic Strain	Yield Stress	Plastic Strain
214	0	118	0	105.6	0	71.16	0	40	0
285.5	0.048	218	0.0296	161.7	0.03	114	0.0393	76.59	0.063
400	0.126	275.5	0.087	208	0.086	140.5	0.1167	90	0.1365
456.7	0.225	359	0.153	250.8	0.116	165	0.1783	95	0.2104
460	0.294	381.5	0.203	289.5	0.136	187	0.2319		
		384.4	0.295	324.24	0.171	204.4	0.2946		
				335.8	0.239	210	0.355		

Note that: The above tabulated data are used to define the stress-strain property of the material for different temperature conditions which is extracted from experimental data.

Appendix-B

Finite Element and Extended Finite Element Method Procedures Followed used in Abaqus Software.

1. Heat Transfer Procedure

A. Part-Module

This module intended for creating the model of the crack

From the ABAQUS/CAE window of menu bar, select Part → Create. Part name '2D_Model'. Space mode is 2D, Deformable Type, Base feature is 'Solid' and approximate size is **2m**. The base feature 2m shows the size of Viewport in which the model drawn. Click continue.

The two-dimensional model of the plate is drawn by selecting the rectangle tool in the left bar and insert the dimension **0.1X0.2m**.

B. Property-Module

From the menu bar, select Material → Create. Material Name-CP_Titanium. Then insert the thermal property of the material CP_Titanium

i. General-Density

ii.Mechanical-Expansion: Insert the value of thermal expansion coefficient. Type-choose Isotropic. Then toggle on the temperature-dependent mode: Insert data **Table A-1**.

iii. Thermal-Conductivity: Insert the value of the thermal conductivity of the material. Type-choose Isotropic. Then toggle on the temperature-dependent mode: Insert data.

From the Main menu bar, select →Create →Name: '2D_Plate' →category is solid, Type: Homogeneous→ Continue. In the Edit section dialogue box, under material pick CP_Titanium. Select the Assign section icon and select the whole plate entire domain then toggle **Done**. In the edit section Assignment dialog box, select 2D_Plate, and CP_Titanium and click **Ok**.

C. Mesh Module

Mesh-Element type-Element library: Standard-Type: Heat Transfer → Select full integration and Element shape: Quad.

Mesh→ Mesh controls→ structured **Quad**.

Mesh→ Seeds→ Assign global seeds by element size as shown in Figure 3-8.

Part→ Assembly→ Instance→ Select 2D_Plate and accept the default then Ok.

D. Step Module

1. From the main menu bar, select Step →Create

2. Name it Step-1. Type of Procedure is General →Heat Transfer.

3. Under the Edit dialog box, insert Time period-1 second. Under type of Heat Transfer procedure toggle on- Steady State

Incrementation: Type-Automatic. Maximum number of increments is **10000**. Increment size is from: **0.01** and minimum is **1E-10** and Maximum is 1.

Under maximum temperatures change per increment: Insert-5

Then click Done.

E. Load and Boundary Condition

1. From the main menu bar, select BC →Create: select Step-1. Category is Others. Select Temperature and then select the boundary of 2D_plate and insert the value of the temperature.

2. Click on the predefined field and type-others-select temperature. Insert the Initial temperature of the plate.

To visualize the output from the analysis in output database the following step needed to follow. Step module →Output →Field output requests→Manager→F-output-1→Edit → thermal select Nodal Temperature

F. Job Module

From the main menu bar, select Job→ Create. Enter any name for the job. Summit the job and monitor the progress. Then Visualization to see the temperature field results.

2. Static General Procedure

A. Part-Module

This module intended for creating the model of the crack

From ABAQUS/CAE window of menu bar, select Part → Create. Part name '2D_Model'. Space mode is 2D, Deformable Type, Base feature is 'Solid' and approximate size is 2. Click continue.

The two dimensional model of the plate is draw by selecting the rectangle tool in the left bar and insert the dimension **0.1X0.2m**.

In this procedure partition around the domain of crack is needed to optimize and get an approximate result.

Open the Part Module →Partition→ Face partition → sketch another rectangular section at the mid of the model.

B. Property-Module

From menu bar, select Material → Create. Material Name-CP_Titanium. Then insert the thermal property of the material CP_Titanium

i. General-Density

ii. Mechanical-Expansion: Insert the value of thermal expansion coefficient. Type-choose Isotropic. Then toggle on the temperature dependent mode: Insert data.

Mechanical →Elasticity →Elastic: Under type choose Isotropic. Put the value of Young's Modulus and the Poisson's ratio.

Mechanical →Plasticity →Plastic: Under type choose Isotropic. Toggle on Temperature dependent→ insert values of mechanical property

Mechanical →Damage for Traction separation laws →MAXPS Damage: Tolerance: 0.005. Put the maximum principal stress of **240E6 (N/m^2).** On the **Sub-options** select Damage Evolution menu section. Use Energy type damage evolution for fracture energy of **24,954 N/m**. The fracture energy value needed because of XFEM method.

On the **Sub-options** menu again select Damage Stabilization-Default

iii. Thermal-Conductivity: Insert the value of the thermal conductivity of the material. Type-choose Isotropic. Then toggle on the temperature dependent mode: Insert data.

From the Main menu bar, select →Create →Name: '2D_Plate' → category is solid, Type: Homogeneous → Continue. In the Edit section dialogue box, under material pick CP_Titanium. Select the Assign section icon and select the whole plate entire domain then toggle Done. In the edit section Assignment dialog box, select 2D_Plate, and CP_Titanium and click Ok

C. Mesh Module

Mesh-Element Type-Element library: Standard-Type: Plane Strain → Select full integration and Element shape: Quad.

Mesh→ Mesh controls→ Structured Quad.

Mesh→ Seeds→ Assign global seeds by element size as shown in Figure 3-6.

Mesh the partition by local element size of **0.00001**

The element type is **CPE4R** stands for: - Two dimensional 4-node plain strain quadratic continuum element.

Part→ Assembly→ Instance→ Select 2D_Plate and accept the default then Ok.

Modelling the CRACK by XFEM

1. Module →Part

Create the crack in part model as wire type. Press Parts. Enter name as 'XFEM_crack', space of the modeling is 2D, Type is Deformable, Base feature is Wire, Approximate size of the window is **2**m. Click **Continue**.

2. On Assembly Module, expand and select the instances-'2D-Plate, and 'XFEM_Crack'. Then click on apply and then cancel. Specify the XFEM crack on appropriate position on the 2D_plate by transition tool.

3. Select 'Interaction' from the main menu, click 'Special'. Name as: 'Crack' Type is XFEM and continue. Then identify the crack location and Crack Domain

D. Step Module

1. From the main menu bar, select Step →Create
2. Name it Step-1. Type of Procedure is General →Static, General.
3. Under the Edit dialog box, insert Time period-1 second.

To consider large plastic deformation, click on **Nlgeom**(Nonlinear geometry). This too used to consider the large deformation and displacements in the analysis and the accuracy of the result.

Incrementation: Type-Automatic. Maximum number of increments is **10000**. Increment size is from: **0.01** and minimum is **1E-20** and Maximum is 1.

Select **other** and General solution controller →Edit →step-1 →continue →Toggle on Specify and Time increment →Ia from **5** to more than **20**. And toggle on Discontinuous analyses. Automatic damage stabilization specify dissipation energy fraction.

Then click Done.

E. Load and Boundary Condition

For the thermo-mechanical analysis: Define the temperature field analyzed in the previous analysis using in the predefined field: Select Predefined Field→Others→Temperature→insert the nodal temperature as ODB file.

1. From the main menu bar, select BC →Create: select step-1. Category is Mechanical. Type for selected step is Symmetry/Antisymmetric/Encastre. Name is Bottom End. Select the bottom of the plate. Click Done and choose ENCASTRE then press continue.
2. Click on the Loads. Enter name as Mechanical Load, category is Mechanical, Type is Pressure, click continue. Insert magnitude of the remote stress vary from 20MPa→100MPa.
3. Click on the predefined field: Enter Name → Temperature: Select→Others→Temperature→ Insert the temperature ODB file from the previous analysis.

In order to visualize the crack in the output database the following changes need to be made to the step module:

Step module →Output →Field output requests→Manager→F-output-1→Edit → Stress and Strain

F. Job Module

From the main menu bar, select Job→ Create. Enter any name for the job. Summit the job and monitor the progress. Then Visualization to see the mechanical and thermo-mechanical stress field results.